Graft Polymers: From Dendrimer Hybrids to Latex Particles

By

Abdul Munam

A thesis
presented to the University of Waterloo
in fulfillment of the
thesis requirement for the degree of
Doctor of Philosophy
in
Chemistry

Waterloo, Ontario, Canada, 2007

I hereby declare that I am the sole author of this thesis. This is a true copy of the thesis, including any required final revisions, as accepted by my examiners.

I understand that my thesis may be made electronically available to the public.

Abstract

The research presented focused on the synthesis and the characterization of graft polymers, of interest either as model systems or for large-scale applications. The materials selected as substrates for grafting reactions were carbosilane dendrimers, linear and branched polystyrenes, and cross-linked polystyrene latex particles. The synthesis of dendrimer-arborescent polymer hybrids was thus achieved by derivatization of the carbosilane dendrimers with dichlorosilane moieties and coupling with 1,4-polybutadiene side chains with $M_n \approx 1000$. A second derivatization and coupling reaction with $M_n \approx 1500$, 5000, or 30000 side chains yielded hybrid polymers with narrow molecular weight distributions ($M_w/M_n \leq 1.16$). In the second part of the thesis, a procedure for the large-scale (100-g) synthesis of arborescent styrene homopolymers and copolymers incorporating poly(2-vinylpyridine) segments is presented. End-capping of the polystyryllithium chains with 1,1-diphenylethylene in the presence of LiCl, followed by the addition of 3 – 6 equivalents of 2-vinylpyridine per side chain, eliminated side reactions and led to grafting yields of up to 95 %. A systematic investigation of the solution properties of polyelectrolytes obtained by protonation of the poly(2-vinylpyridine) arborescent copolymers with a strong acid (trifluoroacetic acid) is also presented. The relative importance of the electrostatic repulsion and the elastic deformation forces on molecular expansion was investigated by examining the solution properties of the copolymers as a function of structure, protonation level, and the presence of salts in polar solvents (methanol, DMF, H_2O). The viscosity of the arborescent copolymer solutions was also found to be much lower than for linear P2VP samples under the same conditions. In the last part of the thesis, the synthesis of model filler particles was achieved by grafting polyisoprene chains onto cross-linked polystyrene latex particles derivatized with acetyl coupling sites.

These substrates, which can be viewed as an extreme case of a dense (hard-sphere) arborescent polymer structure, were used to investigate the influence of filler-matrix polymer interactions on the rheological behavior of filled polyisoprene samples. The influence of the filler structure on the rheological behavior of the blends was examined by dynamic mechanical analysis in terms of frequency-dependent complex viscosity, storage modulus, and damping factor. All the blends exhibited enhanced complex viscosity, storage modulus, and decreased damping factor values relative to the matrix polymer.

Acknowledgements

I would like to take this opportunity to express my gratitude and appreciation to my supervisor, Professor Mario Gauthier, for his guidance and support over the course of this study.

I would like to express my thanks to the Supervisory Committee Members, Professors, Jean Duhamel, Eric Fillion, and Costas Tzoganakis, for their valuable time and helpful suggestions.

I would like to thank Mr. Dale Weber in the Department of Biology, University of Waterloo for running SEM samples and to Dr. Alexandra Smith in the Department of Food Science, University of Guelph for running the Cryo SEM experiments.

I would also like to thank all my co-workers at the University of Waterloo for their assistance and friendship over the course of this research, but particularly Jieming Li, Zongshun Yuan, Steven J. Teertstra, Gabriel Ngole Njikang, Jason Dockendorff, Olivier Nguon, Shahla Aliakbari, Wai-Yau Lin, and Dr. Firmin Moingeon.

My special thanks go to my wife Maimoona for her love, understanding, and support.

Financial support from the Natural Sciences & Engineering Research Council of Canada (NSERC) is gratefully acknowledged.

I dedicate this work to

my mother Zakia Khatoon and wife Maimoona for their

indefatigable patience, support, and encouragement.

Table of Contents

List of Tables

List of Figures

List of Schemes

List of Abbreviations and Symbols

AB_n	Monomer containing 2 types of polymerizable functional groups
B	Bulk modulus
BD	Butadiene
C	Concentration
C_s	Number of coupling sites on the substrate
CDMSS	4-(Chlorodimethylsilyl)styrene
CMC	Critical micelle concentration
CMME	Chloromethyl methyl ether
DMF	*N*,*N*-Dimethylformamide
DMSO	Dimethylsulfoxide
d*n*/d*c*	Refractive index increment
DPE	1,1-Diphenylethylene
DRI	Differential refractometer detector
DVB	Divinylbenzene
E	Young's modulus
EGDMA	Ethylene glycol dimethacrylate
FTIR	Fourier transform infrared spectroscopy
$(F_w)_{DS}$	Formula weight of dendrimers substrate
f_n	Number-average branching functionality
G	Generation number
G	Shear modulus
G′	Storage modulus
G″	Loss modulus
G*	Complex dynamic modulus
^{1}H NMR	Proton nuclear magnetic resonance
HPLC	High pressure liquid chromatography
K	Proportionality constant
k'	Huggins constant

LHAA	6-Lithiohexyl acetaldehyde acetal
LPIP	Linear polyisoprene
MALLS	Multi-angle laser light scattering
M_{BD}	Molecular weight of the butadiene unit
M_n	Number-average molecular weight
$(M_n)_{star}$	Absolute number-average molecular weight of the graft polymer
$(M_n)_{arm}$	Absolute number-average molecular weight of the side chains
M_c'	Molecular weight of the core (substrate)
M_c	Molecular weight of the dendrimer substrate
M_e	Entanglements molecular weight
$(M_n)_{core}$	Number-average molecular weight of the star-like polymer used as substrate
$M_n(G)$	Estimated number-average molecular weight of graft polymers of generation G
$M_n(G-1)$	Absolute number-average molecular weight of the preceding generation
M_n^{br}	Absolute number-average molecular weight of the side chains
M_S	Molecular weight of the styrene unit
mol%	Molar percentage
M_w	Weight-average molecular weight
MWD	Molecular weight distribution
M_w/M_n	Polydispersity index
PANa	Sodium Polyacrylate
PANaL	Linear Sodium Polyacrylate
PACs	Cesium Polyacrylate
PARb	Rubidium Polyacrylate
P2VP	Poly(2-vinylpyridine)
PBD	Polybutadiene
PDI	Polydispersity index
PIP	Polyisoprene
PMMA	Poly(methyl methacrylate)
PS	Polystyrene

PSVP	Vinylphenol-modified polystyrene
PTFE	Poly(tetrafluoroethylene)
SAN	Acrylonitrile-styrene copolymer
SBR	Styrene-butadiene rubber
SEC	Size-exclusion chromatography
SEC-MALLS	Size-exclusion chromatography-laser light scattering detector
SEM	Scanning electron microscopy
TFA	Trifluoroacetic acid
T_g	Glass transition temperature
THF	Tetrahydrofuran
TMEDA	*N*,*N*,*N*',*N*'-Tetramethylethylenediamine
VP	Vinylpyridine
2VP	2-Vinylpyridine
v/v	Fraction by volume
VBC	Vinylbenzyl chloride
w/w	Weight fraction
ε	Dielectric constant or strain
η	Viscosity of Solution
η_o	Viscosity of Solvent
$[\eta]$	Intrinsic viscosity
η^*	Complex dynamic viscosity
η'	Dynamic storage viscosity
η''	Dynamic loss viscosity
η_{sp}	Specific viscosity
σ	Shear stress
Φ	Volume fraction
ω	Angular frequency
τ^*	Complex stress
γ^*	Complex strain
δ	Phase angle
$\tan\delta$	Damping factor

Chapter 1

Foreword

1.0 Opening Remarks

Branched polymers are of interest because of their distinctive physical properties. Among branched macromolecules, star-branched[1] and arborescent polymers[2] are particularly significant because of their well-defined architectures enabling the establishment of structure-property relations. Both polymer families are synthesized mostly by the living anionic polymerization technique. Under ideal conditions, the absence of termination and chain transfer in these reactions allows the preparation of polymers possessing predictable molecular weights and narrow molecular weight distributions, with a degree of control difficult to attain by other means.

Arborescent polymers, specifically, are highly branched macromolecules characterized by a tree-like architecture with multiple branching levels, resulting from cycles of anionic polymerization and grafting reactions.[2] In contrast to the other dendritic polymer families, arborescent polymers are constructed from linear chain segments rather than small molecule monomers, so that very high molecular weights are attained in a few steps. For that reason, arborescent polymers may prove to be more useful than other dendritic polymers for large scale applications.

1.1 Research Objectives and Thesis Outline

The research presented in this Thesis is intended to explore the synthesis and the physical characterization of arborescent polymers and other closely related graft polymers of potential interest for large-scale applications. Following a general overview in Chapter 2 on the synthesis of branched polymers, and other background information relevant to the thesis work, four different projects are examined. In Chapter 3, the

synthesis and characterization of dendrimer-arborescent polymer hybrids derived from carbosilane dendrimer substrates and 1,4-polybutadiene side chains is described. These materials are of interest because of the very low entanglement molecular weight of the polybutadiene chains, that should lead to exceptional elastomeric properties.[3,4] A method for the large-scale (100 g) synthesis of arborescent graft polymers using acetyl coupling sites is then considered in Chapter 4. The synthesis of styrene homopolymers and of copolymers incorporating polystyrene and poly(2-vinylpyridine) segments was achieved. A systematic investigation of the solution properties of polyelectrolytes obtained by protonation of the poly(2-vinylpyridine) arborescent copolymers is then presented in Chapter 5. Finally the synthesis of model filler particles, obtained by grafting polyisoprene chains onto cross-linked polystyrene latex particles according to the acetyl coupling site chemistry discussed in Chapter 4, is reported in Chapter 6. These materials, which can be viewed as an extreme case of an arborescent copolymer structure, are then used to investigate the influence of filler-matrix polymer interactions on the rheological behavior of linear polyisoprene blends. The Thesis is concluded with Chapter 7, providing a summary of the original contributions to knowledge arising from the research and some recommendations for future work.

In agreement with the University of Waterloo Thesis Guidelines, Chapters 3-6 are written in the format of individual papers to be submitted for publication in scientific journals. Each chapter therefore includes an abstract, an introduction on relevant background material, the description of the experimental procedures used, the presentation and discussion of the results obtained, concluding remarks, and a list of references.

1.2 References

1. (a) Rempp, P.; Franta, E.; Herz, J.-E. *Adv. Polym. Sci*. **1988**, *86*, 145. (b) Hsieh, H. L.; Quirk, R. P. *Anionic Polymerization*: *Principles and Practical Applications*; Dekker: New York, 1996; Chapter 13.
2. For a recent review on arborescent and other dendrigraft polymers see Teertstra, S. J.; Gauthier, M. *Prog. Polym. Sci.* **2004**, *29*, 277.
3. Teertstra, S. J.; Gauthier, M. *Macromolecules* **2007**, *40*, 1657.
4. Hempenius, M. A.; Zoetelief, W. F.; Gauthier, M.; Möller, M. *Macromolecules* **1998**, *31*, 2299.

Chapter 2

Background Information and Literature Review

2.0 Scope of the Review

This Chapter is concerned mainly with the synthesis of branched polymers from vinyl and diene monomers using living anionic polymerization techniques. To have a better understanding of the material presented in the following chapters it is therefore necessary to start our discussion with a description of the different branched polymer architectures and the strategies implemented for their synthesis. The non-aqueous solution behavior of polyelectrolytes is then reviewed from a "general" point of view. The role of early studies in establishing the basic understanding of polyelectrolyte solutions in relation to Chapter 5 is of particular interest. A brief discussion of emulsion polymerization techniques serving to synthesize the latex particles investigated in Chapter 6 is then provided, before a likewise brief discussion of the rheology of filled polymers.

2.1 Branched Polymers

A branched polymer can be defined as a molecule containing more than one backbone chain, i.e. having a non-linear chain architecture.[1] Long-chain branching, in particular, is characterized by the presence of one or more branching points linking at least three chain segments, or alternately by the presence of at least three chain ends in the molecule.

2.2 Classification of Branched Polymers

Branched polymers can be classified into three main types: (1) star-branched polymers, with a central branching point linking a number of branches,[1] (2) comb-branched polymers, with a main linear backbone and branches randomly distributed along the backbone,[2] and (3) dendritic polymers, with a multi-level (dendritic) branched architecture. The latter may be

further subdivided into three families based on the specific characteristics of the molecules, namely dendrimers,[3-6] hyperbranched polymers,[7,8] and dendrigraft[9] (also called Comb-burst or arborescent) polymers.[10] These different branched polymer structures are represented schematically in Figure 2.1. The synthetic methods used to obtain these branched polymers are discussed in more details in the subsequent sections.

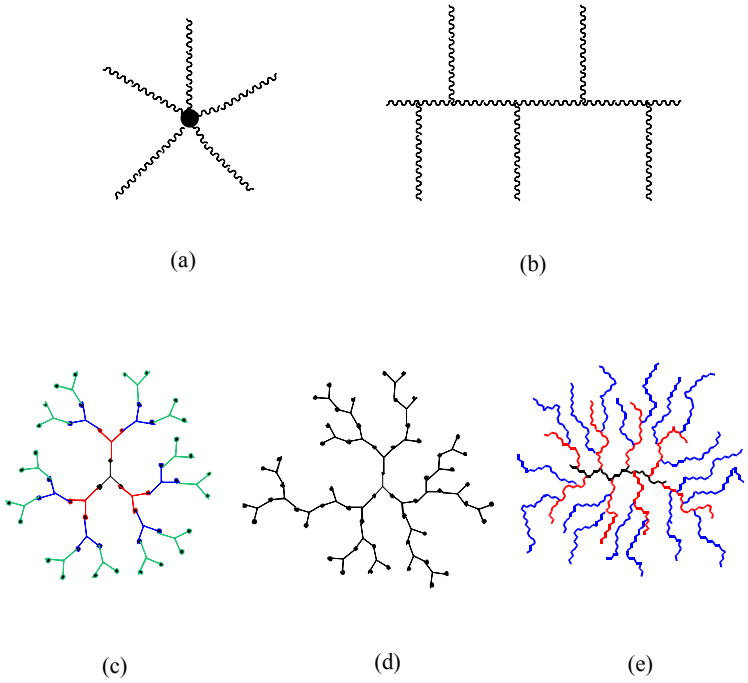

Figure 2.1 Schematic representation of branched polymers: (a) star-branched polymer, (b) comb-branched polymer, (c) dendrimer, (d) hyperbranched polymer, and (e) dendrigraft polymer.

2.2.1 Star-branched Polymers

Star polymers are the simplest branched polymer structures, because they contain a single branching point linking a number of branches (arms or side chains) per molecule.

Ideally the molecules contain a well-defined number of arms of equal length (regular star polymers), and are therefore monodispersed in size. In practice, star polymers are polydispersed due to variations in the size of the side chains or in the number of chains attached. Palm tree[11] or umbrella polymers,[12] containing a single chain with a molecular weight different from the other arms, can also be viewed like asymmetric star polymers.[13] Star-branched polymers are very helpful as model systems to study the influence of branching on the properties of polymers in solution and in the molten state for comparison to their linear counterparts.[14,15] They are also useful as viscosity modifiers in paints and coatings, and for their enhanced processability and desirable mechanical properties.

Star-branched homo- and copolymers are mostly synthesized by the living anionic polymerization technique. The absence of termination and chain transfer in these reactions allows the preparation of chain segments with predictable molecular weights and narrow molecular weight distributions (MWD). Three main methods[2] have been applied to the synthesis of tailor-made star-branched polymers, as depicted in Scheme 2.1:

(1) Multifunctional organometallic initiators.

(2) Reaction of a living precursor polymer with a multifunctional linking reagent.

(3) Block copolymerization of two monomers, the second one being a divinyl monomer.

The first procedure, usually known as the "core-first" methodology (Scheme 2.1a), using a multifunctional initiator and the simultaneous growth of all the side chains from the central core, is not widely used for the synthesis of model star polymers. This is due to difficulties in preparing pure multifunctional organometallic compounds, and to the poor solubility of these compounds in most anionic polymerization solvents. Furthermore, it is impossible to characterize the size and the homogeneity of the branches formed by this method

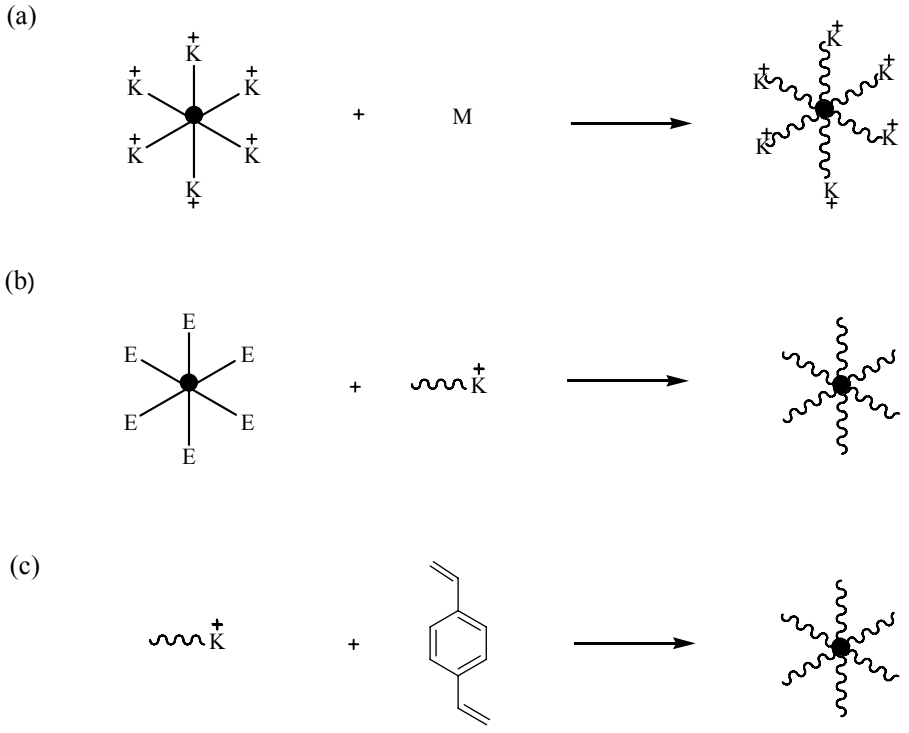

Scheme 2.1. Synthesis of star-branched polymers (a) using a multifunctional initiator, (b) by coupling with a multifunctional linking agent, and (c) by sequential copolymerization with a divinyl compound.

in most cases. This approach was first applied by Eschwey and Burchard[16] to the synthesis of star polymers with very high molecular weights, using polyfunctional organometallic nanoparticle initiators derived from divinylbenzene. Later on, this method was extended to the synthesis of star-branched polymers with functional groups at the chain ends.[17,18] More recently, the "core-first" method was applied to the synthesis of star polymers using novel hydrocarbon-soluble organolithium initiators such as 1,3,5-tris(1-phenylethenyl)benzene.[19] Series of 4-, 8-, and 16-arm star poly(ethylene oxide)s were also synthesized using multifunctional initiators derived from hydroxyl-terminated carbosilane dendrimers.[20] The last

two methods described are best suited to the generation of well-defined star polymers based on a core-first methodology.

The second procedure, known as an "arms-first" methodology (Scheme 2.1b), is the most efficient way to synthesize well-defined star-branched polymers. It starts with the synthesis of a living precursor by anionic polymerization, followed by the reaction of the living chains with a multifunctional electrophile acting as a linking agent (core or substrate).[21] After the sequential polymerization of two or more monomers, linking of the living chains can also serve to generate star-branched block copolymers with identical arms.[22] Multifunctional chlorosilanes (Si-Cl) have been used extensively as linking agents for the synthesis of regular stars.[23-26] Series of 4- to 18-arm polystyrenes[27-29] and polyisoprenes [30-32] were thus synthesized. Polybutadiene stars with up to 128 arms,[33] and "miktoarm" stars incorporating four different types of branches[34] are other examples of star-branched polymers synthesized by this "arms-first" coupling chemistry.

The third procedure (Scheme 2.1c) is also referred to as an "arms-first" methodology, but it is distinct in terms of the coupling procedure. In this case the linking agent is a divinyl monomer (divinylbenzene, ethylene dimethacrylate, etc.) which, when added to the living anionic polymer precursor, leads to the formation of small tightly cross-linked nodules linking the arms.[35] To synthesize star polymers with polystyrene branches,[36] for example, the linking reaction of polystyryllithium with divinylbenzene (DVB) can be viewed as a block copolymerization of DVB followed by coupling of the anionic propagating centers with the pendent vinyl groups within the DVB blocks. The rate constant for the crossover reaction from polystyryllithium to DVB is comparable with that for the homopolymerization of DVB, but it is about 10 times faster than the rate constant for the reaction of the living chain ends with the

residual double bond in DVB. The DVB blocks thus formed are relatively uniform in size and the linking reaction occurs efficiently after the formation of the blocks.

2.2.2 Comb-branched Polymers

Comb-branched polymers are graft polymers incorporating a main linear backbone chain linked to well-defined branches of identical or different compositions, and randomly distributed along the backbone.[2,37]

Comb-branched polymers with side chains of uniform size can be synthesized by anionic grafting. Since living anionic polymerization allows the synthesis of chains with narrow MWD and predictable molecular weights, branches of uniform size can be produced. Two schemes for the synthesis of comb-branched polymers known as the *grafting onto* and the *grafting from* methods[2,37,38] are depicted in Scheme 2.2.

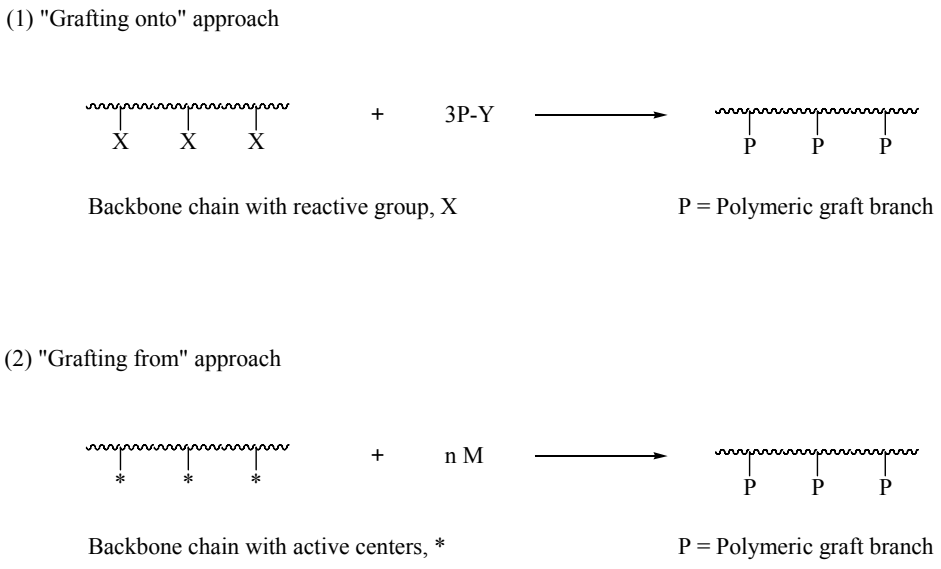

Scheme 2.2 *Grafting onto* and *grafting from* schemes for the synthesis of comb-branched polymers.

The *grafting onto* approach is most commonly used, because anionic propagating centers are highly reactive towards a wide variety of electrophilic functional groups. This method relies on the introduction of coupling sites (functional groups) on the linear substrate and their reaction with the living chains. The coupling sites are typically introduced by chemical modification of the backbone polymer, and therefore randomly distributed along the chain. Different functionalities such as ester, anhydride, halide, nitrile, chlorosilane, epoxide, pyridine, and acetyl have been used with varying degrees of success.[39-42] The *grafting onto* approach has the advantage that the backbone polymer and the side chains can be characterized separately. By measuring the total molecular weight of the graft polymer, the number of side chains introduced and the average spacing between side chains can be thus calculated.

In the Gauthier group in particular, chloromethyl[41,43,44] and acetyl[42,45,46] functionalities have been introduced on polystyrene for the preparation of comb-branched styrene homo- and copolymers. After optimizing the reaction conditions, comb polymers were obtained in up to 96 % yield when coupling polystyryl, polyisoprenyl, and poly(2-vinylpyridinyl) anions with linear polystyrene substrates as depicted in Scheme 2.3. The graft polymers obtained had narrow MWD ($M_w/M_n < 1.1$).

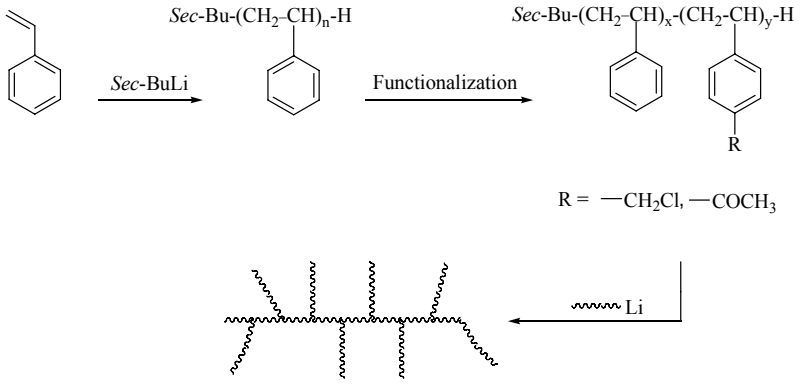

Scheme 2.3 Synthesis of comb-branched polymers by the *grafting onto* approach.

The anionic *grafting from* approach relies on the generation on the backbone polymer of carbanionic sites able to initiate the polymerization of a second monomer. The sites can be introduced by metallation of carbon-hydrogen bonds on the backbone with organometallic compounds (e.g. *n*-butyllithium, *sec*-butyllithium) with chelating compounds such as N,N,N',N'-tetramethylethylenediamine (TMEDA).[47] These reactive complexes can metallate allylic, benzylic, and even aromatic C-H bonds. The initiating sites are generally distributed randomly along the polymer backbone. A monomer is then added, resulting in the growth of side chains from the backbone polymer. Limitations of this method include poor backbone solubility due to aggregation of the charged polymeric substrate, often leading to heterogeneous reactions and a broad MWD prohibiting the reliable estimation of the number and the size of the side chains formed. Incomplete consumption of the metallating agent also leads to the generation of linear polymeric contaminant.

To improve the uniformity of the side chains, the rate of initiation for the metallated sites must be at least of the same order of magnitude as propagation. This is readily achieved for styrene and diene monomers,[48] but cannot be assumed when the metallated sites are stabilized as allylic, benzylic, or aryl anions. Slow initiation typically leads to chains of non-uniform size in these cases.

Complexes of *n*-butyllithium and TMEDA were thus used to metallate polyisoprene or polybutadiene, which were grafted with styrene to generate comb-branched copolymers (Scheme 2.4).[49-51] Degradation of the backbone was observed in the metallation of the polydienes at 50 ^{o}C, the extent of degradation increasing with the amount of *n*-butyllithium-TMEDA complex used. Less degradation was observed with *tert*-butyllithium-alkali metal

alkoxide complexes at 50 °C[50] and for *sec*-butyllithium-TMEDA at room temperature.[52] It was estimated that 65-97% of the metallated sites participated in the grafting reactions.

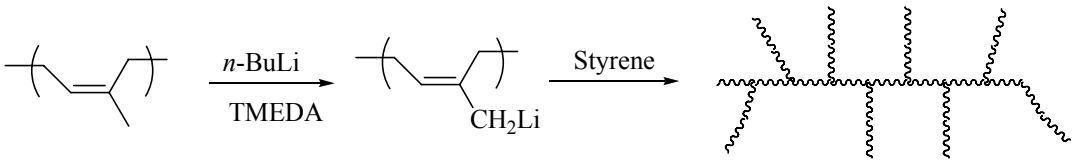

Scheme 2.4 Synthesis of comb-branched polymer by a *grafting from* approach using a metallated substrate initiator.

2.2.3 Dendritic Polymers

Polymers with a dendritic (multi-level) branched architecture have been investigated extensively over the past twenty years. Three families of dendritic polymers can be identified, namely dendrimers, hyperbranched polymers, and dendrigraft polymers. The synthesis of dendrimers (Figure 2.1c) is performed according to either divergent (core first)[3] or convergent (arm first)[53] methods, using cycles of protection, condensation, and deprotection of AB_n-type monomers (n = 2 or 3). The structure of these macromolecules is strictly controlled, leading to very narrow MWD ($M_w/M_n < 1.01$) and precisely predictable molecular weights, in spite of a number of limitations. Since small molecules are used as building blocks, the increase in molecular weight per generation (reaction cycle) is relatively low and many reaction cycles are required to reach high ($> 10^5$) molecular weights. Dendrimer growth is very sensitive to incomplete or side reactions, causing structural defects affecting the topology of the molecules. To overcome these problems large excesses of reagents are used in the synthesis, making dendrimers difficult to purify prior to subsequent reaction steps.

The second family of dendritic polymers is hyperbranched polymers (Figure 2.1d), obtained in one-pot self-condensation reactions of AB_n monomers.[7,8] Moderate to high molecular weight randomly branched polymers are produced by this approach, while avoiding the complex reaction sequences encountered in the synthesis of dendrimers. The control attained over molecular weight and branching is much more limited, however, and the branching density of the molecules is typically much lower than for dendrimers. The random nature of the condensation reaction leads to polymers with many structural flaws, and broad MWD ($M_w/M_n > 2$) are obtained in most cases.

The third family of dendritic polymers is the dendrigraft polymers (Figure 2.1e), also called Comb-burst® polymers by Tomalia et al.[9] and arborescent polymers by Gauthier and Möller.[41] These polymers are synthesized in a generation-based scheme similar to dendrimers with cycles of ionic polymerization and grafting reactions, but using polymeric chains rather than small molecules as building blocks. This approach minimizes some of the problems encountered in the synthesis of dendrimers and hyperbranched polymers. Since the building blocks are polymeric chains, a very rapid molecular weight growth is observed and high molecular weights are obtained in a few steps. The increase in molecular weight and branching functionality is typically 10- to 15-fold per generation for arborescent polymers, as compared to 2- to 3-fold for dendrimers. In contrast to dendrimers, the branches are distributed randomly on the grafting substrate rather than strictly at the chain ends. The random distribution of coupling sites is advantageous because it makes polymer growth less sensitive to side reactions: These affect all molecules to the same extent and in a similar manner on average. While the architecture of dendrigraft polymers is not as strictly defined as in dendrimers, the MWD achieved is usually fairly narrow ($M_w/M_n<1.1$).

2.2.4 Synthetic Strategies for Dendrigraft or Arborescent Polymers

Dendrigraft polymers have been synthesized by both divergent (core first) and convergent (arm first) approaches. The divergent scheme includes both *grafting onto* and *grafting from* methods, whereas a *grafting through* method also developed is a convergent technique conceptually more closely related to the hyperbranched polymer syntheses. Since the synthetic work presented in the thesis is mostly based on the divergent *grafting onto* method, it will be reviewed in more detail while the *grafting from* and *grafting through* methods will only be discussed briefly.

2.2.4.1 Divergent *Grafting onto* Methods

A divergent *grafting onto* method was first applied by Gauthier and Möller for the synthesis of arborescent polystyrenes, using cycles of chloromethylation and anionic grafting.[41,42] A generation-based nomenclature system (G0, G1, G2, etc.) was proposed to refer to graft polymers obtained from successive reactions as depicted in Scheme 2.5.

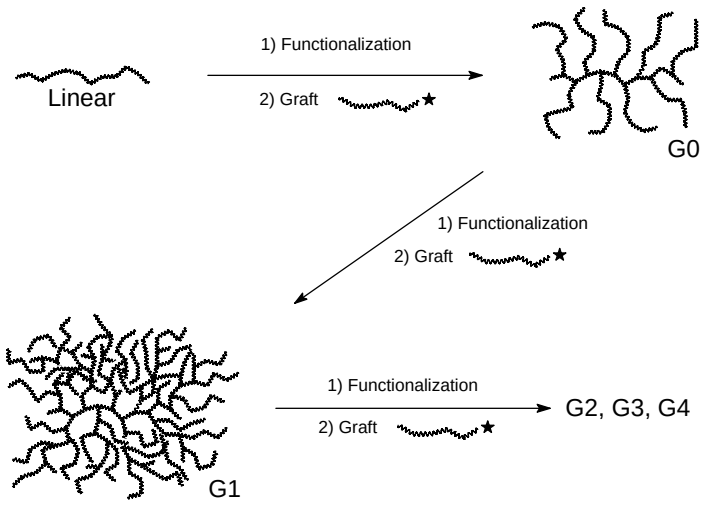

Scheme 2.5 *Grafting onto* method for the synthesis of dendrigraft polymers.

A linear polymer substrate with a narrow MWD serving as core is first randomly functionalized with coupling sites and reacted with the living macroanions to yield a comb-branched (generation 0 or G0) polymer. A key step in the arborescent polymer synthesis is the ability to introduce coupling sites on the newly grafted side chains. If this can be achieved, repetition of the functionalization and grafting cycles leads to higher generation (G1, G2, etc.) arborescent polymers, with molecular weights and branching functionalities increasing geometrically for successive generations.

Several requirements must be met to obtain well-defined graft polymers by this approach.[54] The macroanions must have good 'living' character, be sufficiently reactive, and ideally have a narrow MWD. The side chains grafted in each generation must allow the introduction of coupling sites without inducing intermolecular cross-linking. Furthermore, the coupling reaction should proceed without side reactions and in high yield.

Styrene is one of the monomers satisfying these requirements: The anionic polymerization of styrene yields reactive macroanions with exceptional living characteristics, and a wide range of functional groups can be introduced on the pendent phenyl rings by electrophilic substitution. Chloromethylation and acetylation reactions,[41,42] in particular, have been used for the synthesis of arborescent polystyrenes. The synthetic steps involved in the synthesis of arborescent polystyrene using chloromethyl coupling sites is illustrated in Scheme 2.6 as an example.[41] The chloromethylated linear substrate is reacted with living polystyryllithium after capping the chains with a 1,1-diphenylethylene (DPE) unit. The use of DPE capping for the polystyryl anions is a key step in avoiding side reactions with the chloromethylated substrate: The coupling reaction of non-capped polystyryllithium and linear chloromethylated polystyrene only proceeds in 50 % yield due to a competing metal-halogen

exchange reaction. In contrast, the yield increases to 96 % in THF at -30 °C after capping with DPE. The branching density can be varied for each generation through the chloromethylation level, allowing the synthesis of arborescent polystyrenes with a wide range of characteristics.

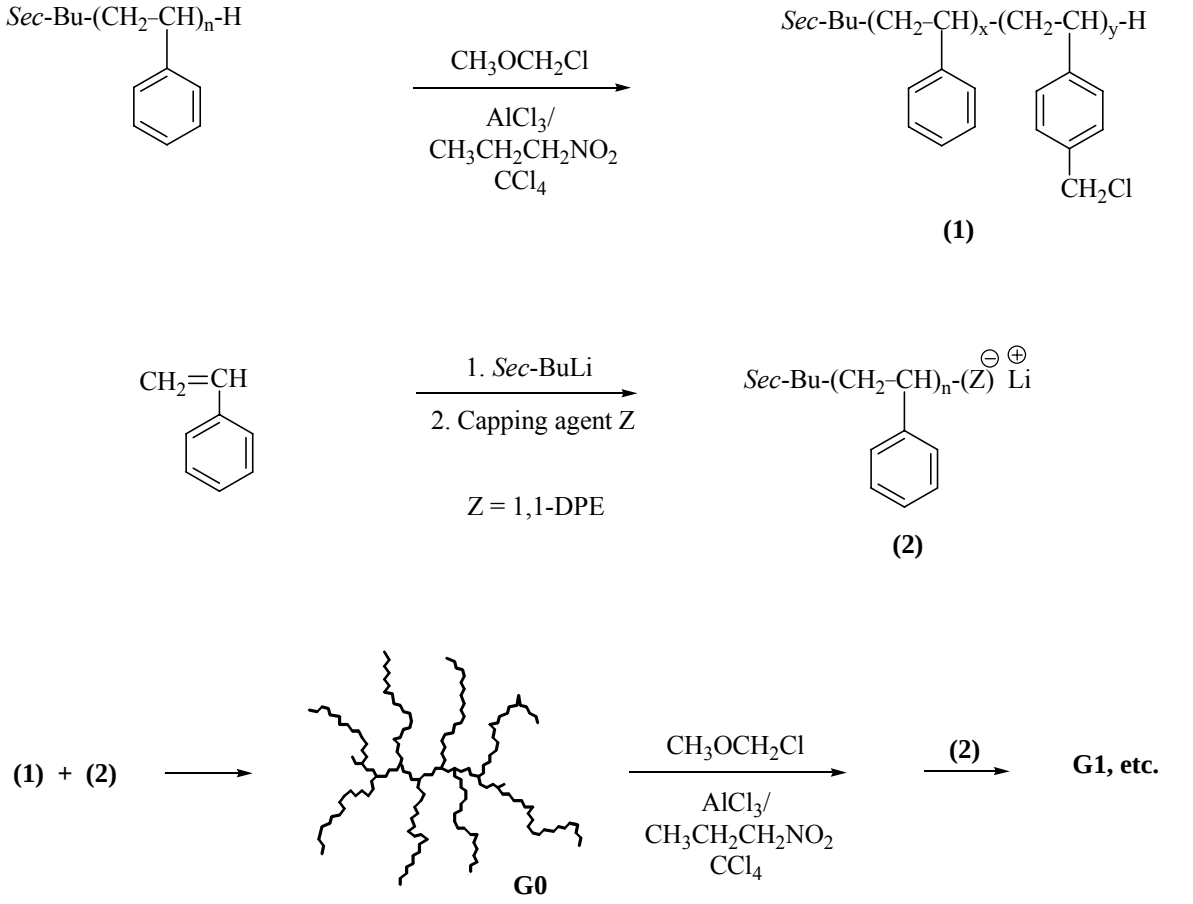

Scheme 2.6 Arborescent polystyrene synthesis by grafting onto chloromethylated polystyrene substrates.

An alternate approach for the synthesis of arborescent polystyrenes based on acetyl coupling sites[42] is illustrated in Scheme 2.7. The main motivation for this work was the elimination of chloromethyl methyl ether and carbon tetrachloride serving in the chloromethylation step, both being hazardous and expensive reagents.

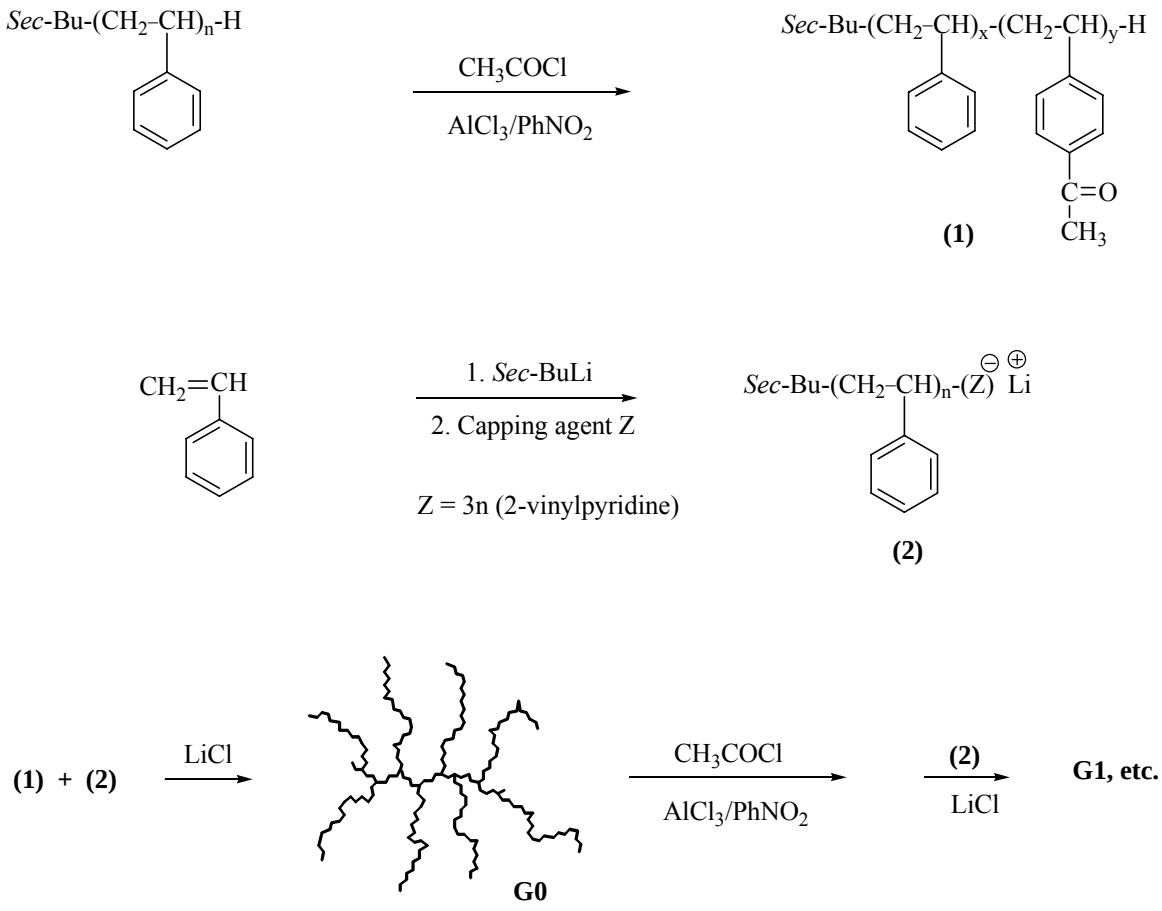

Scheme 2.7 Arborescent polystyrene synthesis by grafting onto acetylated polystyrene substrates.

The synthesis starts with the random acetylation of linear polystyrene with acetyl chloride in nitrobenzene, followed by coupling with polystyryllithium capped with a few 2-vinylpyridine units. Capping was also necessary in this case to attenuate the reactivity of the macroanions and increase the grafting yield. The coupling reaction of non-capped polystyryllithium and linear acetylated polystyrene proceeded in only 65 % yield, due to a competing proton abstraction reaction from the acetyl functionality. The grafting yield increased to 79 % in THF at -30 °C after capping of the living chains with at least 3 equivalents of 2-vinylpyridine, and reached 95 %, even at 25 °C, when 2-vinylpyridine

capping was used in combination with 5 equivalents of LiCl. Repetition of the acetylation and grafting reaction cycles led to arborescent polystyrenes of generations G1 – G3 in 43 – 89 % yield, depending on the substrate generation and the molecular weight of the side chains.

The synthesis of arborescent polyisoprenes was also reported more recently by Gauthier et al.[55] This involved successive functionalization (epoxidation) and anionic grafting cycles, in analogy to the arborescent polystyrene syntheses. A linear polyisoprene sample with a high (ca. 95 %) 1,4-isoprene units content was first synthesized and partially (~ 25 %) epoxidized with performic acid. Coupling of the epoxidized substrate with 1,4-polyisoprenyllithium yielded a comb-branched (G0) polymer. A grafting yield increase from 78 % to 92 % was achieved for a linear substrate upon addition of a lithium salt (LiCl or LiBr) as a promoter for the coupling reaction. Further epoxidation and grafting reaction cycles yielded G1 and G2 arborescent polyisoprenes. A geometric increase in molecular weight and branching functionality was observed for successive generations, in analogy to arborescent polystyrenes, and a relatively low polydispersity index ($M_w/M_n \leq 1.05$) was maintained.

A *grafting onto* strategy has also been applied to the synthesis of arborescent polybutadienes by Hempenius et al.[56] The synthetic scheme used (Scheme 2.8) relied on the anionic polymerization of 1,3-butadiene in hexane, to give a microstructure with ca. 6 % 1,2-butadiene units along the backbone. These vinyl groups were converted into electrophilic coupling sites by hydrosilylation with chlorodimethylsilane, and reacted with an excess of polybutadienyllithium to give a comb-branched (G0) polymer. An excess of living chains was used to ensure the complete reaction of the chlorosilyl moieties because polybutadienyl anions are essentially colourless, making it difficult to monitor the stoichiometry of the grafting reaction visually. Repetition of the hydrosilylation and grafting reactions yielded G1 and G2

arborescent polybutadienes with a geometric increase in molecular weight and branching functionality, and polydispersity indices $M_w/M_n \leq 1.3$.

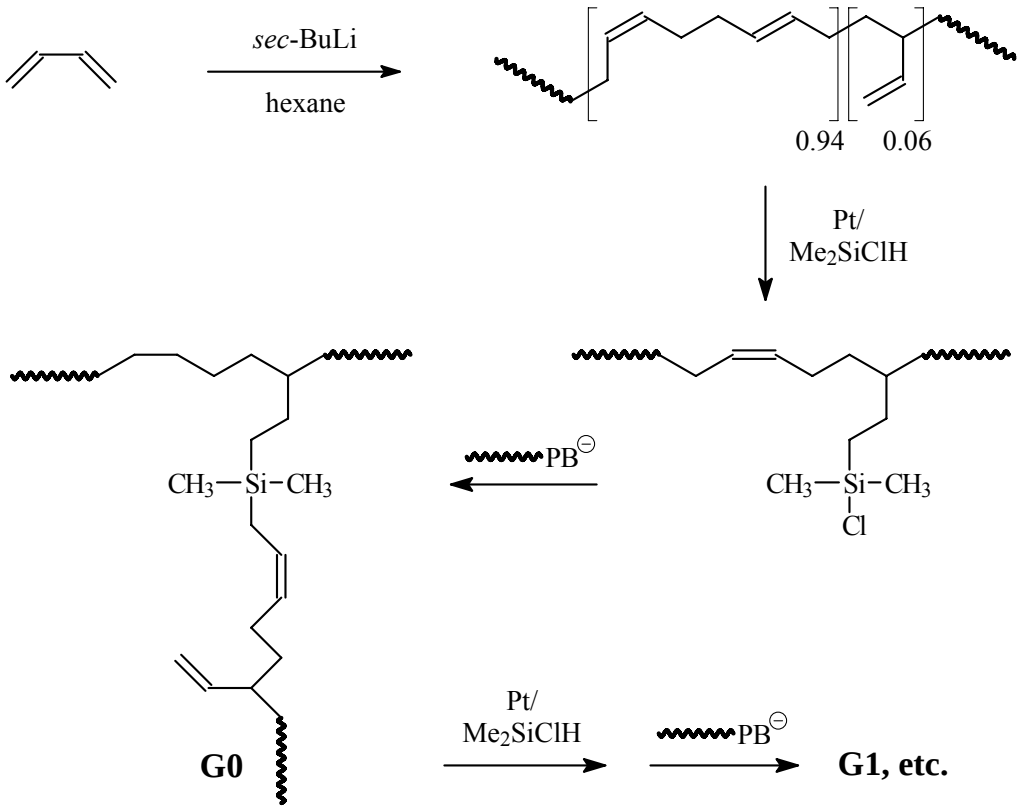

Scheme 2.8 Arborescent polybutadiene synthesis by grafting onto hydrosilylated polybutadiene substrates.

Apart from the arborescent styrene, isoprene, and butadiene homopolymer syntheses described, different arborescent copolymers were also obtained by grafting poly(*tert*-butyl methacrylate),[57] polyisoprene,[43,45] and poly(2-vinylpyridine)[44,46] macroanions onto arborescent polystyrene substrates using variations of the basic schemes discussed, to broaden the range of physical properties observed and to produce materials useful for a wider range of applications.

2.2.4.2 Divergent *Grafting from* Methods

The examples discussed so far are all based upon divergent *grafting onto* methodologies. An alternate procedure involves the growth of side chains from the substrate in a divergent *grafting from* scheme. Unfortunately the structure of the dendrigraft polymers obtained by this approach is difficult to characterize, and the MWD of the products tends to be broader. In spite of these limitations, *grafting from* schemes have allowed the synthesis of novel macromolecular architectures inaccessible by other methods.

The synthesis of amphiphilic arborescent copolymers incorporating a branched polystyrene core with end-linked poly(ethylene oxide) chains forming an outer 'shell' was thus reported by Gauthier et al.[58] The arborescent polystyrenes serving as grafting substrates were synthesized by a variation of the *grafting onto* method described above to introduce hydroxyl chain ends near the surface of the molecules in the last grafting reaction. The synthesis of a hydroxyl-functionalized G1 polystyrene core and the addition of a poly(ethylene oxide) shell are described in Scheme 2.9.

In the example provided, a bifunctional initiator (6-lithiohexyl acetaldehyde acetal, LHAA) containing a protected hydroxyl functionality served to initiate the polymerization of styrene. The living anions, upon capping with DPE and reaction with a chloromethylated G0 polystyrene substrate, yielded a G1 polymer with protected hydroxyl end-groups. Deprotection of the acetal functionalities and deactivation of the residual chloromethyl groups on the substrate were followed by titration with potassium naphthalide and the addition of ethylene oxide. Variation in the amount of ethylene oxide added in the shell growth step provided control over the 'thickness' of the hydrophilic polymer layer, and copolymers with poly(ethylene oxide) contents ranging from ~ 19 – 66 % by weight were obtained.

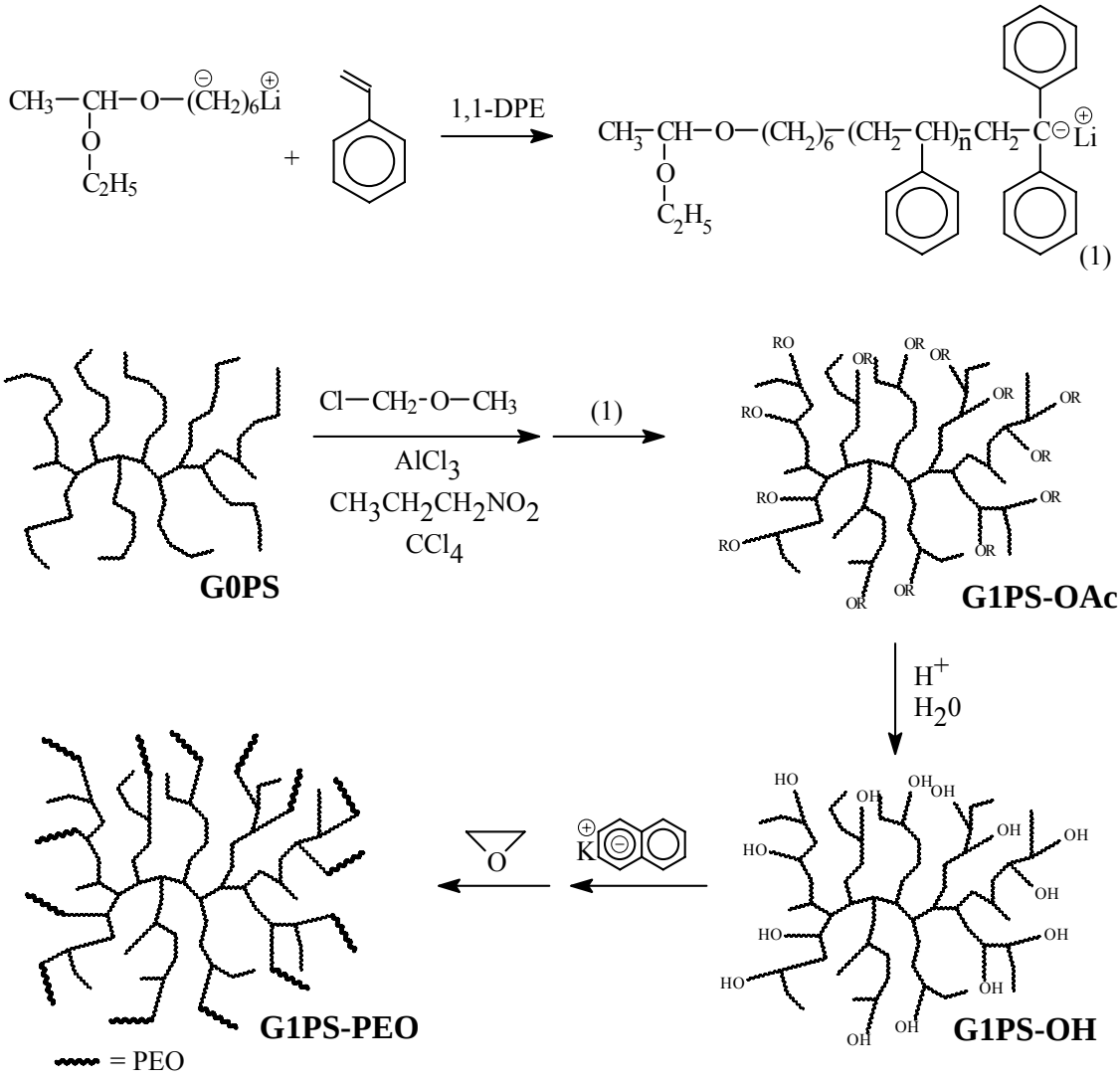

Scheme 2.9 Synthesis of amphiphilic arborescent polystyrene-*graft*-poly(ethylene oxide) by a *grafting from* scheme.

2.2.4.3 Convergent *Grafting through* Methods

The last approach discussed for the synthesis of dendrigraft polymers is a one-pot self-branching convergent synthesis technique suggested by the group of Knauss.[59,60] It relies on the formation of macromonomers in situ from living macroanions and a "bifunctional" monomer carrying a polymerizable vinyl group and a second chemical functionality able to

couple with the living chains. When the coupling agent is added slowly, the macromonomers formed react with living chains to produce branched polymers with a relatively narrow MWD.

The synthesis of dendritic polystyrenes was demonstrated using either 4-(chlorodimethylsilyl)styrene[59] (CDMSS) or vinylbenzyl chloride[60] (VBC) as bifunctional monomers (Scheme 2.10). Linear polystyrene segments were synthesized anionically, and the bifunctional monomer (CDMSS or VBC) was added to the living polymer. In the presence of THF, the chlorosilyl and chloromethyl functionalities react with polystyryllithium at a faster rate than propagation through the vinyl group, yielding macromonomers with a terminal vinyl group. These macromonomers then dimerize by reacting through their vinyl groups with the leftover living chains, if a less than stoichiometric amount of coupling agent is added. This produces branched polystyrene molecules with one single propagating centre located at the center (focal point) of the molecule. To favor dendritic growth and avoid premature chain termination, the addition rate of the coupling agent must be slow enough to allow the reaction of both reactive moieties. Since the propagating center is always located at the focal point, steric hindrance increases with the branching functionality and ultimately limits molecular growth. It is thus difficult to synthesize branched polymers with both a high molecular weight and a high branching density by this method. One way to alleviate this problem is to add a mixture of the coupling agent and styrene, to introduce polystyrene spacer segments between branching points (Scheme 2.10). With a molecular weight of 1000 for the primary polystyrene chains and a styrene : coupling agent (VBC) molar ratio of 5, for example, the molecular weight of the dendrigraft polymer was limited to M_n = 24000, while it reached 41000 for a styrene : coupling agent (VBC) ratio of 15. The downside of this approach is that the branching density decreases as the styrene : coupling agent ratio is increased.

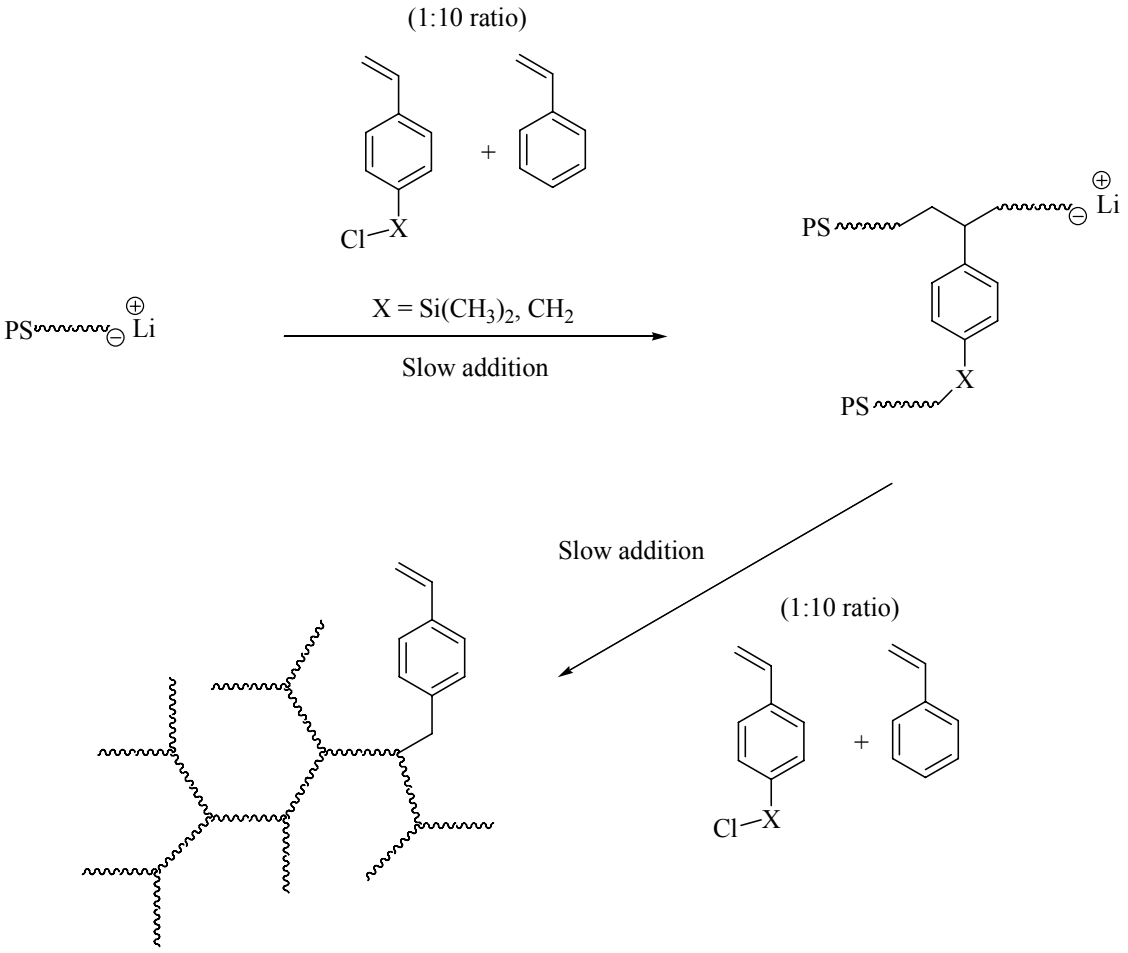

Scheme 2.10 Synthesis of dendritic polystyrene by convergent anionic polymerization.

2.3 Polyelectrolytes

Polyelectrolytes are polymers containing ionic groups covalently bonded either directly to the backbone or to a pendent group. These materials can be defined as polyanions, polycations, or polyampholytes, depending on whether the polymer-bound ions are anionic, cationic, or a mixture of anionic and cationic functionalities. Since the behavior of polyampholytes is complicated by the fact that both ion types are bonded to the polymer, the subsequent discussion will be limited to the properties of polyanions and polycations. In solution, polyelectrolytes can dissociate to different extents into polyvalent macroions

(polyions) and a large number of small ions of opposite charge (counterions), always present in equivalent amount by the condition of electroneutrality. The high charge density of the macroion produces a strong electric field that attracts the counterions, leading to counterion condensation (fixation). The strong electrostatic interactions between the charges on the polyion and with the counterions are at the origin of the characteristic properties of polyelectrolytes. Most macroions are long flexible chains with a coiled structure in solution, but their size depends strongly on the net charge on the backbone and the interactions with counterions. For increasing charge density along the backbone uncompensated by closely associated counterions, the ions along the chain repel each other intramolecularly and cause expansion of the coiled molecule. This correlation between the molecular conformation and the electric charge density is believed to be at the origin of many of the characteristic properties of polyelectrolytes. Since the interactions among ionic groups are amplified by their close proximity along the chain, a small difference in interactions due to changes in solvent or counterion, or the presence of salts may have a huge influence on the properties of polyelectrolytes.[61] One major factor controlling the solution properties of polyelectrolytes is the balance between intramolecular and intermolecular interactions. Intramolecular interactions typically dominate at low polymer concentrations, while intermolecular interactions dominate at higher concentrations.[62] Another property characteristic of polyelectrolytes concerns the influence of simple electrolytes (added salts), which screen the electrostatic interactions between the macroion and the counterions.

Systematic studies of polyelectrolyte solutions have been carried out, more commonly in aqueous solutions than in non-aqueous media.[63] This is partly because of the strong interest in naturally occurring polyelectrolytes such as proteins, nucleic acids, and polysaccharides, and

partly because many polyelectrolytes are insoluble even in polar organic solvents in their ionized state.[63] Nonetheless, the study of polyelectrolytes in non-aqueous solutions is important because it can offer insight into the fundamental understanding of polyelectrolytes. This is because the electrostatic interaction energy varies inversely with the dielectric constant of the medium. Water is a very polar compound (dielectric constant $\varepsilon = 80$), whereas ε varies widely for organic solvents. The influence of electrostatic interactions on the solution behavior of polyelectrolytes can be thus investigated by varying the solvent used in the measurements. Furthermore, water is a complex solvent dissociating partly to small ions (H^+ and OH^-) that can act like added salts and affect the behavior of salt-free solutions.[63] Consequently, the investigation of polyelectrolytes in non-aqueous solutions provides information applicable to a wider range of conditions than those encountered in aqueous media.[63]

The study of polyelectrolytes in non-aqueous solutions has yielded a large body of literature, and a detailed review of this field is beyond the scope of the present overview. Since the primary goal of this section is to provide some basic information about the properties of polyelectrolyte solutions, the discussion will be limited to the viscosity of these materials in non-aqueous solutions. For convenience, the discussion starts with linear polyelectrolytes and is then extended to branched systems. The emphasis is set on the degree of ionization and the influence of the dielectric constant of the solvent on viscosity. In cases where the behavior in non-aqueous solutions is unknown, examples are also provided for aqueous solutions.

2.3.1 Viscosity of Salt-free Polyelectrolyte Solutions

According to the Huggins equation[64] for a neutral polymer solution, a plot of the reduced viscosity (η_{sp}/C) against concentration (C) yields a straight line: according to Equation 2.1.

$$\eta_{sp}/C = [\eta] + k'[\eta]^2 C \quad (2.1)$$

The specific viscosity η_{sp} is defined as $(\eta-\eta_0) / \eta_0$, where η and η_0 are the viscosities of the solution and the solvent, respectively, $[\eta]$ is the limiting (intrinsic) viscosity, and k' is the Huggins constant, which is a measure of solvent quality. The intrinsic viscosity is related to the hydrodynamic volume of the molecules. The solution viscosity of neutral polymers is generally lower than for polyelectrolytes of comparable molecular weight.

Polyelectrolyte research starting from the 1950s can be used to illustrate the main features of these materials. The viscosity behavior of a polyelectrolyte obtained by quaternization of a styrene/4-vinylpyridine copolymer with *n*-butyl bromide[65] shown in Figure 2.2 is typical of linear polyelectrolytes in non-aqueous solutions. Three different compositions of nitromethane-dioxane mixtures were used in the experiments to vary the dielectric constant ε within the 23.1 – 39.4 range. It is clear that the reduced viscosity of the polyelectrolyte solution increases with the solvent polarity and is much higher than for the parent polymer. The strong upward curvature of the reduced viscosity plots contrasts with the linear plots obtained for neutral polymer solutions. The upturn in the viscosity curve is more pronounced for higher weight ratios of nitromethane (i.e. increasing ε), illustrating the influence of the dielectric constant. Two fundamental polyelectrolyte concepts, namely counterion condensation and chain expansion due to intramolecular repulsive forces, are used to explain the characteristics observed in Figure 2.2. For higher dielectric constant solvents the electrostatic interaction energy between the polyion and the counterions decreases, which

suppresses counterion condensation or increases the net charge of the polyion. With increasing charge density, the ionic charges along the polyion chain repel each other and lead to chain expansion. The reduced viscosity thus increases with the dielectric constant of the solvent. The increase in reduced viscosity at lower polyelectrolyte concentrations can also be viewed as a consequence of the increased free volume available to the molecules, favoring the dissociation of the condensed ions from the polyions and promoting coil expansion.

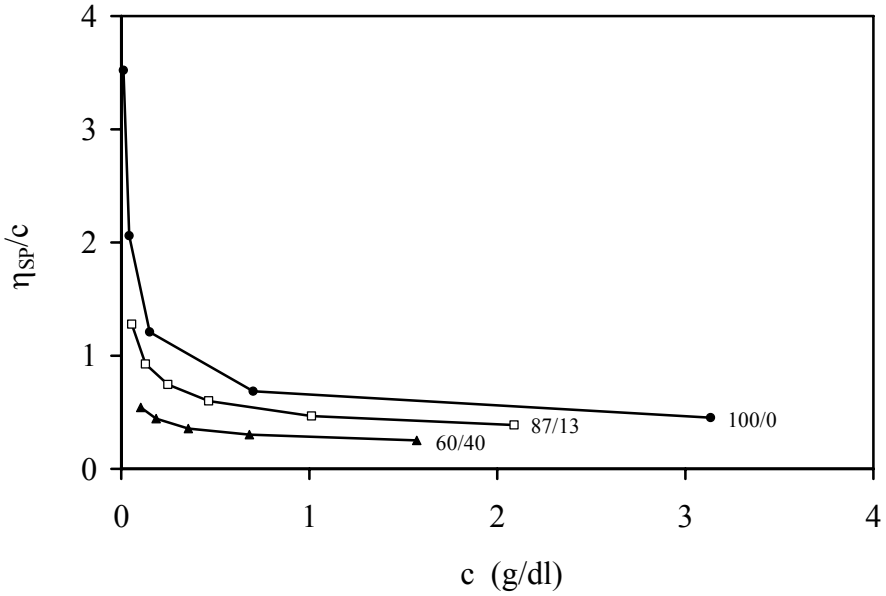

Figure 2.2 Reduced viscosity curves for 4-vinylpyridine/styrene copolymer quaternized with *n*-butyl bromide in nitromethane-dioxane mixtures (the numbers are the weight ratios).[65]

Another example is provided below to illustrate the influence of the dielectric constant of different solvents on the reduced viscosity of polyelectrolytes, in this case for poly(2-vinylpyridine) partially quaternized with methyl bromide and *n*-butyl bromide. The solvents used were methanol, ethanol, nitromethane, and water.[66] Typical polyelectrolyte behavior is again observed, the reduced viscosity increasing with the dielectric constant of the solvent

(Figure 2.3). Similar effects were also reported for poly(4-vinylpyridine) quaternized with *n*-butyl bromide in ethanol-water mixtures[67] and for poly(4-vinylpyridine) protonated with hydrogen chloride in methanol.[68]

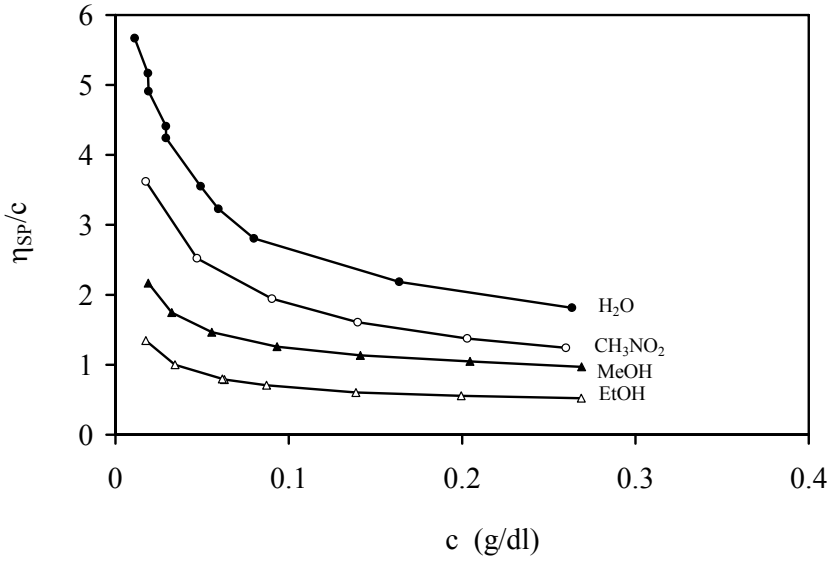

Figure 2.3 Reduced viscosity of poly(2-vinylpyridine) partially quaternized with *n*-butyl bromide in different solvents.[66]

The studies described so far used linear polyelectrolytes to elucidate the basic characteristics of these systems and the influence of the dielectric constant of the solvent. Another family of ion-containing polymers also investigated extensively in non-aqueous solutions is the ionomers, which are copolymers containing typically less than 10-15% of ionic units. For example, random copolymers consisting of partly sulfonated polystyrene with ion contents reaching up to 5.6 mol% (5.6 % sodium styrenesulfonate units per 100 monomer units on average) were investigated in DMF (Figure 2.4).[62] It is clear that while the reduced viscosity increases even at very low ion contents (e.g. 0.94 mol %) in analogy to polyelectrolytes, the upturn is more pronounced for higher ion contents. Even though the main

characteristics of ionomer solutions are similar to those of polyelectrolytes, the significant reduced viscosity increase observed at low charge densities is rarely seen for polyelectrolytes, because it is difficult to achieve a low charge density in these systems simply by controlling the degree of neutralization in salt-free polyelectrolyte solutions. Similar polyelectrolyte behavior was also reported for the sodium salts of sulfonated polystyrene ionomers in DMSO and in α-methoxyethanol.[69] Other ionomer viscosity investigations in nonaqueous solutions including styrene-methacrylic acid copolymers in DMF[70] and *n*-butylmethacrylate-methacrylic acid copolymers in DMF[71] led to conclusions similar to the sulfonated polystyrene ionomers.

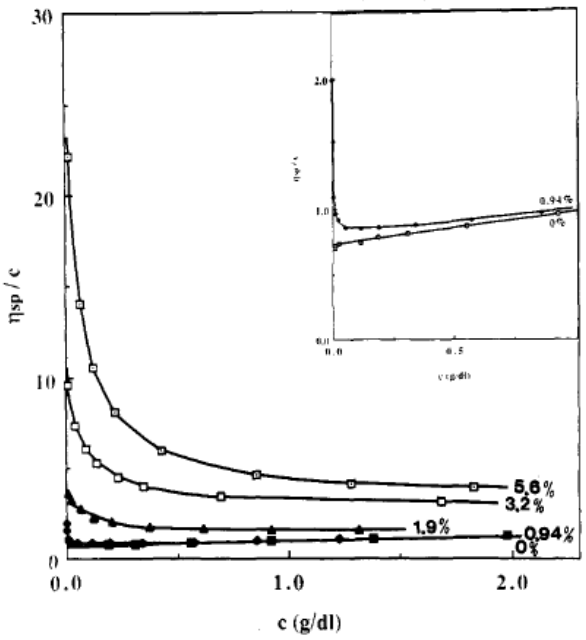

Figure 2.4 Viscosity curves for sulfonated polystyrene ionomers ($M_w = 4.0 \times 10^5$; Na salt) in DMF with ion contents as indicated.[62]

Ionomers are also known to aggregate in low polarity solvents,[62,69] leading to the typical behavior shown in Figure 2.5 for the sodium salts of partially sulfonated polystyrenes in THF (ε = 7.6). Two striking features of this system are that the reduced viscosity in the low

concentration range is lower for the ionomers than for the parent polystyrene from which they were derived, and that strong curvature is present in the high concentration range. This can be explained in terms of the counterion condensation effect described earlier. The electrostatic interaction energy being much higher in low polarity solvents, dissociation of the counterions is suppressed (counterion condensation is favored) and the ion pairs formed further coalesce into ionic aggregates. This leads to lower intramolecular repulsion forces and to ionomer chain contraction. Correspondingly, the reduced viscosity of the ionomer solutions is lower than for the parent polystyrene sample. On the other hand, intermolecular association dominates at high polymer concentrations and the reduced viscosity is again larger than for the parent polystyrene. This explains why while the viscosity decreases for increasing ion contents at low polymer concentrations, the upturn at high concentrations also increases with the ion content.

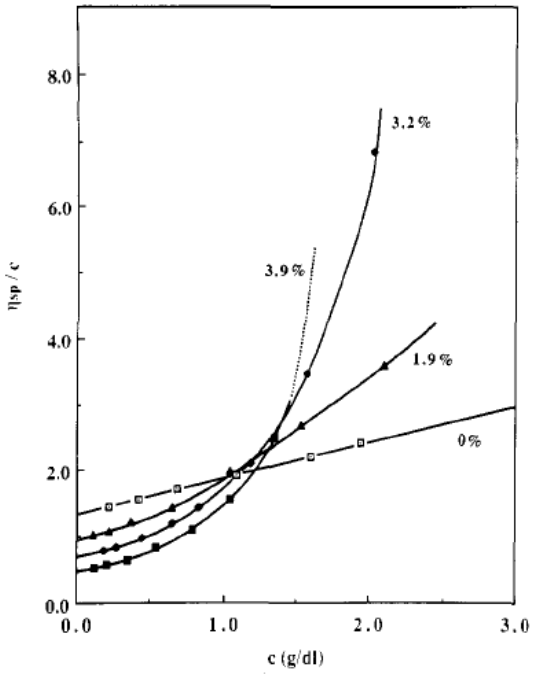

Figure 2.5 Viscosity in THF of sulfonated polystyrene ionomers (M_w = 4.0 × 10^5; Na salt) with ion contents as indicated.[62]

Another characteristic of ion-containing polymer solutions (ionomers and polyelectrolytes) concerns the effect of added salts on viscosity, illustrated in Figure 2.6 for the lithium salt of sulfonated polystyrene in DMF with added LiCl.[72] The reduced viscosity of the ionomer solutions in the low concentration range is suppressed dramatically even at very low salt concentrations (e.g. 10^{-4} M), a maximum appearing in the viscosity curve. At salt concentrations of 10^{-3} M and above, linear scaling of the reduced viscosity with concentration is observed, in analogy to neutral polymers. Again, counterion condensation and chain expansion due to intramolecular repulsion can be used to explain this phenomenon. In the presence of salts, the dissociation equilibrium is shifted to the condensed counterion state and the net charge of the polyion decreases, leading to decreased intramolecular repulsion and contraction of the polymer chain. More recently, screening of the electrostatic interactions between the polymer-bound ions by the salt ions has also been invoked to explain the added salt effect.[73]

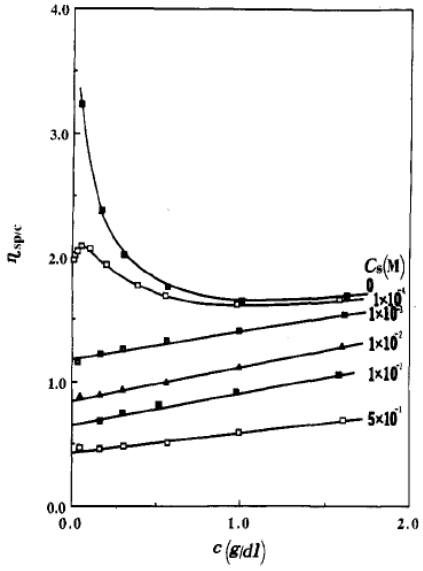

Figure 2.6 Viscosity of sulfonated polystyrene ionomers (M_w = 4.0 × 10^5; Li salt) in DMF at various LiCl concentrations as indicated.[72]

The polyelectrolyte behavior was also investigated for block copolymers of polystyrene and poly(1-azabicyclooctane[4,2,0]) in DMF with the amine moieties either protonated or alkylated.[74] Several organic acids including *p*-toluenesulfonic acid were used for protonation, whereas alkyl iodides served for quaternization. The block copolymers exhibited typical polyelectrolyte behavior (Figure 2.7), even though the magnitude of the effects was much more important for the methyl iodide-quaternized homopolymer (V128) than for the block copolymers (V124, V125) and the protonated sample (V123, M_n = 19800 and 21000 for the polystyrene and the polyamine blocks, respectively). There was no apparent correlation between the molecular weight of the polyelectrolyte block and the intrinsic viscosity. When comparing viscometric data for the homopolymer and the block copolymers at the same concentrations, the ionic strength is necessarily lower for the latter. If the polyelectrolyte block alone affects the solution properties, the copolymers should exhibit a stronger polyelectrolyte effect than the homopolymer. The results obtained show an opposite trend, suggesting that the polystyrene block hinders the expansion of the polyelectrolyte block. The much less pronounced polyelectrolyte effect observed for the protonated copolymer was attributed to the reversibility of the protonation reaction. Residual acid can ionize and act like an added salt, screening the electrostatic interactions.

Hyperbranched polyesters with terminal carboxylic acid groups were investigated recently after conversion to their water-soluble ammonium and sodium salts.[75] These samples also displayed an increase in reduced viscosity at low polymer concentrations, the effect being suppressed by added salts. Unfortunately no comparison could be done with a linear analogue, nor was the behavior of these polymers investigated in non-aqueous solutions.

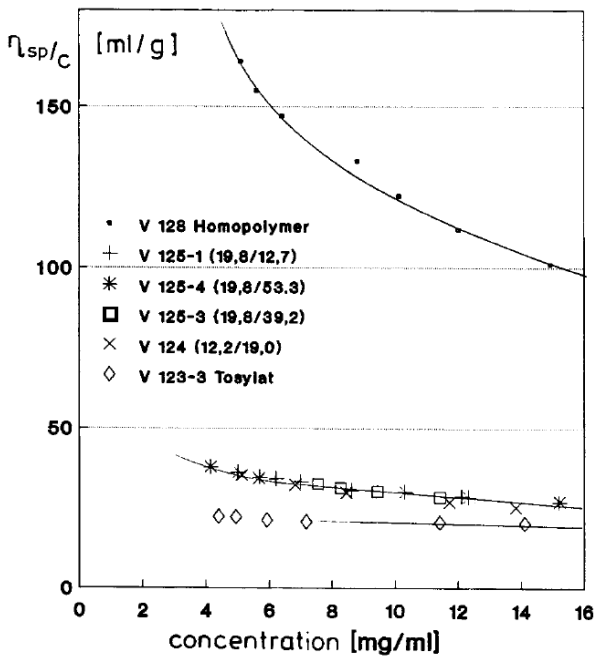

Figure 2.7 Viscosity of poly(1-azabicyclooctane[4,4,0]) homopolymer quaternized with methyl iodide (V128, M_n = 1.1 × 10^5), a block copolymer protonated with *p*-toluenesulfonic acid (V123-3, M_n = 19800 and 21000 for the polystyrene and the polyamine blocks, respectively), and different block copolymers in DMF at 25 °C (the numbers in brackets are $M_n \times 10^{-3}$ for the polystyrene and the polyamine blocks).[74]

The dilute aqueous solution properties of star-branched polyelectrolytes were likewise investigated recently.[76] The systems examined included four- and six-arm star-branched polyacrylates in their sodium, cesium, and rubidium salt forms (PANa, PACs, PARb). The reduced viscosity of the star-branched polyelectrolytes was compared with that of linear analogues. The results obtained for the Na salts (Figure 2.8) were similar for the Cs and Rb samples. The reduced viscosity is enhanced at low concentrations, chain expansion being more pronounced for the linear polyacrylate than for the star molecules of comparable molecular

weight. The maximum in the reduced viscosity is found at the same polyelectrolyte concentrations for the linear and the star polyelectrolytes carrying the same counterion.

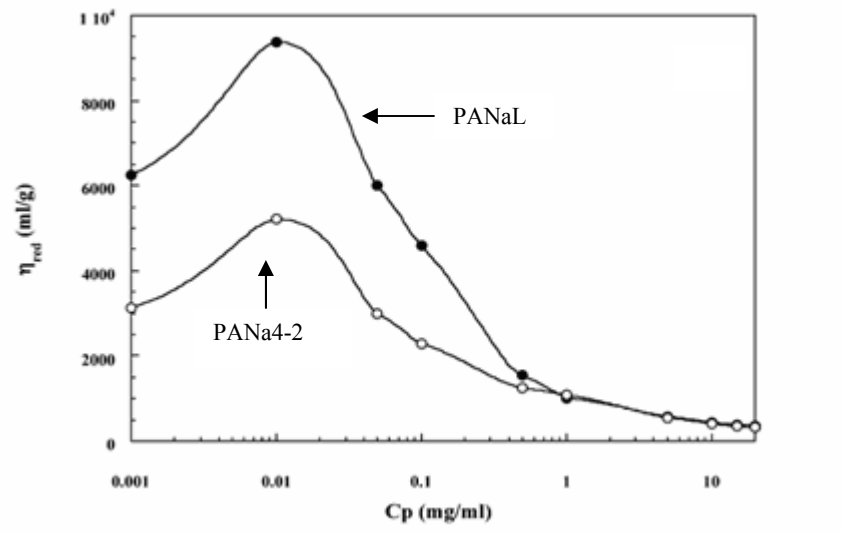

Figure 2.8 Comparison of reduced viscosity in aqueous solutions for 4-arm sodium polyacrylate (PANa4-2, M_n = 77613) and linear sodium polyacrylate (PANaL, M_n = 75302).[76]

The appearance of a maximum may be due to the presence of residual ionic impurities.[77] The position of the maximum was indeed also found to be independent of molecular weight by Cohen et al. in their studies of sulfonated polystyrene.[78] This indicates that the viscosity maximum does not arise from intermolecular entanglements. Furthermore, the peak position is very sensitive to the presence of free ions from excess salts or acid, which implies that its origin is related to the electrostatic interactions. This leads to the following qualitative interpretation of the occurrence of a maximum in the reduced viscosity curve: As the polyelectrolyte solution is diluted with a solvent contaminated with a trace amount of residual salt the total ionic strength, which is a combination of contributions from the polyion, the counterions, and the salt contaminant in the solvent, decreases. At very low polyelectrolyte concentrations, however, since the contributions from the polyion and the counterions become

very small, the contribution from the salt contaminant becomes significant and sufficient to induce ion condensation, and the polymer chain contracts.

The reduced viscosity of the polyacrylates was also compared in terms of the overall molecular weight and the number of arms in the stars (Figure 2.9). At constant branching functionality, the reduced viscosity decreased for decreasing overall molecular weights (i.e. for decreasing arm size); at constant overall molecular weight, the reduced viscosity also decreased for increasing branching functionality (again for shorter arms). This was attributed to the lower degree of freedom of the chains in the star polymers for increasing branching functionalities and for shorter, stiffer side chains.[76]

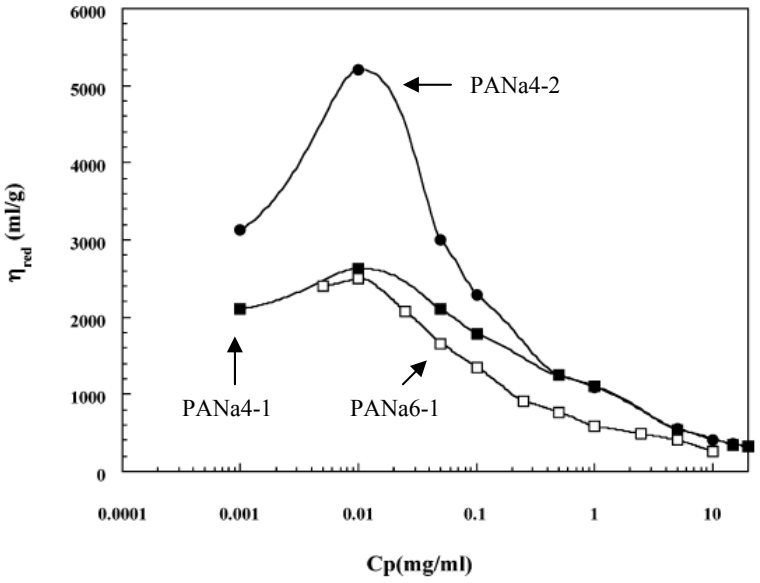

Figure 2.9 Comparison of reduced viscosity in aqueous solutions for 4-arm sodium polyacrylates (PANa4-1, M_n = 56614; PANa4-2, M_n = 77613) and 6-arm sodium polyacrylate (PANa6-1, M_n = 57856).[76]

Molecular expansion due to ionic forces was very briefly examined for arborescent polystyrene-*graft*-poly(2-vinylpyridine) copolymers using dynamic light scattering

measurements in dilute solutions to clarify the influence of structure. The ionization of the 2-vinylpyridine units was achieved by dissolving the samples in methanol acidified with HCl, for comparison to the neutral polymers in methanol.[44] The excess HCl present ensured screening of the intermolecular interactions. The hydrodynamic volume expansion factor, expressed as the ratio of hydrodynamic volume in methanol-HCl (ionized) to that in pure methanol (neutral), was compared for linear P2VP samples and for two series of arborescent poly(2-vinylpyridine) copolymers with either short ($M_w \approx 5000$, P2VP5) or long ($M_w \approx 30\,000$, P2VP30) side chains (Figure 2.10).

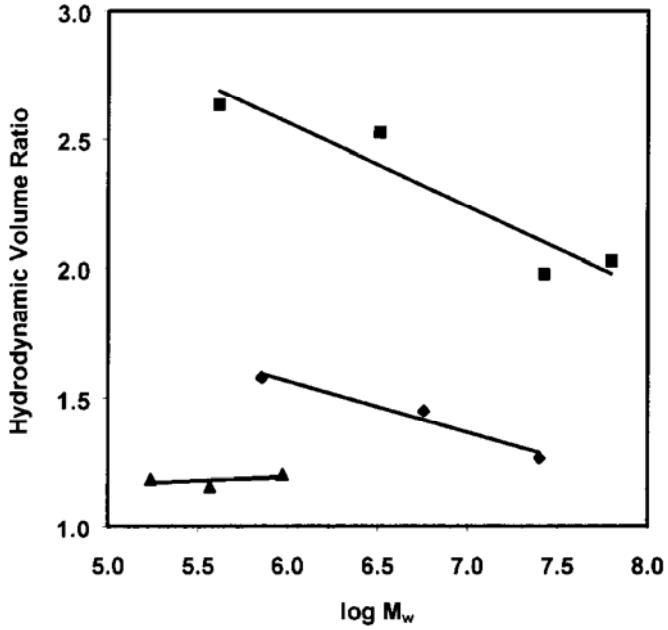

Figure 2.10 Molecular weight dependence of hydrodynamic volume expansion: (▲) linear P2VP; (♦) GxPS-P2VP5 copolymers; (■) GxPS-P2VP30 copolymers (x = 0, 1, 2, 3). Volume expansion is expressed as the ratio of hydrodynamic volumes in acidic methanol (ionized) and in pure methanol (neutral).[44]

Much larger expansion ratios observed for the branched copolymers than for the linear P2VP samples were attributed to the increased charge density and electrostatic repulsions within the branched molecules. The largest expansion ratios were observed for the copolymers with the long, flexible (P2VP30) side chains. Interestingly, the volume expansion ratio decreased for higher generations within each copolymers series, most likely due to enhanced structural rigidity. Since molecular expansion due to electrostatic repulsion forces is opposed by the elastic deformation forces for the molecules, the latter should be more important for the higher branching functionality, more rigid macromolecules.

2.4 Emulsion Polymerization

Polymeric microspheres have found a wide range of applications in analytical chemistry, biology, biomedicine, and in separation techniques such as chromatography.[79] Methods for the preparation of polymeric particles have been developed using suspension, dispersion, and emulsion polymerization. Suspension polymerization typically produces large particles in a size range from 50 μm to several mm, with a broad size distribution. Dispersion polymerization was developed to synthesize particles of uniform size but uses an organic solvent as the continuous phase, which causes some environmental concerns. The fact that emulsion polymerization takes place in aqueous dispersion media partly explains its increasing popularity. The reactions can be carried out with or without emulsifiers, to obtain submicron-sized particles of uniform size.

Emulsion polymerization was developed during World War II for the large scale production of synthetic rubber from 1,3-butadiene and styrene. Since then emulsion polymerization has been applied to the production of a wide range of polymeric products from

engineering plastics to architectural coatings.[80] Emulsion polymerization relies mainly on free radical reactions, and can be performed by different methods known as 'batch', 'semi-continuous', and 'continuous' polymerization processes. The batch process is simplest and refers to a polymerization where all the ingredients are charged in the reactor at the beginning of the reaction and removed at the end. This can be problematic for copolymerization reactions, since differing comonomer reactivity ratios can lead to highly heterogeneous products. In the semi-continuous process, some of the ingredients (e.g. one or both comonomers) are added over the course of the reaction. If the addition rate of the monomer(s) is slower than the polymerization rate, this becomes the rate-limiting step and the reaction is said to be starve-fed. In the continuous process, reactants are added and the reaction mixture is removed simultaneously from the reaction.

The most popular model for emulsion polymerization, proposed by Harkins,[81] explains the formation of particles in a reaction where an emulsifier (surfactant) is used to disperse the monomer phase. The emulsifying agents or surfactants, small molecules possessing a hydrophilic polar head and a hydrophobic tail, play a central role in this model. Harkins considers an emulsifier solution in water initially containing a water-insoluble monomer and a water-soluble initiator, paying attention to the presence of each species in the various phases of the heterogeneous reaction. The emulsifier molecules is partitioned in the aqueous phase, at the surface of monomer droplets, and as micelles swollen by monomer (Figure 2.11). The latter form when the surfactant concentration lies above a certain minimum value known as the critical micelle concentration (CMC).

Free radicals are produced in the aqueous phase either through a redox reaction or by thermal decomposition of the water-soluble initiator. During the first stage of the

polymerization process, the initiating radicals (primary radicals or oligomeric radicals formed by initiation in the aqueous phase) enter the monomer-swollen micelles and start the reaction.

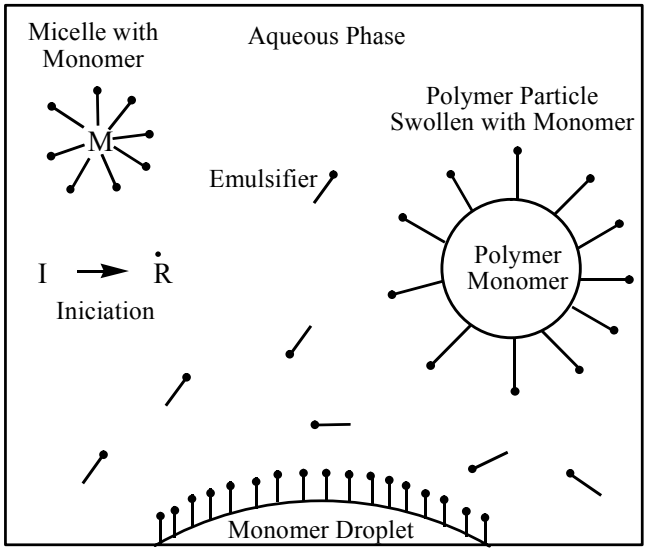

Figure 2.11 Harkins' model for emulsion polymerization.

The polymerization takes place predominantly in the micelles rather than the monomer droplets, due to the very high surface area of the micelles making radical capture by these species much more likely. Following initiation, monomer diffuses from the droplets into the micelles as it is consumed in the polymerization reaction. The polymer particles formed thus grow, become colloidally unstable, and undergo multiple coagulation events with other growing particles and micelles. The number of particles and micelles present decreases with time due to these coagulation events, to eventually stabilize by the end of the first stage of the reaction. During stage two, the polymerization proceeds within the particles by diffusion of the monomer from the monomer droplets and oligomeric radical entry from the water phase, and the rate of polymerization remains constant. The end of stage two is defined by the

disappearance of the monomer droplets. Stage three is characterized by a decreasing rate of polymerization, due to the fact that the concentration of monomer within the particles decreases with time, since the monomer droplets have disappeared. The kinetics of emulsion polymerization has been quantified,[82] however a comprehensive review of this topic is beyond the scope of this thesis.

2.4.1 Surfactant-free Emulsion Polymerization

The polystyrene latex particles used for the synthesis of model filler particles grafted with polyisoprene chains in Chapter 6 were synthesized by the surfactant-free emulsion polymerization technique. For that reason, this variation of the classical emulsion polymerization technique is briefly reviewed. The surfactants added to impart colloidal stability to the latex particles in emulsion polymerization can affect the properties of the material. They can also interfere with subsequent modification reactions such as the anionic grafting reactions investigated in Chapter 6. Post-polymerization removal of these surfactants is a tedious endeavor and generally leads to coagulation of the latex. For these reasons, a surfactant-free emulsion polymerization technique was used to produce particles stabilized by ionic groups covalently bonded to the surface of the particles.

Matsumoto and Ochi showed in 1965 that stable polystyrene latices could be obtained in the absence of surfactant, using potassium persulfate ($K_2S_2O_8$) to generate charged free radicals upon thermal decomposition.[83] This initiator not only initiates the free radical polymerization, but the sulfate ionic chain ends also impart electrostatic stabilization to the polymer particles in analogy to small molecule surfactants. The mechanism of surfactant-free polymerization is thought to involve four reaction steps similar to classical emulsion

polymerization, namely initiation, nucleation, coagulation, and particle growth. While the water solubility of most monomers is low, a small amount of monomer does dissolve in the aqueous phase, allowing the growth of oligomeric radicals.[84,85] These amphiphilic oligomers become increasingly hydrophobic as they grow and become insoluble in the reaction medium, so they tend to associate into micelles or adsorb onto growing latex particles, in analogy to surfactant molecules. A schematic illustration of the mechanism of surfactant-free emulsion polymerization is shown in Figure 2.12.

Cross-linked particles of uniform size have been obtained by emulsifier-free polymerization of various monomers including styrene, methyl methacrylate, and methacrylonitrile with divinyl monomers.[86-89] Notably, cross-linked spherical polystyrene particles with diameters from 200 ~ 800 nm could be obtained in a single reaction step.[86] Due to the initiation mechanism of surfactant-free emulsion polymerization the latex particles are still contaminated with spectator ions, ionic byproducts due to inefficient initiation, and surface-active oligomeric species.[90] The spectator ions are usually the counterions for the sulfate groups derived from the persulfate initiator [e.g. NH_4^+ from $(NH_4)_2S_2O_8$]. Byproducts due to inefficient persulfate initiation include residual persulfate ions ($S_2O_8^{2-}$) and bisulfate ions (HSO_4^-) resulting from the hydrolysis of the sulfate groups. Surface-active oligomers, also known as *in situ* surfactants, coexist with the latex particles throughout the polymerization.[91]

2.5 Rheology

Rheology is the science investigating the deformation and flow of matter. It is concerned with the response of materials to mechanical deformations. That response may be irreversible flow, reversible elastic deformation, or a combination of both.[92]

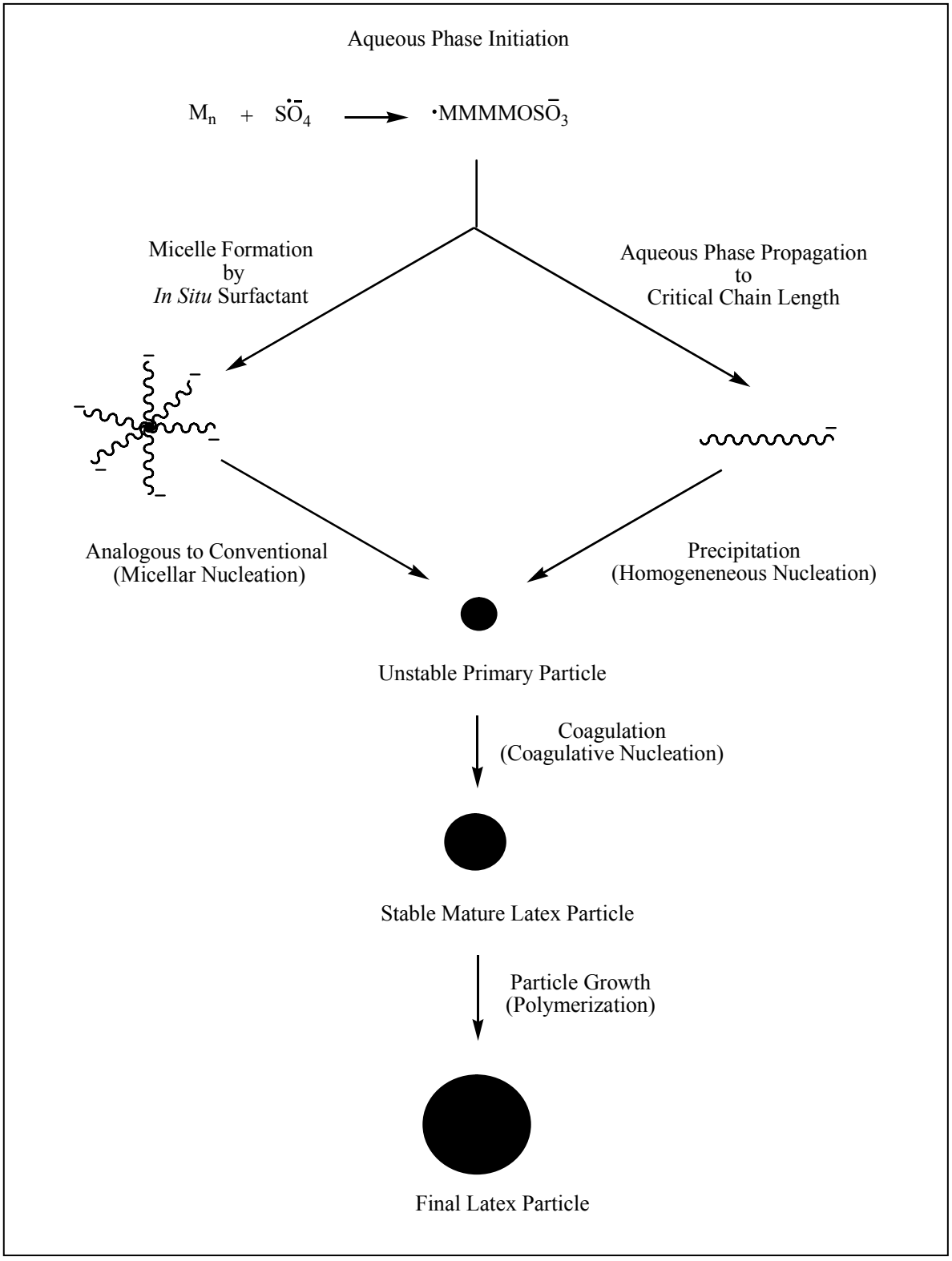

Figure 2.12 Schematic illustration of the surfactant-free emulsion polymerization mechanism.

2.5.1 Viscosity

A liquid is a material that continues to deform as long as it is subjected to a tensile or shear stress. For a liquid under shear the rate of deformation or shear rate is proportional to the shearing stress applied. The original expression of this relationship is Newton's law, stating that the ratio of the stress to the deformation rate is a constant defined as the viscosity. According to Newton's law, viscosity is independent of shear rate, which is true for ideal or Newtonian liquids. The viscosity of many liquids (including most polymers) depends on the shear rate, and these are accordingly called non-Newtonian liquids. These materials most commonly exhibit shear thinning (a decrease in viscosity for increasing shear rates), whereas others display shear thickening. Some liquids also behave like elastic solids until the shear stress exceeds a certain value (the yield stress), after which they flow readily. Some commonly observed flow behaviors are illustrated on Figure 2.13 as the dependence of shear stress on the shear rate. These plots are called flow curves and are frequently used to illustrate the rheological behavior of liquids. Newtonian flow corresponds to a straight line, and curvature is observed for shear thinning and thickening. A yield stress corresponds to a non-zero intercept on the y-axis.

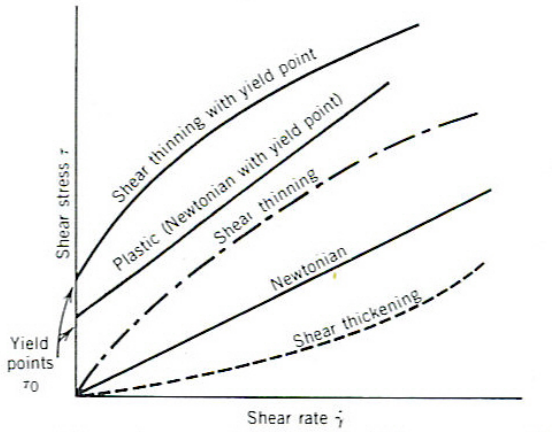

Figure 2.13 Flow curves for different types of materials.[92]

2.5.2 Elasticity and Viscoelasticity

The magnitude of an elastic deformation is a function of the applied stress and is expressed in terms of relative changes in dimensions (volume or length), depending on the nature of stress. An ideal elastic or Hookean solid[92] is a material deforming reversibly and for which the strain (deformation) is proportional to the applied stress according to Hooke's Law, with immediate recovery of the original shape when the stress is released. The proportionality constant K between the stress σ and the strain ε in Equation 2.2 is called the elasticity modulus.

$$\sigma = K\,\varepsilon \tag{2.2}$$

For homogeneous, isotropic solids, three moduli may be defined. Young's modulus E relates the tensile stress to the tensile strain. The shear modulus G relates the shear stress to the shear strain. The bulk modulus B relates the change in volume to the hydrostatic pressure.

Polymers and their solutions often display both elastic and viscous character to different extents. Because a complex rheological response is difficult to visualize, mechanical models are often used to represent the viscous response to applied stress. Thus a perfectly viscous material (Newtonian fluid) is represented by a dashpot (a piston in a cylinder filled with the Newtonian fluid), while the elastic response is represented by a spring. The dashpot represents the dissipation of energy as heat, whereas the spring represents energy storage.

2.5.3 Dynamic Mechanical Behavior

By subjecting a specimen to an oscillatory stress and monitoring the time-dependent deformation (response), information on both the elastic and viscous (damping) characteristics of the material can be obtained. Elastic materials store energy, i.e. they convert mechanical work into recoverable potential energy. Because an elastic material recovers instantly from a

deformation, the stress and strain signals are in phase with each other. Liquids, in contrast, do not store energy when deformed but rather dissipate it as heat while flowing. This results in highly damped motions, and the strain is out of phase with the applied stress in the dynamic measurements. When a viscoelastic material is subjected to a cyclic stress such as a sine wave (solid line in Figure 2.14), the deformation amplitude (strain) is proportional to the stress but lags the stress signal by some angle δ varying between 0 and 90° (dashed curve), depending on whether the material has more elastic or viscous character, respectively.

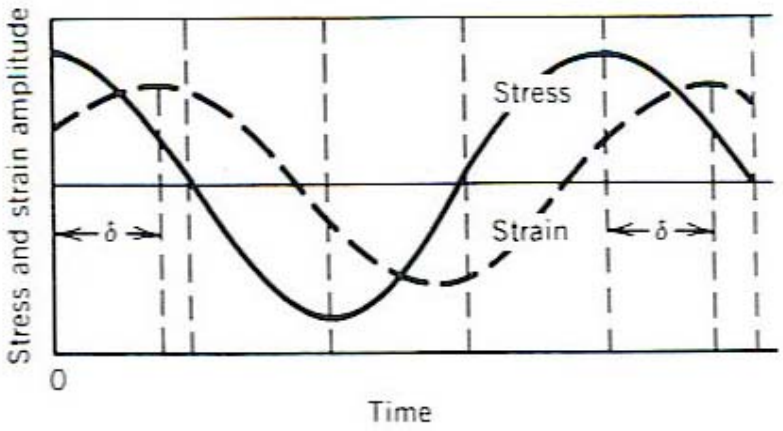

Figure 2.14 Time-dependent viscoelastic material response; δ is the lag angle for the strain curve. [92]

This behavior is usually represented by complex variables combinint the elastic and viscous contributions. The complex stress (τ*) and the complex strain (γ*) can be represented by Equations 2.3 and 2.4, respectively

$$\tau^* = \tau_0 e^{i\omega t} \tag{2.3}$$

$$\gamma^* = \gamma_0 e^{i(\omega t-\delta)} \tag{2.4}$$

where $i = \sqrt{-1}$, ω is the angular frequency ($\omega = 2\pi f$), and δ is the phase angle. The complex strain and stress can be resolved into their real (in phase) and imaginary (90° out-of-phase) components using Equations 2.5 and 2.6, respectively.

$$\gamma^* = \gamma' + i\gamma'' \tag{2.5}$$

$$\tau^* = \tau' + i\tau'' \tag{2.6}$$

The shear modulus can also be represented using complex variable notation, the complex dynamic modulus (G^*) being the ratio of the complex stress and the complex strain:

$$G^* = \tau^* / \gamma^* \tag{2.7}$$

The dynamic modulus can also be resolved into two components using Equations 2.8-2.9.

$$G' = |G^*| \cos\delta \tag{2.8}$$

$$G'' = |G^*| \cos\delta \tag{2.9}$$

The storage modulus (G') is linked to the in-phase components of γ^* and τ^*, and is a measure of elasticity. It is approximately equal to the elastic modulus determined in creep or stress relaxation experiments. The loss modulus (G'') is related to the out-of phase component of γ^* and τ^*, and is associated with viscous energy dissipation or damping. The ratio of G'' and G' is another measure of damping called the dissipation factor or loss tangent:

$$\tan\delta = G''/G' \tag{2.10}$$

Alternately the complex dynamic viscosity of a viscoelastic material, directly related to the storage and loss moduli, is defined by Equations 2.11-2.14.

$$\eta^* = \eta' + i\eta'' \tag{2.11}$$

$$\eta^* = G^*/i\omega \tag{2.12}$$

$$\eta' = G''/\omega \tag{2.13}$$

$$\eta'' = G'/\omega \tag{2.14}$$

2.5.4 Rheology of Filled Polymers

Plastics and rubbers are often mixed with solid particulates, either to enhance the mechanical properties (reinforcing fillers) or to reduce the cost of the materials (non-reinforcing fillers).[93-95] Different solids including carbon black, calcium carbonate, mica, and talc have been investigated as fillers,[94-96] but these often have a complex structure impeding the interpretation of the rheological results. For reinforcing fillers, the properties of the composites depend primarily on the interactions between the matrix and the filler particles (e.g. carbon black), although interparticle interactions are also important in some cases (e.g. silica fillers).[97] Consequently, the influence of these materials on the rheology of polymers can be very complex.[98,99] Strong interactions between the matrix polymer and the filler particles tend to increase the viscosity and the dynamic moduli, because strong adsorption of the polymer on the filler surface restricts chain mobility within the matrix. The nature and surface composition of the particles, as well as matrix properties such as the polarity and the molecular weight also influence the rheology of the mixtures.[98] Model fillers such as spherical glass beads and cross-linked polymer particles have been used to help understand the influence of these different parameters on the rheology of filled polymers.[96,98,100-102] While a comprehensive review of each variable is beyond the scope of the present work, the influence of particle-matrix interactions on rheology will be reviewed briefly using selected examples from the literature.

The composition of the filler and the matrix plays a critical role in the rheology of filled polymers.[101] Thus when both components are "chemically compatible", the filler particles can be dispersed uniformly within the matrix, and increases in viscosity and modulus are observed. The influence of filler composition on the rheological properties of filled polymers was explored using monodispersed particles (0.3 μm diameter) of different chemical compositions

including polystyrene (PS), vinylphenol-modified polystyrene (PSVP) crosslinked with divinylbenzene (DVB), and poly(methyl methacrylate) (PMMA) crosslinked with ethylene glycol dimethacrylate (EGDMA). The particles were synthesized by emulsifier-free emulsion polymerization. Blends of a low molecular weight liquid polysulfide (M_w = 8000) with the different fillers were investigated.[103] The dependence of the storage modulus G' and the complex dynamic viscosity η* on frequency are compared in Figure 2.15 for the different filler compositions. The filled polymers display reinforcement and shear thinning behavior to different extents, depending on the interactions between the filler particles and the matrix. The interactions between the PS particles and the polysulfide matrix being relatively weak dispersive forces, these particles are considered to be incompatible with the matrix. The interactions between the PMMA particles and the polysulfide matrix are mainly dipole-dipole interactions, and weak hydrogen-bonding interactions between the carbonyl groups of PMMA and the terminal mercaptan (-SH) groups of the polymer. The PSVP particles bearing phenol groups (PSVP05 and PSVP10 containing 5 and 10 mol % phenol moieties, respectively) have strong intermolecular hydrogen-bonding interactions with the polysulfide chains leading to significant matrix adsorption onto the particles. The strength of the interactions between the different fillers and the matrix should translate into corresponding increases in modulus and viscosity. The modulus and viscosity enhancement of the filled polysulfide indeed varies in the order PSVP > PMMA > PS, the more strongly interacting systems displaying the largest G' and η* values. While polar and hydrogen bonding interactions improve the filler dispersion, they also promote the adsorption of polymer chains on the surface of the particles. A network structure is thus formed consisting of particles with an immobilized polymer layer on their surface, each particle acting as a physical cross-linking site.

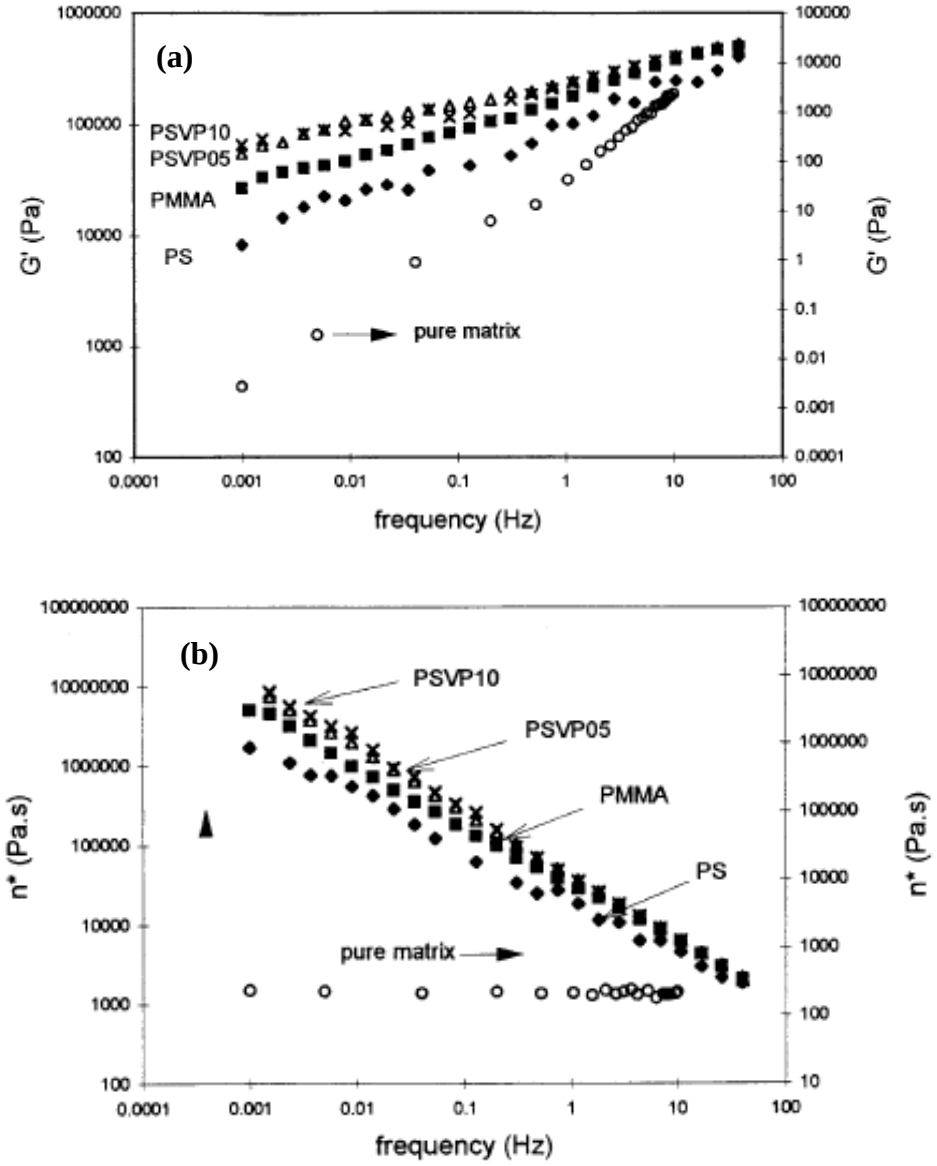

Figure 2.15 Storage modulus G' (a) and complex dynamic viscosity η* (b) of polysulfide blends with filler particles of different chemical compositions.[103]

Another approach to demonstrate a reinforcement effect was not based on physical interactions between the filler and the rubber matrix (as in the first example), but rather on chemical bonds formed by grafting the rubber matrix onto the surface of the filler particles during vulcanization.[104] A styrene-butadiene rubber (SBR) sample was thus mixed with cross-

linked PMMA lattices containing azo functions that decomposed thermally while processing the rubber, leading to covalent coupling of the particles with the unsaturated units of the SBR matrix. Reinforcement was very strong under these conditions as compared to unmodified PMMA particles (without azo groups). It was however found to be very difficult to achieve a uniform dispersion of the azo-modified PMMA particles due to their incompatibility with the matrix, and repetitive loading cycles led to a dramatic drop in tensile strength. This was attributed to breaking of some bonds between the filler and the matrix.

The problems encountered in the previous example were solved when using filler particles with a core-shell morphology, incorporating a highly cross-linked PMMA core and a polystyrene shell compatible with the matrix. The shell was added on the particles by emulsion polymerization using a *grafting from* method based on the azo-modified seed latexes.[105] The dynamic mechanical properties were compared for SBR matrix filled with the core-shell particles and with carbon black as a function of the deformation amplitude (% strain), as shown in Figure 2.16.

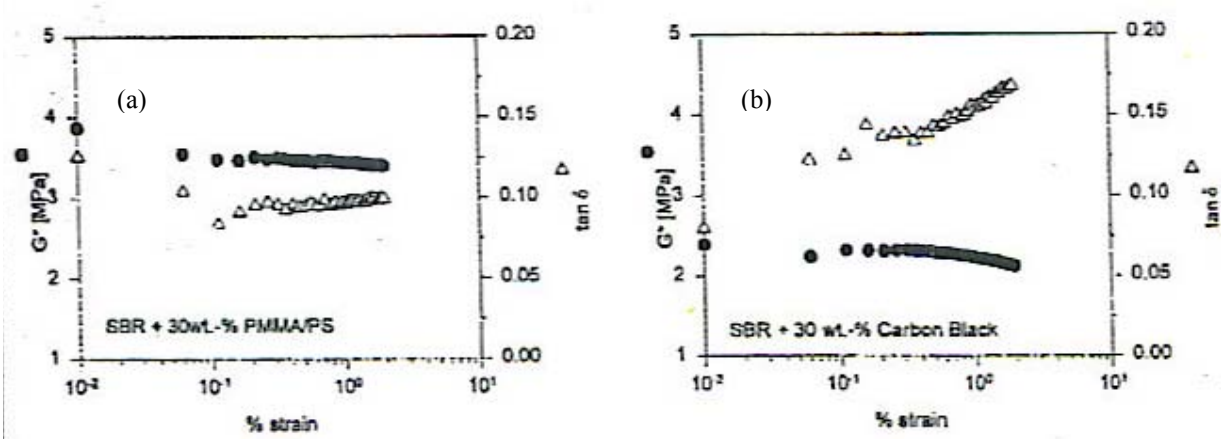

Figure 2.16 Dynamic modulus of cross-linked SBR filled with (a) 30 wt % PMMA/PS core-shell polymer and (b) 30 wt % carbon black.[105]

The storage modulus (G') remained constant for strains up to 2 % for both filled samples, but it was about 1.8 times larger for the core-shell filler. The loss tangent (tan δ) also remained constant for the core-shell filled elastomer within the same amplitude range, but decreased for the carbon black-filled sample in the low amplitude range. This confirms that the core-shell particles were better dispersed than the carbon black particles, and hence led to higher modulus values.[105]

The use of core-shell particles as fillers has also been investigated. Some other examples include a PMMA matrix in combination with cross-linked poly(butyl acrylate-*co*-styrene) particles incorporating a covalently grafted shell of PMMA,[106] and a polystyrene matrix in combination with cross-linked PMMA particles with a shell of covalently grafted carboxylic-acid terminated polystyrene chains.[107]

Considering the many examples available in the literature, core-shell polymers appear to be excellent as model systems to study the reinforcement of elastomers by fillers because their size, shape, and surface functionality can be controlled. This is particularly true when a matrix-compatible shell is covalently grafted onto highly cross-linked, rigid particles.

2.6 References

1. Roovers, J. In *Encyclopedia of Polymer Science and Engineering*, 2nd ed., Vol. 2; Kroschwitz, J. I. Ed.; Wiley: New York, 1985; p 478.
2. Rempp, P.; Franta, E.; Herz, J.-E. *Adv. Polym. Sci.* **1988**, *86*, 145.
3. Tomalia, D. A.; Naylor, A. M.; Goddard, W. A. *Angew. Chem., Int. Ed. Engl.* **1990**, *29*, 138.
4. Dvornic, P. R.; Tomalia, D. A. *Curr. Opin. Colloid Interface Sci.* **1996**, *1*, 221.

5. Newkome, G. R.; Moorefield, C. N.; Vögtle, F. *Dendritic Molecules*, *Concepts*, *Syntheses*, *Perspectives*; VCH: New York, 1996.

6. Majoral, J.-P.; Caminade, A.-M. *Chem*. *Rev*. **1999**, *99*, 845.

7. Kim, Y. H. *Adv*. *Mater*. **1992**, *4*, 764.

8. Voit, B. I. *Acta Polym*. **1995**, *46*, 87.

9. Tomalia, D. A.; Hedstrand, D. M.; Ferritto, M. S. *Macromolecules* **1991**, *24*, 1435.

10. Gauthier, M. In *Ionic Polymerizations and Related Processes*; Puskas, J. E., Ed.; NATO ASI Series E359; Kluwer Academic: Dordrecht, 1999, p 239.

11. Bayer, U.; Stadler, R. *Macromol*. *Chem*. *Phys*. **1994**, *195*, 2709.

12. Wang, F.; Roovers, J.; Toporowski, P. M. *Macromol*. *Symp*. **1995**, *95*, 255.

13. Hadjichristidis, N.; Pispas, S.; Pitsikalis, M.; Iatrou, H.; Vlahos, C. *Adv*. *Polym*. *Sci*. **1999**, *142*, 71.

14. Cloutet, E.; Filaut, J. L.; Astruc, D.; Gnanou, Y. *Macromolecules* **1998**, *31*, 6748.

15. Simms, J. A.; Spinelli, H. J. *J*. *Coat*. *Technol*. **1987**, *59*, 125.

16. Eschwey, H.; Burchard, W. *Polymer* **1975**, *16*, 180.

17. Lutz, P.; Rempp, P. *Makromol*. *Chem*. **1988**, *189*, 1051.

18. Tsitsilianis, C.; Lutz, P.; Graff, S.; Lamps, J. P.; Rempp, P. *Macromolecules* **1991**, *24*, 5897.

19. Quirk, R. P.; Tsai, Y. *Macromolecules* **1998**, *31*, 8016.

20. Comanita, B.; Noren, B.; Roovers, J. *Macromolecules* **1999**, *32*, 1069.

21. Hsieh, H. L. *Rubber Chem*. *Tech*. **1976**, *49*, 1305.

22. Quirk, R. P.; Kinning, D. J.; Fetters, L. J. In *Comprehensive Polymer Science*, Vol.7; Allen, G; Bevington, J. C. Eds.; Pergamon: New York, 1989; p 1.

23. Morton, M.; Helminiak, T. E.; Gadkary, S. D.; Bueche, F. *J. Polym. Sci.* **1962**, *57*, 471.

24. Zelinski, R. P.; Wofford, C. F. *J. Polym. Sci. Part A* **1965**, *3*, 93.

25. (a) Gervasi, J. A.; Gosnell, A. B. *J. Polym. Sci. Part A-1* **1966**, *4*, 1391. (b) Gervasi, J. A.; Gosnell, A. B. *J. Polym. Sci. Part A-1* **1966**, *4*, 1401.

26. Masuda, T.; Ohta, Y.; Onogi, S. *Macromolecules* **1971**, *4*, 763.

27. Roovers, J.; Bywater, S. *Macromolecules* **1972**, *5*, 384.

28. Roovers, J.; Bywater, S. *Macromolecules* **1974**, *7*, 443.

29. Roovers, J.; Hadjichristidis, N.; Fetters, L. J. *Macromolecules* **1983**, *16*, 214.

30. Hadjichristidis, N.; Roovers, J. *J. Polym. Sci., Part B: Polym. Phys. Ed.* **1974**, *12*, 2521.

31. Hadjichristidis, N.; Guyot, A.; Fetters, L. J. *Macromolecules* **1978**, *11*, 668.

32. Hadjichristidis, N.; Fetters, L. J. *Macromolecules* **1980**, *13*, 191.

33. Roovers, J.; Zhou, L. L; Toporowski, P. M.; van der Zwan, M.; Iatrou, H.; Hadjichristidis, N. *Macromolecules* **1993**, *26*, 4324.

34. Iatrou, H.; Hadjichristidis, N. *Macromolecules* **1993**, *26*, 2479.

35. Quack, G.; Fetters L. J.; Hadjichristidis, N.; Young R. N. *Ind. Eng. Chem. Prod. Res. Dev.* **1980**, *19*, 587.

36. Worsfold, D. J. *Macromolecules* **1970**, *3*, 514.

37. Pitsikalis, M.; Pispas, S.; Mays, J. W.; Hadjichristidis, N. *Adv. Polym. Sci.* **1998**, *135*, 1.

38. Dreyfuss, P.; Quirk, R. P. In *Encyclopedia of Polymer Science and Engineering*, Vol. 7; Kroschwitz, J. I. Ed.; Wiley: New York, 1987; p 551.

39. Rempp, P.; Lutz, P. In *Comprehensive Polymer Science*, Vol. 6; Eastmond, G. C.; Ledwith, A.; Russo, S.; Sigwalt, P. Eds., Pergamon: Elmsford, 1989; p 403.

40. Bywater, S. *Prog*. *Polym*. *Sci*. **1974**, *4*, 27.

41. Gauthier, M.; Möller, M. *Macromolecules* **1991**, *24*, 4548.

42. Li, J.; Gauthier, M. *Macromolecules* **2001**, *34*, 8918.

43. Kee, R. A.; Gauthier, M. *Macromolecules* **1999**, *32*, 6478.

44. Kee, R. A.; Gauthier, M. *Macromolecules* **2002**, *35*, 6526.

45. Li, J.; Gauthier, M.; Teertstra, S. J.; Xu, H.; Sheiko, S. S. *Macromolecules* **2004**, *37*, 795.

46. Gauthier, M.; Li, J.; Dockendorff, J. *Macromolecules* **2003**, *36*, 2642.

47. Langer, A. W. Jr. In *Polyamine Chelated Alkali Metal Compounds*; Langer, A. W. Ed.; Adv. Chem. Ser. 130; Am. Chem. Soc.: Washington, D.C, 1974; p 1.

48. Hsieh, H. L.; McKinney, O. F. *Polym*. *Lett*. **1966**, *4*, 843.

49. Tate, D. P.; Halasa, A. F.; Webb, F. J.; Koch, R. W.; Oberster, A. E. *J*. *Polym*. *Sci*. Part A-1 **1971**, *9*, 139.

50. Halasa, A. F.; Mitchell, G. B.; Stayer, M.; Tate, D. P.; Oberster, A. E.; Koch, R. W. *J*. *Polym*. *Sci*., *Polym*. *Chem*. *Ed*. **1976**, *14*, 497.

51. Hadjichristidis, N.; Roovers, J. *J*. *Polym*. *Sci*., *Part B*: *Polym*. *Phys*. *Ed.* **1978**, *16*, 851.

52. Falk, J. C.; Schlott, R. J.; Hoeg, D. F.; Pendleton, J. F. *Rubber Chem*. *Technol*. **1973**, *46*, 1044.

53. Hawker, C. J.; Fréchet, J. M. J. *J*. *Am*. *Chem*. *Soc*. **1990**, *112*, 7638.

54. Kee, R. A.; Gauthier, M.; Tomalia, D. A. *Dendrimers and Other Dendritic Polymers*. Fréchet, J. M. J.; Tomalia, D. A. Eds.; Wiley: New York, 2001; p. 212.

55. Yuan, Z.; Gauthier, M. *Macromolecules* **2005**, *38*, 4124.

56. Hempenius, M. A.; Michelberger, W.; Möller, M. *Macromolecules* **1997**, *30*, 5602.

57. (a) Kee, R. A.; Gauthier, M. *Am*. *Chem*. *Soc. Div*. *Polym*. *Chem*. *Prepr*. **1999**, *40(2)*, 165. (b) Kee, R. A. *Ph.D. Thesis*, University of Waterloo, Waterloo, **2001**.

58. Gauthier, M.; Tichagwa, L.; Downey, J. S.; Gao, S. *Macromolecules* **1996**, *29*, 519.

59. Knauss, D. M.; Al-Muallem, H. A.; Huang, T.; Wu, D. T. *Macromolecules* **2000**, *33*, 3557.

60. Knauss, D. M.; Al-Muallem, H. A. *J*. *Polym*. *Sci*. *Part A*: *Polym*. *Chem*. **2000**, *38*, 4289.

61. Dobrynin, A.V.; Rubinstein, M. *Prog*. *Polym*. *Sci*. **2005**, *30*, 1049.

62. Hara, M.; Wu, J.; Lee, A. H. *Macromolecules* **1988**, *21*, 2214.

63. *Polyelectrolytes: Science and Technology*; Hara, M. Ed.; Dekker: New York, 1993; p 193.

64. Huggins, M. L. *J*. *Am*. *Chem*. *Soc*. **1942**, *64*, 2716.

65. Fuoss, R. M.; Cathers, G. I. *J*. *Polym*. *Sci*. **1949**, *4*, 97.

66. Maclay, W. N.; Fuoss, R. M. *J*. *Polym*. *Sci*. **1951**, *6*, 511.

67. Fuoss, R. M.; Strauss, U. P. *J*. *Polym*. *Sci*. **1948**, *3*, 246.

68. Fuoss, R. M.; Maclay, W. N. *J*. *Polym*. *Sci*. **1951**, *6*, 305.

69. Lundberg, R. D.; Phillips, R. R. *J*. *Polym*. *Sci*. *Part B*: *Polym*. *Phys*. **1982**, *20*, 1143.

70. Hara, M.; Lee, A. H.; Wu, J. *J*. *Polym*. *Sci*. *Part B*: *Polym*. *Phys*. **1987**, *25*, 1407.

71. Niezette, J.; Vandershueren, J.; Aras, L. *J*. *Polym*. *Sci*. *Part B*: *Polym*. *Phys*. **1984**, *22*, 1845.

72. Hara, M.; Wu, J.; Lee, A. H. *Macromolecules* **1989**, *22*, 754.

73. Oosawa, F. *Polyelectrolytes*; Dekker: New York, 1971; Chapter 7.

74. Mühlbach, K.; Schulz, R. C. *Acta Polym*. **1995**, *46*, 130.

75. Turner, S. R.; Walter, F.; Voit, B. I.; Mourey, T. H. *Macromolecules* **1994**, *27*, 1611.

76. Moinard, D.; Borsali, R.; Taton, D.; Gnanou, Y. *Macromolecules* **2005**, *38*, 7105.

77. (a) Darskus, R. L.; Jordan, D. O.; Kurucsev, T.; Martin, M. L. *J. Polym. Sci., Part A* **1965**, *3*, 1941. (b) Hodgson, D. F.; Amis, E. J. In *Polyelectrolytes Science and Technology*, Hara, M. Ed.; Marcel Dekker: New York, 1993; p127.

78. Cohen, J.; Priel, Z.; Rabin, Y. *J. Chem. Phys.* **1998**, *88,* 7111.

79. (a) Ugelstad, J.; Mørk, P. C.; Schmid, R. ; Ellingsen, T. ; Berge, A. *Polym. Int.* **1993**, 30, 157. (b) Liang, Yi-C. ; Svec, F. ; Fréchet, J. M. J. *J. Polym. Sci. Part A: Polym. Chem.* **1995**, *33*, 2639.

80. Odian, G. *Principles of polymerization*, 3rd ed., Wiley: New York, 1991; Chapter 4.

81. Harkins, W. D. *J. Am. Chem. Soc.* **1947**, *69*, 1428.

82. Nomura, M.; Tobita, H.; Suzuki, K. *Adv. Polym. Sci.* **2005**, *175*, 1.

83. Matsumoto, T.; Ochi, A. *Kobunshi Kagaku* **1965**, *22*, 481. [Cited: (a) Gauthier, M.; Frank, P. C. *Reactive and functional Polymer*. **1996**, 31, 67. (b) Xu, X-J. ; Slow, K-S. ; Wong, M-K. ; Gan, L-M. *J. Polym. Sci. Part A: Polym. Chem.* **2001**, *39*, 1634.]

84. Shouldice, G. T.; Vandezande, G. A.; Rudin, A. *Eur. Polym. J.* **1994**, *30*, 179.

85. Gardon, J. L. In *Polymerization Processes*; Schildknecht, C. E. Ed.; Wiley: New York, 1977; Chapter 6.

86. Zou, D.; Derlich, V.; Gandhi, K.; Park, M.; Sun, L.; Kriz, D.; Lee, Y. D.; Kim, G.; Aklonis, J. J.; Salovey, R. *J. Polym. Sci. Part A Polym. Chem.* **1990**, *28*, 1909.

87. Zou, D.; Ma, S.; Guan, R.; Park, M.; Sun, L.; Aklonis, J. J.; Salovey, R. *J. Polym. Sci. Part A Polym. Chem.* **1992**, *30*, 137.

88. Ding, Z.; Ma, S.; Kriz, D.; Aklonis, J. J.; Salovey, R. *J*. *Polym*. *Sci*. *Part B Polym*. *Phys*. **1992**, *30*, 1189.

89. Zou, D.; Aklonis, J. J.; Salovey, R. *J*. *Polym*. *Sci*. *Part A Polym*. *Chem*. **1992**, *30*, 2443.

90. Wang, Z.; Paine, A. J.; Rudin, A. *J*. *Polym*. *Sci*. *Part A Polym*. *Chem*. **1995**, *33*, 1597.

91. Hergeth, W. D.; Lebek, W.; Kakuschke, R.; Schmutzler, K. *Makromol*. *Chem*. **1991**, *192*, 2265.

92. *Polymers: Polymer Characterization and analysis*; Kroschwitz, J. I. Ed.; Wiley: New York, 1990; p 637.

93. Byers, T. J.; Wayner, M.P. In *Rubber Technology*, 3rd ed; Morton, M. Ed.; Van Nostrand Reinhold: New York, 1987; Chapter 3.

94. Metzner, A. B. *J*. *Rheol*. **1985**, *29*, 739.

95. Kamel, M. R.; Mutel, A. *J*. *Polym*. *Eng*. **1985**, 5, 293.

96. Yilmazer, U.; Farris, R. J. *J*. *Appl*. *Polym*. *Sci*. **1983**, *28*, 3369.

97. Wolff, S.; Wang, M. *Rubber Chem*. *Technol*. **1992**, *65*, 329.

98. Agarwal, S.; Salovey, R. *Polym*. *Eng*. *Sci*. **1995**, *35*, 1241.

99. Zhu, J.; Ou, Y.; Feng, Y. *Polym*. *Int*. **1995**, *37*, 105.

100. Park, M.; Gandhi, K.; Sun, L.; Aklonis, J. J.; Salovey, R. *Polym*. *Eng*. *Sci*. **1990**, *30*, 1158.

101. (a) Sun, L.; Park, M.; Salovey, R. *Polym*. *Eng*. *Sci*. **1992**, *32*, 777. (b) Sun, L.; Park, M.; Salovey, R. *Polym*. *Eng*. *Sci*. **1992**, *32*, 1418.

102. Sun, L.; Aklonis, J. J.; Salovey, R. *Polym*. *Eng*. *Sci*. **1993**, *33*, 1308.

103. Cai, J. J.; Salovey, R. *J*. *Polym*. *Sci*., *Part B Polym*. *Phys*. **1999**, *37*, 815.

104. Nuyken, O.; Bayer, R. *Kautsch*. *Gummi Kunstst*. **1995**, *48*, 704.

105. Nuyken, O.; Ko, S.-K.; Voit, B.; Yang, D. *Kautsch*. *Gummi Kunstst*. **1995**, *48*, 784.

106. Bousmina, M.; Muller, R. *J. Rheol*. **1993**, *37*, 663.

107. Fahrländer, M.; Bruch, M.; Menke, T.; Friedrich, C. *Rheol*. *Acta* **2001**, *40*, 1.

Chapter 3

Synthesis of 1,4-Polybutadiene

Dendrimer – Arborescent Polymer Hybrids

3.0 Abstract

A divergent synthetic scheme was developed for the preparation of high branching functionality hybrid polymers from carbosilane dendrimer substrates and 1,4-polybutadiene side chains. Carbosilane dendrimers containing either 32, 64, or 128 peripheral Si-Cl functional groups were first coupled with 1,2-polybutadienyllithium chains with a number-average molecular weight $M_n \approx 1000$ and a narrow molecular weight distribution. The polybutadiene-grafted substrates were then hydrosilylated with dichloromethylsilane and reacted with high 1,4-microstructure content polybutadienyllithium chains to generate high branching functionality arborescent-dendrimer hybrids. Three series of hybrid polymers were synthesized containing 1,4-polybutadiene side chains with a number-average molecular weight $M_n \approx 1500$, 5000, or 30000. Size exclusion chromatography analysis of the polymers confirmed that a narrow molecular weight distribution was maintained ($M_w/M_n \leq 1.16$). The branching functionality of the arborescent hybrids varied from 140 − 335, 160 − 1115, and 360 − 2830 for the 32-, 64-, and 128-site coupling precursors, respectively. The experimental branching functionalities attained were lower than the theoretical values due to decreased coupling efficiency within each series, in particular for polymers with longer polybutadiene side chains, as a result of steric limitations in the grafting reaction.

3.1 Introduction

Branched polymers are of interest, among others, because of their peculiar physical properties[1-3] and their potential usefulness as rheological modifiers for other polymers.[4] Star-branched and arborescent (dendrigraft) polymers are two families of branched polymers of particular importance because their controllable architectures enable fundamental investigations of structure-property relations. The physical properties of these materials can be fine-tuned through variations in parameters such as their side chain molecular weight and composition, branching functionality, the presence of functional end groups, etc. The molecular weight distribution (MWD) of star-branched and arborescent polymers is often very narrow, because their synthesis typically relies on living polymerization techniques. As a result, these polymers are ideal for the elucidation of the influence of structural parameters on the molecular (polymeric) and intermolecular (colloidal) properties of branched polymers.

Different methods have been developed for the synthesis of star-branched polybutadienes, but the coupling reaction of living polybutadienyllithium chains with chlorosilane substrates is clearly most successful.[5] This technique was further extended to the synthesis of 32-, 64-, and 128-arm regular star polybutadienes by using dendrimers with chlorosilane functionalities as coupling substrates.[6,7] The method is highly versatile, but the dendrimeric coupling agents eventually restrict the growth of the molecules due to steric limitations and observed broadening of the MWD. Grafting of 1,4-polybutadiene chains onto an 18-arm 1,2-polybutadiene star-branched polymer hydrosilylated with dichloromethylsilane has also been explored for the synthesis of high branching functionality stars.[8] For a hydrosilylation level corresponding to 270 coupling sites per

substrate molecule, the branching functionality attained for the stars ranged from 180-200, corresponding to coupling efficiencies of 67-74%. A core-first strategy using dendrimeric initiators was also reported for the synthesis of 4-, 8-, and 16-arm star polymers.[9] When a narrow MWD is required, this method is only practical if a rapid exchange exists between active and dormant propagating centers. Evidence against fast initiation has also been observed in these systems,[10] and proper characterization of the side chains cannot be carried out unless they are attached to the core through selectively cleavable bonds.

The synthesis of arborescent (dendrigraft) polymers relies on a generation-based scheme to obtain dendritic (multi-level) graft polymer architectures.[11] A linear polymer substrate is modified to introduce coupling sites serving in a grafting reaction for linear chains. The comb (or generation G0 arborescent) polymer obtained is then subjected to additional cycles of functionalization and grafting reactions to yield higher generation (G1, G2…) arborescent polymers, with a branching functionality and molecular weight increasing geometrically for each cycle. The random distribution of coupling sites on the substrates makes these molecules less sensitive to incomplete reactions, because all the molecules are affected to the same extent when a large number of coupling sites are present on the substrate. Consequently, a narrow MWD ($M_w/M_n \sim 1.1$) is achieved for these materials even for very high branching functionalities.

A strategy combining carbosilane dendrimer substrates and arborescent polymer chemistry is now presented for the synthesis of high branching functionality dendrimer-arborescent polybutadiene hybrid polymers. Carbosilane dendrimer substrates bearing 32, 64, or 128 peripheral Si-Cl functional groups are first coupled with short 1,2-

polybutadienyllithium segments and hydrosilylated with dichloromethylsilane. The polyfunctional substrates are then reacted with polybutadienyllithium chains of different number-average molecular weights (M_n = 1500, 5000, and 30000) with a high 1,4-microstructure content. This approach yielded substrates with up to 2830 side chains, significantly higher than for the star-branched polymers reported previously.

3.2 Experimental Section

3.2.1 Solvent and Reagent Purification

Tetrahydrofuran (THF; Caledon, reagent grade) was purified by distillation from sodium-benzophenone ketyl under nitrogen. Cyclohexane (BDH, HPLC grade) was purified by refluxing with oligostyryllithium under nitrogen. The dry solvents were introduced directly from the stills into the polymerization reactor or ampule preparation manifolds through polytetrafluoroethylene (PTFE) tubing. *n*-Butyllithium (*n*-BuLi, Aldrich, 2.5 M in hexane) and *tert*-butyllithium (*tert*-BuLi, Aldrich, 1.7 M in heptane) solutions were used as received; the exact activity of the *tert*-BuLi solution was determined by the method of Lipton et al.[12] 2,2′-Bipyridyl (Aldrich, 99+%) was dissolved in dry cyclohexane to give a 0.10 M solution. All reagent ampules used in the polymerization and coupling procedures were prepared using high-vacuum techniques and filled with dry nitrogen.[13] The ampules, equipped with PTFE stopcocks and ground glass joints, were designed to be mounted directly on the polymerization reactor. 1,3-Butadiene (Praxair, 99 %) was purified by stirring over *n*-butyllithium (1 mL for 20 mL monomer) for 30 min at 0 °C and condensation to an ampule under vacuum. The monomer was diluted by condensing an equal volume of dry THF or cyclohexane under

vacuum, and the ampule was stored at -20 °C until used. Dichloromethylsilane (Aldrich, 99 %) was purified on a high-vacuum manifold by three freezing – evacuation – thawing cycles, and slow distillation to a glass ampule. Tetravinylsilane (Gelest, 95 %), vinylmagnesium chloride (Aldrich, 1.6 M solution in THF), and platinum(0)-1,3-divinyl-1,1,3,3-tetramethyldisiloxane complex (Aldrich, 3 wt% solution in xylene) were used as received.

3.2.2 Synthesis of Carbosilane Dendrimers

All carbosilane dendrimer generations (i.e. 8-, 16-, 32-, and 64-arm) were synthesized using a modification of the procedure reported by Zhou and Roovers.[14] Only procedures differing significantly from those reported previously are described. A detailed procedure for the synthesis of an 8-arm carbosilane dendrimer is described as an example.

8-Arm (G1) Carbosilane Dendrimer. Ampule 1 containing freshly distilled dichloromethylsilane (17.7 mL, 19.6 g, 170 mmol), the dry THF inlet, and an empty ampule 2 were mounted on the high-vacuum manifold shown in Figure 3.1. Except for ampule 1, the manifold was evacuated, flamed, cooled to room temperature, and filled with nitrogen before removing the stopcock from the ampule 2 and adding tetravinylsilane (4.4 mL, 3.5 g, 26 mmol) with a syringe.

The vinylsilane compound was dried with three azeotropic distillation cycles by evacuating the manifold, adding 20 mL portions of dry THF in flask A, condensation to ampule 2, and recondensation to flask B. The vinylsilane was then redissolved in 40 mL of dry THF. The dichloromethylsilane (6.5 equivalents, 63 % excess vs. tetravinylsilane)

was then condensed from ampule 1 to ampule 2 under vacuum, the apparatus was filled with nitrogen, and platinum(0)-1,3-divinyl-1,1,3,3-tetramethyldisiloxane complex in xylene (75 μL) was added to ampule 2 with a syringe.

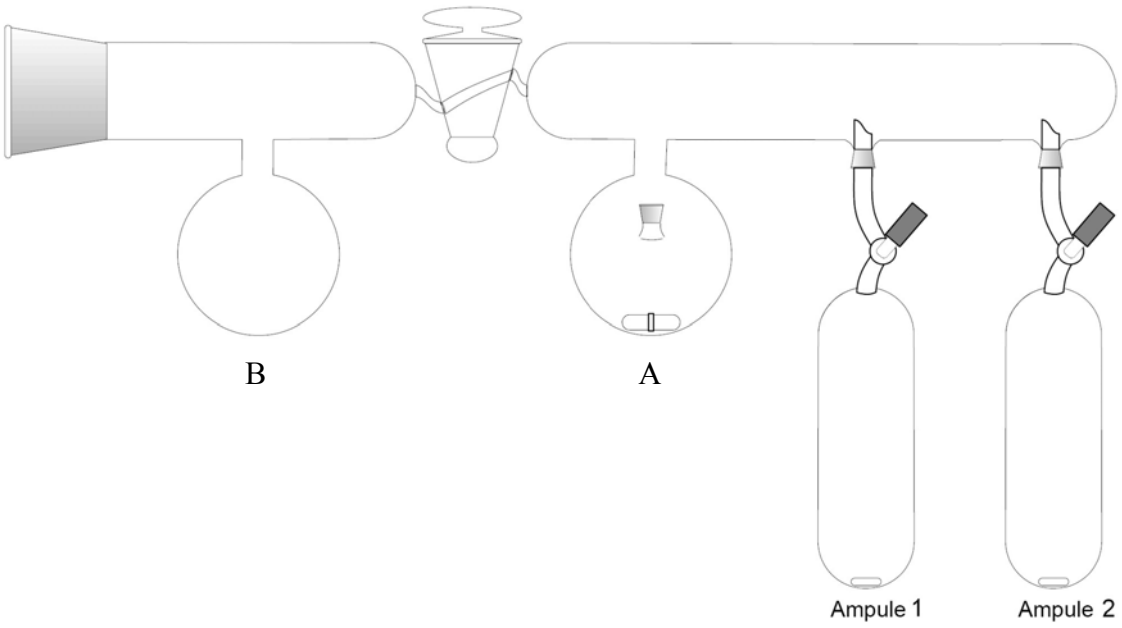

Figure 3.1 Manifold for hydrosilylation reaction.

The reaction mixture was then heated to 50 °C in an oil bath and maintained under N_2. Within 5 min, the reaction started refluxing. The ampule was removed from the oil bath and cooled in an ice-water bath to control the reaction. After 30 min, the ampule was heated again in the oil bath at 50 °C for 4 h. After cooling to room temperature, the excess dichloromethylsilane and the THF were condensed to flask B under vacuum. Two fresh portions of dry THF (40 ml) were transferred to ampule 2 and condensed to flask B. A last 40 mL portion of dry THF was transferred to ampule 2, which was filled with N_2. Vinylmagnesium chloride (1.6 M in THF, 234 mL, 374 mmol, 80 % excess vs. Cl-Si

groups) was then added over a period of 30 min to ampule 2. The ampule was sealed and the reaction was allowed to proceed at room temperature for seven days. Hexane (200 mL) was then added, and the mixture was washed twice with 200 mL portions of water and once with 200 mL of saturated aqueous NaCl solution. The organic solution was dried over anhydrous $MgSO_4$, the solvent was removed on a rotary evaporator, and the 14-g solid residue was purified by flash chromatography on a silica gel column (230-400 mesh, 15 cm length × 6 cm diameter), eluting with a solution of 0.25 % ethyl acetate in hexane, to give 7.2 g of the pure 8-arm carbosilane dendrimer or first generation (G1) in 52 % yield as an oily product.

The conditions used for the synthesis of the 16-, 32-, and 64-arm carbosilane dendrimers were identical with those described in the procedure provided unless otherwise noted, with the amounts of reagents specified below.

16-Arm (G2) Carbosilane Dendrimer. G1 carbosilane dendrimer (8-arm) 3.8 g (7.2 mmol); dichloromethylsilane 11.3 g (10.22 mL, 98 mmol, 13.6 equiv, 70 % excess); total hydrosilylation reaction time 5 h; vinylmagnesium chloride 173 mL (277 mmol, 140 % excess). Total reaction time was 15 days. Raw product (10 g) purified by flash chromatography on a silica gel column (230-400 mesh, 15 cm length × 6 cm diameter), eluting with a solution of 0.25 % ethyl acetate in hexane to give 4.6 g of the pure 16-arm (G2) carbosilane dendrimer in 48 % yield as an oily product.

32-Arm (G3) Carbosilane Dendrimer. G2 carbosilane dendrimer (16-arm) 2.6 g (2.0 mmol); dichloromethylsilane 6.5 g (5.8 mL, 57 mmol, 28.5 equiv, 78 % excess); total hydrosilylation reaction time 5 h; vinylmagnesium chloride 120 mL (192 mmol, 200 % excess). Total reaction time was 30 days. Raw product (6 g) purified by flash

chromatography on a silica gel column (230-400 mesh, 8 cm length × 6 cm diameter), eluting with a solution of 8 drops of ethyl acetate in 500 mL of hexane, to give 2.5 g of the pure 32-arm (G3) carbosilane dendrimer in 44 % yield as a viscous liquid product.

64-Arm (G4) Carbosilane Dendrimer. G3 carbosilane dendrimer (32-arm) 1.0 g (0.35 mmol); dichloromethylsilane 3.0 g (2.7 mL, 26 mmol, 74.0 equiv, 132 % excess); total hydrosilylation reaction time 6 h; vinylmagnesium chloride (1.6 M in THF) 42.5 mL (68 mmol, 200 % excess). Total reaction time was 60 days. Raw product (2.2 g) purified by flash chromatography on a silica gel column (230-400 mesh, 5 cm length × 6 cm diameter), eluting with a solution of 8 drops of ethyl acetate in 500 mL of hexane, to give 0.5 g of the pure 64-arm (G4) carbosilane dendrimer in 24 % yield as a viscous liquid product.

3.2.3 Synthesis of Carbosilane-*graft*-1,2-polybutadiene Star-like Hybrids

The star-like hybrid polymers were synthesized from the 16-, 32- and 64-arm carbosilane dendritic cores and side chains with a number-average molecular weight $M_n \approx 1000$ by adapting a reported procedure.[7] The procedure for the synthesis of a 32-arm star-like hybrid is provided as an example below.

Hydrosilylation Reaction. G2 carbosilane dendrimer (16-arm) 0.25 g (0.2 mmol) in 10 mL THF; dichloromethylsilane: 0.63 g (0.57 mL, 5.5 mmol, 27.5 equiv, 72 % excess); platinum divinyltetramethyldisiloxane complex 25 μL; total hydrosilylation reaction time 5 h. Substrate dissolved in 10 mL THF, purged with N_2, and stored at room temperature until the coupling reaction.

Anionic Polymerization and Coupling. The anionic polymerization of 1,3-butadiene was carried out in THF at 0 ^{o}C for 4 h, to yield a mixed microstructure with 52 % of 1,2-units.[13] 1,3-Butadiene (7.7 g, 142.4 mmol, 12 mL at 0 °C) was stirred with *n*-butyllithium (0.6 mL) in a high-vacuum manifold for 30 min at 0 °C, condensed into a calibrated ampule, and diluted with 15 mL of THF. The ampule was stored at -20 °C until the polymerization. Ampules containing the G2 star-like chlorosilane coupling agent (6.4 meq chlorosilane groups) in THF, 1,3-butadiene (142.4 mmol in THF), the dry THF inlet, and a septum were mounted on the reactor. After evacuation, flaming, and purging with N_2, THF (150 mL) and a few drops of 1,3-butadiene were added, and residual impurities were titrated at -78 °C with *tert*-BuLi to a persistent light yellow color. The calculated amount of *tert*-BuLi (4.5 mL, 7.7 mmol, for a target M_n = 1000) was then added, followed by the monomer over 5 min; the light yellow color changed to deep yellow. After 5 min the reactor was warmed to 0 °C, the polymerization was allowed to proceed for 4 h, and a side chain sample was removed and terminated with N_2-purged methanol (measured side chain M_n = 540). The reactor was warmed to 23 ^{o}C, and the coupling agent solution was added over 5 min. Fading of the deep yellow color of the polybutadienyllithium solution was noticeable within 2 min, and after 30 min the reaction mixture was light yellow. The coupling reaction was allowed to proceed further for 24 h at 23 °C, and residual macroanions were terminated with N_2-purged methanol. The crude product (5.0 g) was recovered by precipitation in methanol, filtration, and drying under vacuum. The pure grafting product (2.5 g, absolute M_n = 19000, M_w/M_n = 1.02, branching functionality f_n = 31) was isolated from the crude product by precipitation fractionation from *n*-hexane/methanol. The purified product was dried under high vacuum and stored

at -80 °C. The same conditions were used for the synthesis of 64-, and 128-arm carbosilane-*graft*-1,2-polybutadiene hybrids, with the reagent amounts given below.

64-Arm Star-like Hybrid. Chlorosilane substrate: G3 carbosilane dendrimer (32-arm) 0.25 g (0.08 mmol) in 10 mL THF; dichloromethylsilane 0.72 g (0.65 mL, 6.2 mmol, 77.5 equiv, 142 % excess); platinum divinyltetramethyldisiloxane 25 μL; total hydrosilylation reaction time 5 h. Coupling reaction: G3 chlorosilane coupling agent 0.25 g (5.5 meq chlorosilane groups) in 10 mL THF; 1,3-butadiene 11 g (18 mL, 203.4 mmol); *tert*-BuLi 6.5 mL (11 mmol). Crude product yield 10 g, fractionated product yield 4.0 g (absolute M_n = 61 000, M_w/M_n = 1.03, branching functionality f_n = 57).

128-Arm Star-like Hybrid. Chlorosilane substrate: G4 carbosilane dendrimer (64-arm) 0.25 g (0.04 mmol) in 10 mL THF; dichloromethylsilane: 0.80 g (0.73 mL, 7.0 mmol, 175 equiv, 173 % excess); platinum divinyltetramethyldisiloxane complex 25 μL; total hydrosilylation reaction time 6 h. Coupling reaction: G4 chlorosilane coupling agent 0.25 g (5.3 meq chlorosilane groups) in 10 mL THF; 1,3-butadiene 10.6 g (16.5 mL, 196 mmol); *tert*-BuLi 6.2 mL (10.6 mmol, for a target M_n = 1000). Crude product yield 9.5 g, fractionated product yield 2.0 g (absolute M_n = 160000, M_w/M_n = 1.16, branching functionality f_n = 126).

3.2.4 Synthesis of Dendrimer-Arborescent Polybutadiene Hybrids

Three series of arborescent hybrids were synthesized by hydrosilylation of the carbosilane-*graft*-1,2-polybutadiene star-like hybrids and coupling with 1,4-polybutadienyllithium side chains with $M_n \approx$ 1500, 5000, 30000. The 1,2-polybutadiene hybrid substrates used all had a microstructure with 52 mol % 1,2-units, and were derived either

from the G2, G3, or G4 carbosilane dendrimers. A procedure for the synthesis of an arborescent hybrid using the G2 substrate and with $M_n \approx 1500$ side chains is provided.

Hydrosilylation Reaction. 32-arm star-like hybrid 0.25 g (G2, dried for 24 h under high vacuum; weight fraction PBD 0.848, 3.92 mmol BD units, 2.04 mmol 1,2-vinyl groups) in 10 mL THF; dichloromethylsilane 0.47 g (0.42 mL, 4.1 mmol, 100 % excess vs. vinyl groups); platinum divinyltetramethyldisiloxane complex 50 μL; total hydrosilylation reaction time 24 h. Chlorosilane coupling agent dried overnight under high vacuum before redissolution in 10 mL THF, ampule filled with N_2 and stored at room temperature. The same conditions were used for the hydrosilylation reaction using either the 64-arm or the 128-arm star-like hybrid, but the total reaction time required for complete hydrosilylation reaction at 50 °C was 30 and 36 h, respectively.

Anionic Polymerization and Coupling. High *cis*-1,4-content polybutadiene was prepared in cyclohexane at 23 °C and the monomer was purified as described earlier.[13] Ampules containing the 32-arm chlorosilane coupling agent 0.25 g (4.1 meq chlorosilane groups) in 10 mL THF, purified 1,3-butadiene (9.2 g, 14.3 mL, 170.1 mmol) in 15 mL THF, the dry cyclohexane inlets, and a septum were mounted on a 2-L glass reactor equipped with a vacuum-tight mechanical stirrer. After evacuation, flaming, and purging with N_2, cyclohexane (300 mL) and 0.5 mL of 0.10 M 2,2′-bipyridyl solution in cyclohexane were added, and the solvent was titrated with *tert*-BuLi to give a persistent light orange colour.[15] The reactor was then cooled to 0 °C and the calculated amount of *tert*-BuLi (3.6 mL, 6.1 mmol, for a target M_n = 1500) was added, followed by the monomer over 5 min. The reactor was warmed to room temperature (23 °C), polymerization was allowed to proceed for 24 h, and a side chain sample was removed

and terminated with N_2-purged methanol (measured side chain M_n = 1200). The coupling agent solution was added to the reactor over 5 min. Fading of the orange color of the polybutadienyllithium solution was noticeable within 5 min, and after 2 h the reaction mixture become almost colorless and hazy. The coupling reaction was allowed to proceed further for 24 h at 23 °C, and residual macroanions were terminated with N_2-purged methanol. The crude product (8.7 g) was recovered by precipitation in methanol, filtration, and drying under vacuum. The pure grafting product (4.0 g, absolute M_n = 430000, M_w/M_n = 1.01, branching functionality f_n = 336) was isolated by precipitation fractionation from *n*-hexane/methanol, dried under high vacuum, and stored at -80 °C. The same conditions were used to achieve the targeted $M_n \approx 5000$ and 30000 for the side chains in 48 h and 72 h polymerization time, respectively. Irrespective of the substrate type used, the coupling reactions for all arborescent hybrids were essentially complete in 24 h.

3.2.5 Polymer Characterization

A size exclusion chromatography (SEC) system calibrated with linear polystyrene standards was routinely used to monitor the polymerization and coupling reactions, as well as sample fractionation. The instrument, operated at room temperature, consisted of a Waters 510 HPLC pump, a 500 mm × 10 mm Jordi DVB linear Mixed-Bed column (molecular weight range 10^2-10^7), and a Waters 410 differential refractometer detector. THF at a flow rate of 1 mL/min served as eluent for the analysis.

The absolute number-average molecular weight (M_n), polydispersity index (M_w/M_n) of the hybrid polymers and the polybutadiene side chains ($M_n \approx 30000$) were

determined by SEC analysis using a Wyatt Dawn DSP-F MALLS (multiangle laser light scattering) detector operating at 632.8 nm. The SEC system consisted of a Waters 590 programmable HPLC pump coupled with Waters Ultrastyragel columns (10^4, 10^5, and 10^6 Å pore sizes) using THF at a flow rate of 1 mL/min. Polymer concentration measurements in the eluent were accomplished with a Waters 2410 DRI detector operating at 660 nm. Molecular weights were obtained from the MALLS and DRI signals, using the Astra Version 4.70.07 software package. The refractive index increment (d*n*/d*c*) values for the polybutadiene side chain samples and the hybrid polymers used in the MALLS analysis were determined in THF at 25 °C on a Brice-Phoenix differential refractometer equipped with a 632 nm band-pass interference filter.

^{1}H NMR spectroscopy served to monitor the hydrosilylation reaction, to confirm the structure of the carbosilane dendrimers synthesized, and to determine the absolute M_n of the polybutadiene side chains with $M_n \approx 1000$, 1500, and 5000. The microstructure of the polybutadiene chains was analyzed by the method of Tanaka et al.[16] All spectra were recorded on a Bruker-300 (300 MHz) instrument in $CDCl_3$ at a concentration of 5 %.

3.3 Results and Discussion

3.3.1 Synthetic Strategy

Carbosilane dendrimers containing 16, 32, and 64 vinyl functionalities were synthesized starting from a tetravinylsilane core, using cycles of hydrosilylation with dichloromethylsilane and nucleophilic displacement with vinylmagnesium chloride as described in the literature.[14] The corresponding chlorosilane coupling precursors with 32, 64, or 128 peripheral Si-Cl groups, were then obtained by hydrosilylation of the

carbosilane dendrimers with dichloromethylsilane, and coupled with short polybutadiene chains containing a high proportion of 1,2-units. These star-like graft polymer hybrids were again subjected to hydrosilylation to introduce a large number of chlorosilane moieties. The star-like substrates were finally reacted with 1,4-polybutadienyllithium chains of different molecular weights, to generate series of high branching functionality dendrimer-arborescent polymer hybrids.

3.3.2 Synthesis of Carbosilane Dendritic Macromolecules

Carbosilane dendritic substrates of generations G1-G4 were synthesized as described previously,[14] but the procedures were adapted to the high-vacuum purification and polymerization techniques routinely used in our laboratory.[13] Since the synthesis of the carbosilane dendrimers was reported previously, the discussion will be limited to a comparison of the results obtained in this work with those reported previously. The progress of the reaction and the formation of side products were monitored by ^{1}H NMR spectroscopy analysis. The ^{1}H NMR spectra obtained for the pure products, provided in Figure 3.2, are characteristic for the perfect carbosilane dendrimer structures, as incomplete reactions and structural defects destroy the symmetry of the spectra.[14]

For each generation three groups of proton resonances are present in the ^{1}H NMR spectra. Taking the carbosilane dendrimer of first generation (G1, 8-arm) as an example, the vinyl protons on the exterior of the molecules (δ 6.01 m, 4H and δ 5.71 m, 2H) are clearly distinguishable, as well as the methyl protons attached to the silicon atoms (δ 0.11 s, 3H). The spectral pattern for the methylene groups (δ 0.43 m, 4H) is more complex,

and most sensitive to the presence of structural defects. The symmetry of these peaks is therefore a good indicator of the structural perfection and purity of the dendrimers.[14]

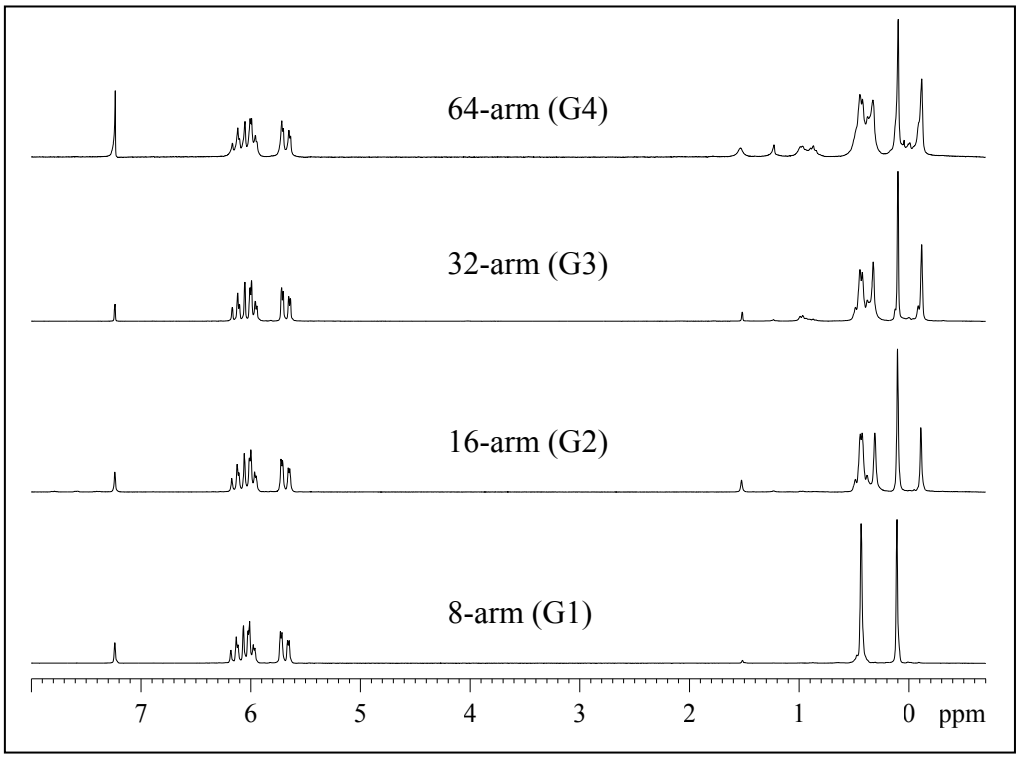

Figure 3.2 300 MHz ^{1}H NMR spectra for the carbosilane dendrimers in $CDCl_3$.

There are two types of methylene protons, one close to the central silicon core, and the other one close to the vinyl groups. For the G2 (16-arm), G3 (32-arm) and G4 (64-arm) dendrimers the coupling patterns are very similar, except for the peaks becoming broader. The methylene proton resonances for these molecules appear in two groups, since the methylene units next to the vinyl groups (δ 0.43) are non-equivalent to the interior methylene protons (δ 0.31). There are also two single peaks for methyl groups in G2-G4 dendrimers. The one at δ 0.10 is for methyl groups next to the vinyl bonds,

while the other at δ -0.10 is for the interior methyl groups. A single peak at δ 1.52 in all ^{1}H NMR spectra are due to traces of water, while the additional single peak at δ 1.24, and multiple peaks centered at δ 0.86 in the ^{1}H NMR spectrum of the G3 and G4 dendrimers correspond to traces of hexane in the products. These peaks match exactly those observed in the ^{1}H NMR spectrum for hexane used in the chromatographic purification procedure and slowly decrease upon drying the samples under high vacuum, but are still detectable even after 1 week. Finally, it should be noted that while the spectra are quite similar, the ratios of integrated peak intensities change among the different generations. The NMR peak intensity ratios obtained are compared in Table 3.1 with those previously reported[14] and with the theoretical ratios calculated based on structure. It is clear that the modified synthetic procedures are equivalent to the ones reported in the literature, as the intensity ratios are very close to the calculated values for both methods.

Size exclusion chromatography (SEC) analysis was used to determine the apparent (polystyrene-equivalent) molecular weight and polydispersity index of the carbosilane dendrimers. The results, reported in Table 3.2, show that a narrow molecular weight distribution was maintained ($M_w/M_n \leq 1.09$) and the apparent molecular weight increased with the generation number. The corresponding SEC elution curves for the dendrimers and for tetravinylsilane (corresponding to generation G0) are provided in Figure 3.3. In spite of the small size of the molecules, the peaks are clearly shifted to lower elution volumes with increasing generation number. This is noticeable even for tetravinylsilane (M = 136), since the columns used had a lower molecular weight limit of 100. The breadth of the peaks is comparable for all samples, suggesting that peak broadening is similar and consistent with the absence of gross structural imperfections in

Table 3.1 Integration Ratios for the ^{1}H NMR Spectra of the Carbosilane Dendrimers

Generation	Structure Ratios					Integrated Intensity Ratios				
	CH_2=CH		CH_2-CH_2	CH_3		CH_2=CH		CH_2-CH_2	CH_3	
G1 (8-arm)	2	1	2	1.5		2/2[a]	1/1[a]	2/1.9[a]	1.5/1.5[a]	
G2 (16-arm)	2	1	3	1.5	0.76	2/2[a]	1/1[a]	2.9/2.9[a]	1.5/1.5[a]	0.76/0.73[a]
G3 (32-arm)	2	1	3.5	1.5	1.1	2/2[a]	1/1[a]	3.5/3.6[a]	1.6/1.5[a]	1.2/1.2[a]
G4 (64-arm)	2	1	3.8	1.5	1.3	2/2[a]	1/1[a]	3.8/3.7[a]	1.8/1.5[a]	1.4/1.3[a]

a) Intensity ratios reported by Zhou and Roovers.[14]

Table 3.2 Molecular Weight and Yield of Carbosilane Dendrimers

Generation	Formula	Formula Weight	Functionality	M_n [a]	M_w/M_n [a]	Yield (%)
G1 (8-arm)	$C_{28}H_{52}Si_5$	528	8	730	1.05	52/55[b]
G2 (16-arm)	$C_{68}H_{132}Si_{13}$	1312	16	1400	1.06	48/48[b]
G3 (32-arm)	$C_{148}H_{292}Si_{29}$	2880	32	2300	1.05	44/41[b]
G4 (64-arm)	$C_{308}H_{612}Si_{61}$	6016	64	3900	1.09	24/26[b]

a) Apparent values determined by SEC analysis based on linear PS standard calibration curve.

b) Yields reported by Zhou and Roovers.[14]

the dendrimers. The yields of purified vinylcarbosilane dendrimers, also reported in Table 3.2 for the G1-G4 substrates, are in good agreement (± 3%) reported by Zhou and Roovers.[14] This again confirms the equivalence of the modified synthetic procedures and the ones reported in the literature.

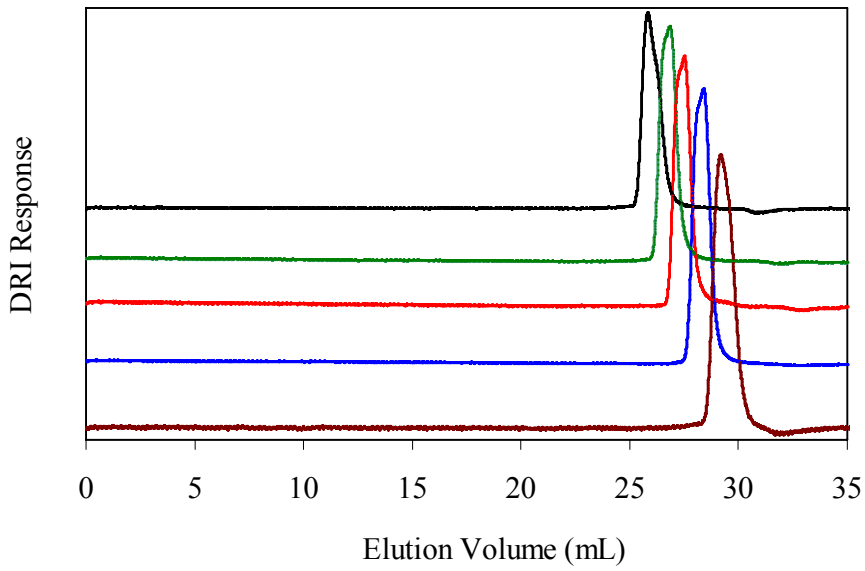

Figure 3.3 SEC elution curves for carbosilane dendrimers, from top to bottom: 64-arm (G4), 32-arm (G3), 16-arm (G2), 8-arm (G1), and tetravinylsilane (G0).

3.3.3 Synthesis of Star-like 1,2-Polybutadiene Hybrids

Three star-like 1,2-polybutadiene hybrids with target branching functionalities of 32-, 64-, and 128-arm were synthesized by a reported procedure[6,7] adapted to the high-vacuum purification and polymerization techniques used in our laboratory.[13] The synthetic procedure is summarized in Scheme 3.1, using the G2 carbosilane dendrimer substrate as an example. The nomenclature used for the star polymers identifies the number of sites on the dendrimer substrate and the molecular weight of the arms used in the synthesis; thus CS32─*m*PBD1 refers to a polymer synthesized by coupling the

carbosilane dendrimer with 32 Si-Cl sites with mixed microstructure polybutadiene arms with $M_n \approx 1000$. It should be noted that it is the 16-arm or G2 carbosilane dendrimer that becomes coupling precursor CS32 after hydrosilylation. Similarly the G3 and G4 dendrimers become the CS64 and CS128 coupling substrates, respectively.

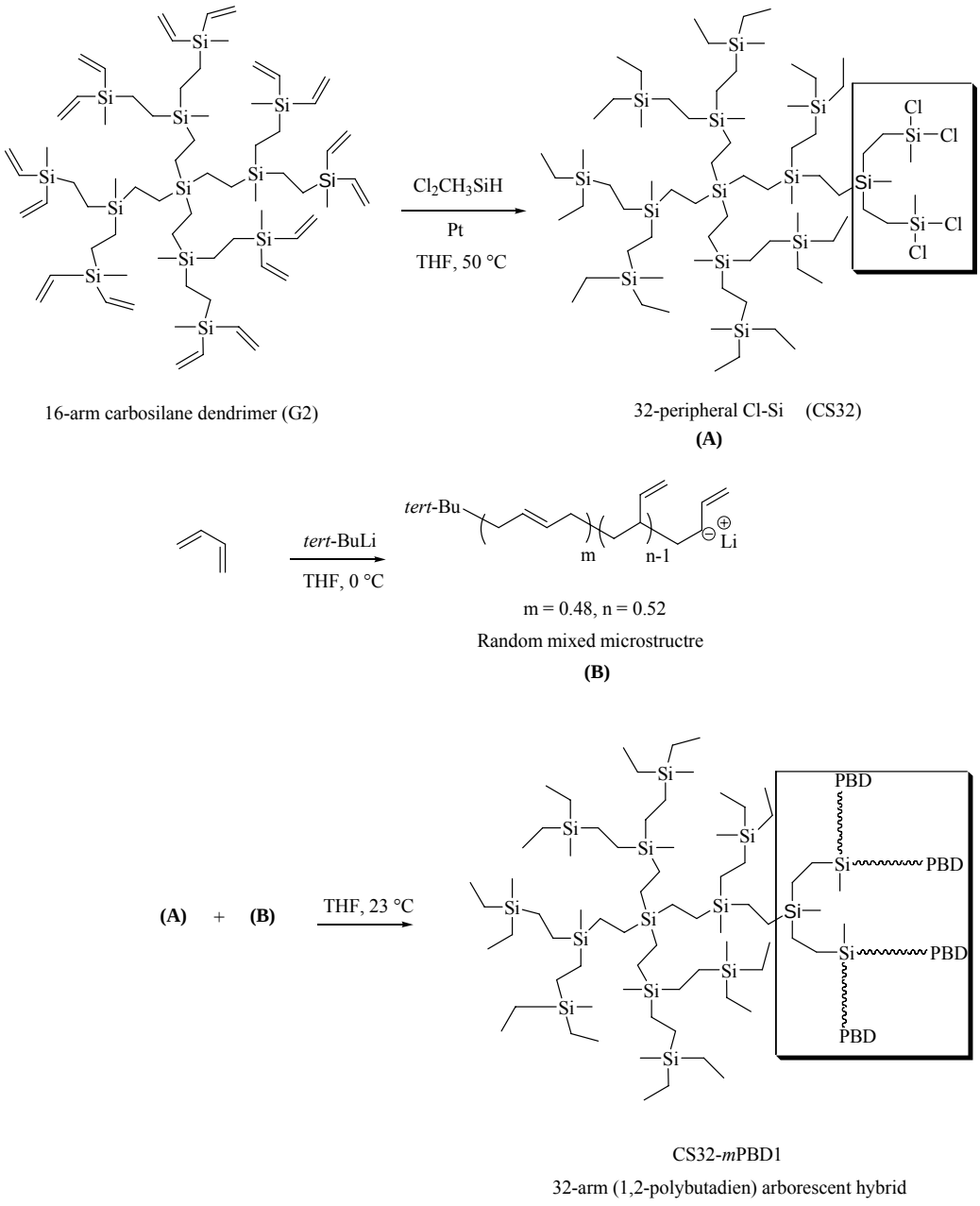

Scheme 3.1 Synthesis of 32-arm 1,2-polybutadiene star-like arborescent hybrid.

The synthesis of the star-like polymers was achieved in THF. An excess of dichloromethylsilane was used in the hydrosilylation reaction to ensure complete hydrosilylation of the vinyl groups on the carbosilane dendrimers. This was achieved in 5 h at 50 °C for the G2 and G3 dendrimers, and in 6 h for the G4 dendrimer, as evidenced by the complete disappearance of the vinyl signal at δ 5.70 and δ 6.01 in the ^{1}H NMR spectrum, and the appearance of a new peak at δ 0.57 due to the ─$SiCH_3(Cl)_2$ units (Figure 3.4b).

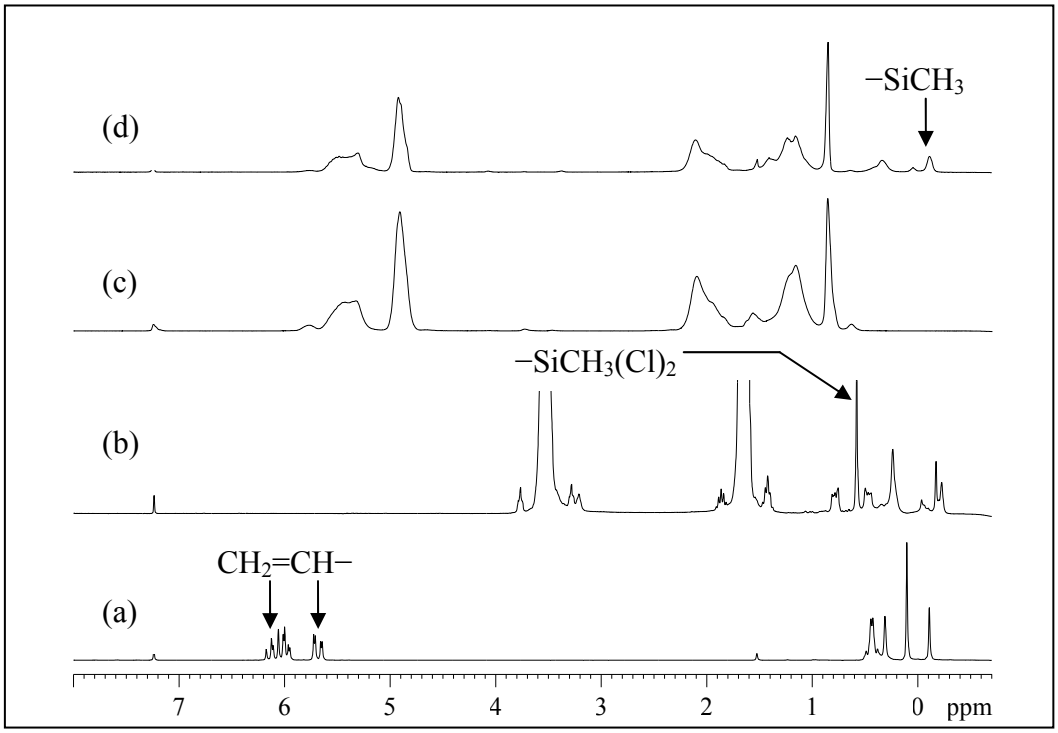

Figure 3.4 300 MHz ^{1}H NMR spectra for the synthesis of sample CS32−*m*PBD1: (a) G2 carbosilane dendrimer before hydrosilylation, (b) hydrosilylated G2 dendrimer, (c) mixed microstructure polybutadiene side chains, (d) fractionated star-like polymer.

The microstructure of polybutadiene derived from organolithium initiators can be varied depending on the reaction conditions.[17,18] Thus a predominantly 1,4-microstructure is obtained in nonpolar (hydrocarbon) solvents, while THF (a more polar solvent) leads to a mixed microstructure with 1,4- and 1,2-butadiene units.[19-22] Accordingly, low molecular weight 1,2-polybutadienyllithium was prepared in THF at 0 °C to produce compact star-like polymers. The ^{1}H NMR spectra in Figure 3.4c illustrate the reaction of the side chains with substrate CS32. The microstructure of the chains was determined from the relative peak areas of the two olefinic proton resonances at δ 5.32-5.76 (2H of the *cis*- and *trans*-1,4-microstructures) and at δ 4.90 (3H of the 1,2-microstructure) by the method of Tanaka et al.[16] This corresponds to 1,4- (*cis*- and *trans*-isomers combined) and 1,2-units contents of 48 and 52 mol %, respectively, for all samples.

The coupling reaction for substrate CS32 was carried out with a 20 % excess of living ends with respect to the Si-Cl groups, whereas a 100 % excess was used for CS64 and CS128. The extent of the coupling reaction was monitored by SEC analysis, from the increase in apparent molecular weight of the star-like polymer and the relative peak areas for the graft polymer and the side chains. Completion of the coupling reaction was also evidenced by ^{1}H NMR analysis of the fractionated product (Figure 3.4d) by the disappearance of the signal at δ 0.57 [─$SiCH_3(Cl)_2$] for the coupling precursor and the appearance of a new peak at δ -0.11 for ─$SiCH_3$ after displacement of the two Cl atoms. SEC analysis confirmed that the coupling reaction was essentially complete within 30 min for CS32, whereas for CS64 and CS128 it required 1 h. Since no further increases in molecular weight were observed even after 24 h, so this reaction time was used for all coupling reactions. This contrasts with the coupling times of 21 days to 8 weeks

necessary in a previous study[6,7] where benzene served as solvent. The longer reaction times necessary are attributed to the lower polarity of the solvent used.

Size exclusion chromatography (SEC) characterization was performed for the side chain samples removed before the grafting reaction, the crude products, and the fractionated star-like polymers. A series of SEC curves is provided in Figure 3.5 to illustrate the synthesis of the star-like polymers. Using sample CS32─*m*PBD1 as an example, the 1,2-polybutadiene side chains have a relatively narrow MWD in spite of their low molecular weight (M_n = 540, M_w/M_n = 1.13, Figure 3.5a). Two peaks, corresponding to the star-like polymer and to the linear contaminant, are observed in the SEC trace for the crude product (Figure 3.5b). The leftmost peak corresponds to the graft polymer while the peak on right, with an elution volume identical to the side chain sample removed before coupling, is mainly due to the 20 % excess of side chains used in the coupling reaction. Complete removal of the linear chain contaminant by fractionation is demonstrated in Figure 3.5c. The successful fractionation of samples CS64─*m*PBD1 and CS128─*m*PBD1 is likewise demonstrated in Figures 3.5d and 3.5e, respectively.

Characterization data for the purified star-like polymers are provided in Table 3.3. The number-average branching functionality f_n was calculated according to the equation

$$f_n = \frac{(M_n)_{star} - M_c}{(M_n)_{arm}} \tag{3.1}$$

where $(M_n)_{star}$ represents the absolute number-average molecular weight of the graft polymer, $(M_n)_{arm}$ is the absolute number-average molecular weight of the side chains and M_c is the mass of the core (coupling substrate) calculated from the equation

$$M_c = n\,(44) + (Fw)_{CSD} \tag{3.2}$$

where n is the number of arms, 44 is the formula weight of CH_3SiH and $(Fw)_{CSD}$ is the corresponding formula weight of the carbosilane dendrimer substrate reported in Table 3.2. The branching functionalities in Table 3.3 are essentially identical with the nominal functionalities for the CS32 and CS128 substrates, and slightly lower for CS64. Since the deviation is relatively low even for CS64 (-8.8 %), this could be due simply to cumulative errors in determining M_n for the star-like polymer and the side chains. The absolute polydispersity indices (M_w/M_n) for the star-like polymers determined by SEC-MALLS analysis (Table 3.3) demonstrate that narrow MWD were achieved.

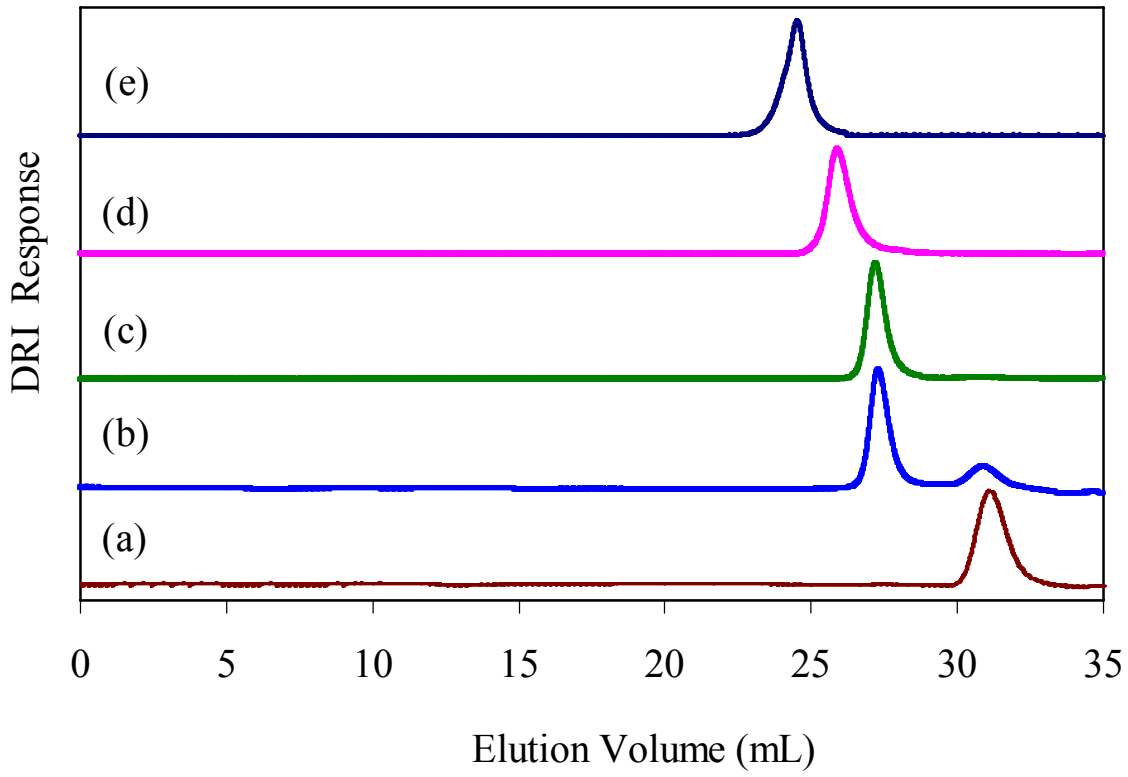

Figure 3.5 Synthesis of star-like 1,2-polybutadienes: SEC traces for (a) side chains, (b) crude grafting product, (c) fractionated sample CS32−*m*PBD1, (d) fractionated sample CS64−*m*PBD1, (e) fractionated sample CS128−*m*PBD1.

Table 3.3 Characteristics of Star-like Polybutadiene Hybrids

Sample	Side Chains [c]			M_c [d]	Star Polymer			
	M_n [a]	M_w/M_n [b]	DP		dn/dc [e]	M_n [f]	M_w/M_n [f]	f_n [g]
CS32−*m*PBD1	540	1.13	10	2016	0.1121	1.9×10^4	1.02	31
CS64−*m*PBD1	1000	1.10	19	4288	0.1021	6.1×10^4	1.03	57
CS128−*m*PBD1	1200	1.10	21	8832	0.1122	1.6×10^5	1.16	126

a) Determined from ^{1}H NMR analysis. b) Apparent values from SEC analysis using a linear polystyrene standards calibration curve. c) All side chains have 52 % 1,2- and 48 % 1,4-butadiene units. d) From equation 3.2. e) Refractive index increment in THF at 25 °C and 632 nm. f) Absolute values from SEC-MALLS analysis. g) Branching functionality determined using Equation 3.1.

3.3.4 Synthesis of Arborescent 1,4-Polybutadiene Hybrids

Three series of dendrimer-arborescent polymer hybrids with 1,4-polybutadiene side chains were synthesized by coupling the hydrosilylated 1,2-polybutadiene star-like substrates with 1,4-polybutadienyllithium of different molecular weights ($M_n \approx 1500, 5000, 30000$) according to Scheme 3.2.

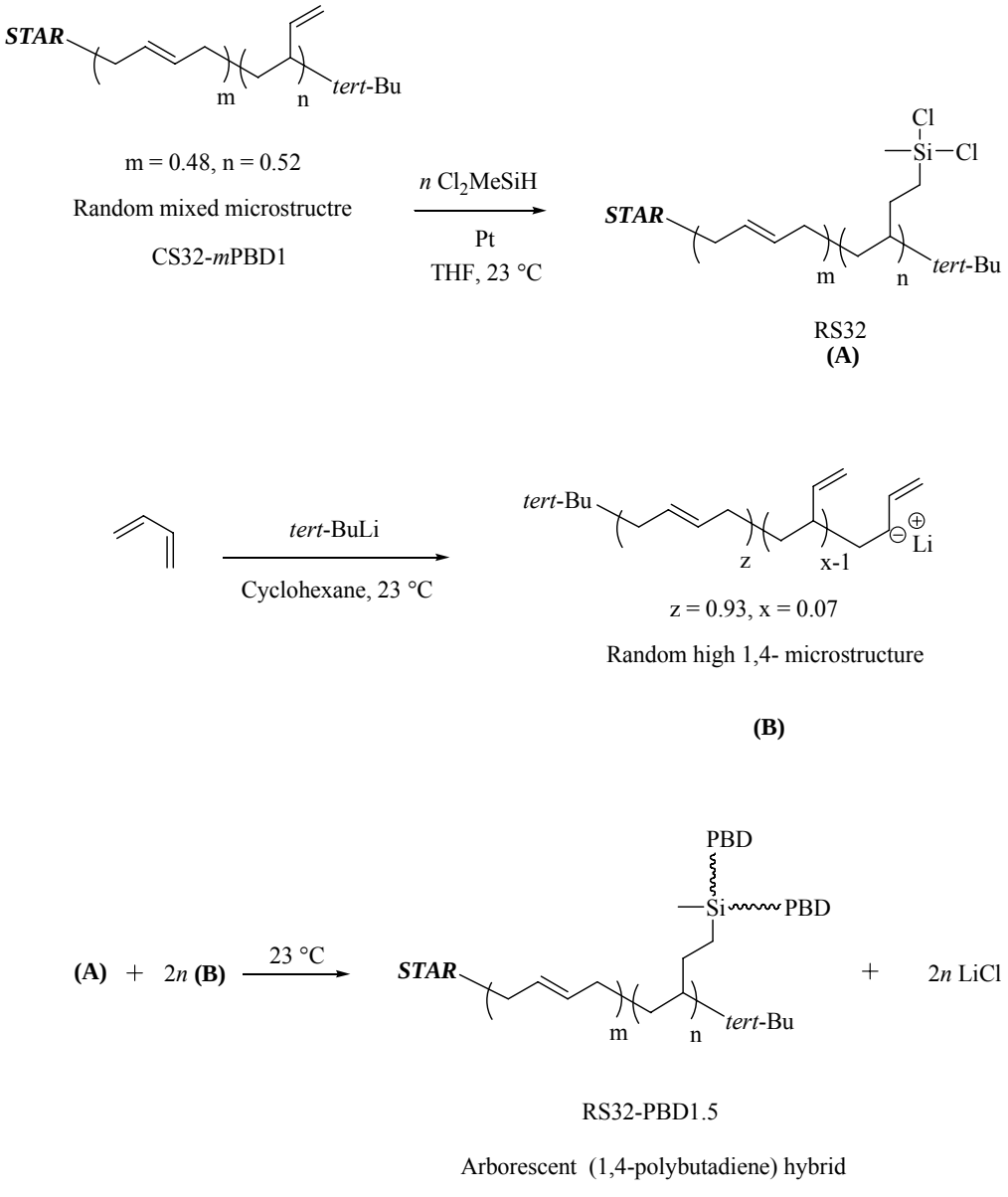

Scheme 3.2 Synthesis of 1,4-polybutadiene dendrimer-arborescent hybrid.

The sample nomenclature used to refer to the arborescent hybrids identifies the hydrosilylated star-like substrate serving in the reaction and the target molecular weight of the side chains. Thus RS32─PBD1.5 refers to an arborescent hybrid synthesized by coupling the hydrosilylated star-like polybutadiene CS32─*m*PBD1 with 1,4-polybutadiene ($M_n \approx 1500$). It should be noted that samples CS64−*m*PBD1 and CS128−*m*PBD1 likewise become RS64 and RS128 upon hydrosilylation, respectively. The vinyl groups of the 1,2-butadiene units were easily converted into coupling sites by hydrosilylation with dichloromethylsilane in THF. Complete hydrosilylation of the vinyl groups was achieved in 24 h at 50 °C for substrate RS32, whereas it required 30 and 36 h for RS64 and RS128, respectively. This is evidenced by the ^{1}H NMR spectrum for RS32 (Figure 3.6b), confirming the complete disappearance of the vinyl resonance at δ 4.90 and the appearance of a new peak at δ 0.57 [─$SiCH_3(Cl)_2$]. The signals for the 1,4-units (δ 5.32-5.76) were unaffected, indicating that the internal double bounds of the polybutadiene chains were unreactive.

The polybutadienyllithium with a predominantly 1,4-microstructure serving as side chains was synthesized in cyclohexane at room temperature. The target $M_n \approx 1500$, 5000 and 30000 were attained in 24, 48, and 72 h polymerization time, respectively. The ^{1}H NMR spectrum shown in Figure 3.6c corresponds to the side chains used in the synthesis of sample RS32−PBD1.5. The microstructure, determined by the method of Tanaka et al.[16] described previously, corresponds to 93 % 1,4-units (*cis*- and *trans*-isomers combined) and 7 % 1,2-units. The microstructure analysis and characterization results for the side chains of all samples are summarized in Table 3.4.

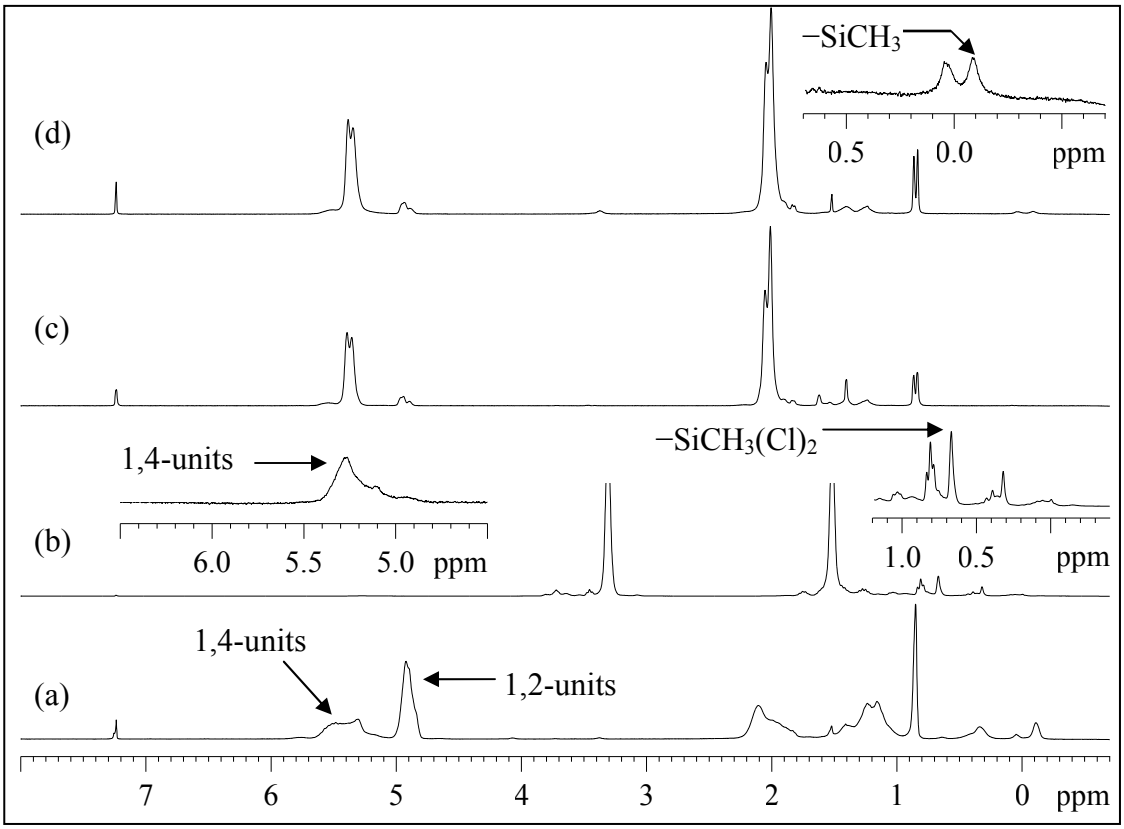

Figure 3.6 300 MHz ^{1}H NMR spectra for the synthesis of sample RS32−PBD1.5: CS32−*m*PBD1 substrate (a) before and (b) after hydrosilylation, (c) 1,4-polybutadiene side chains, (d) fractionated arborescent hybrid.

The arborescent hybrids with a side chain $M_n \approx 1500$ were synthesized with a 50 % excess of living chains vs. Si-Cl groups, whereas for side chains with $M_n \approx 5000$ and 30000 the living chains were in 75 % and 100 % excess, respectively. Since the concentration of living chains decreases for higher molecular weights, the larger excesses used ensured a reasonably fast coupling reaction rate. The reaction of the coupling substrate is evidenced by the complete disappearance in the ^{1}H NMR spectrum (Figure 3.6d) of the signal at δ 0.57 [─$SiCH_3(Cl)_2$], and the appearance of a new peak at δ -0.11 [─$SiCH_3$] following the loss of the two Cl atoms. SEC monitoring of the reaction also

confirmed that the coupling reaction for all arborescent hybrids was essentially complete in 24 h, as their molecular weight became constant.

Size exclusion chromatography (SEC) analysis was performed for the side chains, the crude products, and the fractionated arborescent hybrids. The chromatograms provided in Figure 3.7 as an example illustrate the synthesis of sample RS32─PBD1.5. The polybutadiene side chains are characterized by a relatively narrow MWD (M_n = 1200, M_w/M_n = 1.10; Figure 3.7a). As in the synthesis of the star-like substrates, the two peaks in the SEC curve for the crude grafting product (Figure 3.7b) correspond to the graft polymer (left) and to linear chain contaminant (right). Interestingly, the peak on the right has a molecular weight twice as large as the side chain sample removed before the coupling reaction (Figure 3.7a). This effect, also reported for the synthesis of 32-arm star polybutadienes from carbosilane substrates,[6] was attributed to coupling of the linear polymer with residual dichloromethylsilane from the hydrosilylation reaction contaminating the coupling precursor. The SEC traces in Figures 3.7c-e confirm the complete removal by fractionation of linear contaminant from samples RS32─PBD1.5, RS32─PBD5, and RS32─PBD30, respectively. SEC curves are also provided in Figures 3.8 and 3.9 to illustrate the synthesis of arborescent polybutadienes based on substrates RS64 and RS128, respectively. Crude sample RS128─PBD1.5 has an extra peak between the linear precursor and the graft polymer (Figure 3.8b), again attributed to coupling of the linear polymer with dichloromethylsilane residues from the hydrosilylation reaction. The chromatograms of Figures 3.8c-e and Figures 3.9c-e likewise confirm the complete removal of linear contaminant by fractionation of the arborescent hybrid samples based on the RS64 and RS128 substrates, respectively.

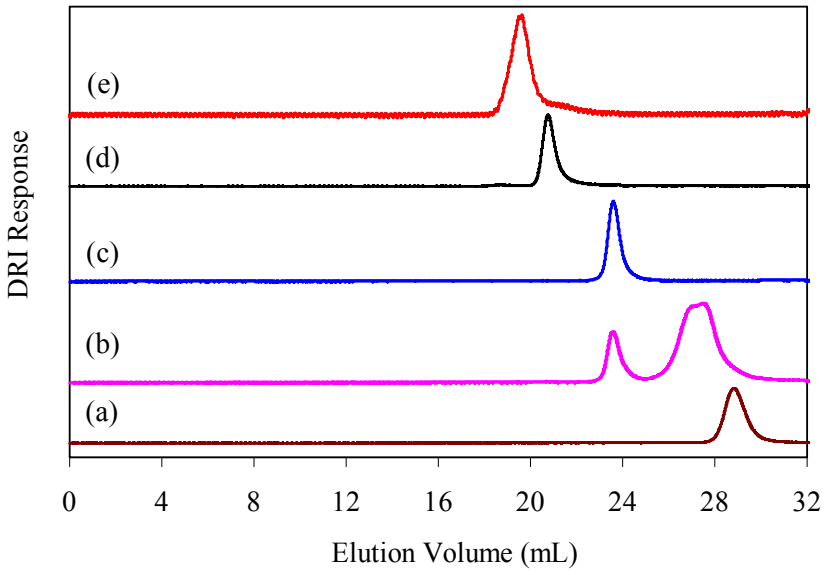

Figure 3.7 Synthesis of arborescent 1,4-polybutadiene hybrids from RS32 core: SEC traces for (a) side chains, (b) crude grafting product, and fractionated samples (c) RS32−PBD1.5, (d) RS32−PBD5, (e) RS32−PBD30.

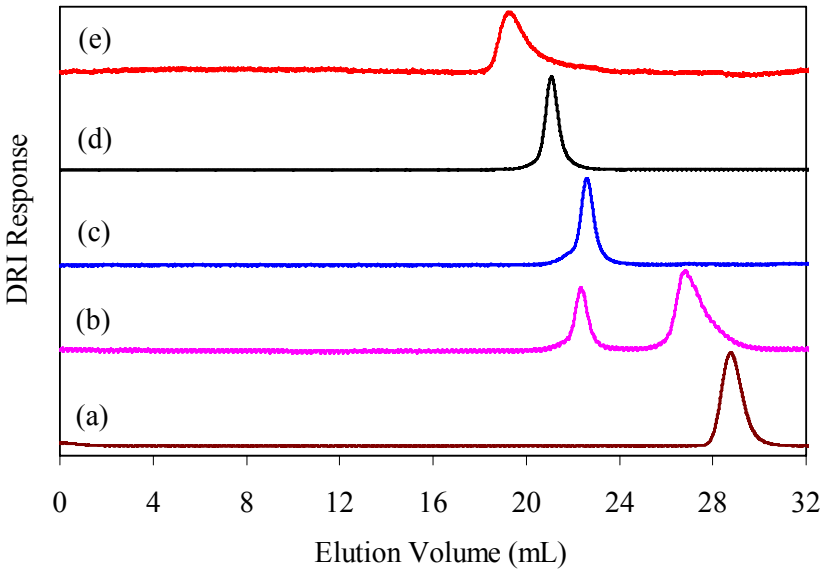

Figure 3.8 Synthesis of arborescent 1,4-polybutadiene hybrids from RS64 core: SEC traces for (a) side chains, (b) crude grafting product, and fractionated samples (c) RS64−PBD1.5, (d) RS64−PBD5, (e) RS64−PBD30.

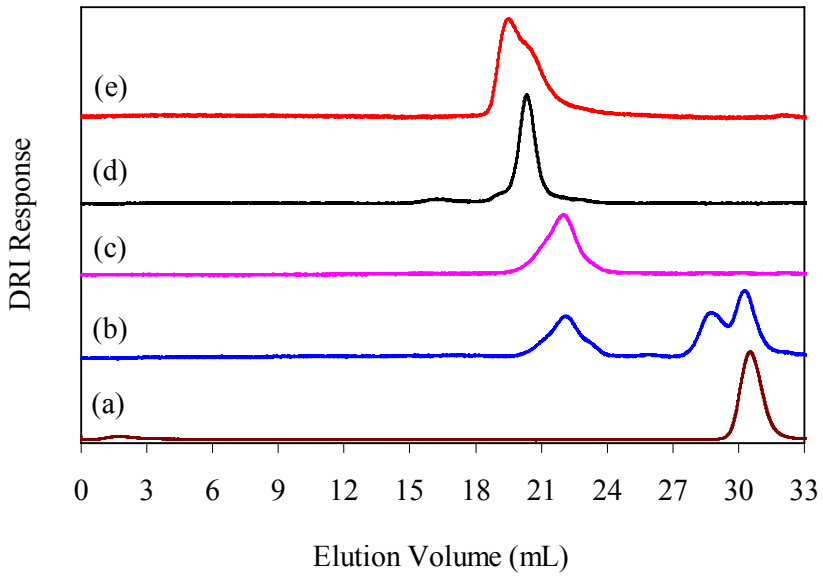

Figure 3.9 Synthesis of arborescent 1,4-polybutadiene hybrids from RS128 core: SEC traces for (a) side chains, (b) crude product, and fractionated samples (c) RS128−PBD1.5, (d) RS128−PBD5, (e) RS128−PBD30.

Characterization data for the arborescent-dendrimer hybrids synthesized are provided in Table 3.4. The number-average branching functionality f_n was calculated according to the equation

$$f_n = \frac{(M_n)_{star} - M_c'}{(M_n)_{arm}} \tag{3.3}$$

where $(M_n)_{star}$ represents the absolute number-average molecular weight of the graft polymer (arborescent-dendrimer hybrid), $(M_n)_{arm}$ is the absolute number-average molecular weight of the side chains, and M_c' is the molecular weight of the core (substrate) calculated according to the equation

$$M_c' = (M_n)_{core} + \frac{[(M_n)_{core} - M_c]}{M_{BD}} \times 0.52 \times 44 \tag{3.4}$$

Table 3.4 Characteristics of 1,4-Polybutadiene Arborescent Hybrids

Sample	Side Chains			M_c' [d]	Hybrid Polymers				Coupling Efficiency (%) [h]
	M_n [a]	M_w/M_n [b]	1,4-Vinyl Groups Mol (%) [c]		dn/dc [e]	M_n [f]	M_w/M_n [f]	f_n [g]	
RS32−PBD1.5	1200	1.10	93		0.1200	4.3×10^5	1.01	336	99
RS32−PBD5	6500	1.11	94	26200	0.1302	2.0×10^6	1.05	304	89
RS32−PBD30	26000 [f]	1.08 [f]	95		0.1364	3.7×10^6	1.03	141	41
RS64−PBD1.5	1270	1.11	94		0.1269	1.5×10^6	1.07	1114	99
RS64−PBD5	4000	1.10	95	85000	0.1300	3.8×10^6	1.03	929	83
RS64−PBD30	29900 [f]	1.09 [f]	96		0.1283	4.9×10^6	1.03	161	14
RS128−PBD1.5	1300	1.10	92		0.1217	3.9×10^6	1.13	2828	95
RS128−PBD5	5800	1.13	95	224000	0.1204	5.3×10^6	1.08	875	29
RS128−PBD30	23000 [f]	1.06 [f]	96		0.1229	8.6×10^6	1.14	364	12

a) Absolute M_n from ^{1}H NMR analysis. b) Apparent polydispersity from SEC analysis using a linear polystyrene standards calibration curve. c) From ^{1}H NMR spectroscopy analysis. d) Substrate M_n calculated from Equation 3.4. e) Refractive index increment in THF at 25 °C and 632 nm. f) Absolute values determined from SEC-MALLS analysis. g) Branching functionality calculated from Equation 3.3. h) Fraction of coupling sites on the substrate consumed.

where $(M_n)_{core}$ represents the number-average molecular weight of the star-like polymer serving as substrate, M_c is the molecular weight of the dendrimer substrate used to synthesize the star-like polymer, 44 is the formula weight of the branching units (CH_3SiH), 0.52 is the mole fraction of 1,2-units in the star-like polymer, and M_{BD} is the molecular weight of the butadiene unit (54.04). The branching functionality f_n and M_c' are reported in Table 3.4 for all samples. The f_n values range from 140 − 335 for the RS32 sample series, from 160 − 1115 for the RS64 series, and from 360 − 2830 for the RS128 series, respectively. The experimental branching functionalities are always lower than the number of coupling sites available on the substrates (column 9 in Table 3.4), the deviations being most significant for graft polymers with longer polybutadiene side chains. This is consistent with previous findings in the synthesis of arborescent polymers,[11] since the accessibility of the chlorosilane coupling sites should be restricted due to steric limitations.

The coupling efficiency, defined as the fraction (percentage) of chlorosilane coupling sites consumed in the reaction, was calculated as the ratio of branching functionality f_n to the number of coupling sites C_s on the substrate, calculated according to the equation

$$C_s = \frac{[(M_n)_{core} - (Fw)_{DS}]}{M_{BD}} \times 0.52 \times 2 \qquad (3.5)$$

where $(M_n)_{core}$ represents the number-average molecular weight of the star-like polymer used as substrate, $(F_W)_{DS}$ represent the formula weight of the dendrimer substrate used for star-like polymer synthesis, 0.52 correspond to the mole fraction of 1,2-units in the arms of the star-like polymer, M_{BD} is the molecular weight of the butadiene unit (54.04), and the factor 2 accounts for the presence of two coupling sites in each dichloromethylsilane

unit added. The coupling efficiency decreases as the length of the polybutadiene side chains increases, and likewise as the number of coupling sites on the substrate increases (column 10 in Table 3.4). This decrease is again attributed to increased congestion of the substrate leading to decreased accessibility of the chlorosilane coupling sites.

The absolute number-average molecular weight (M_n) and polydispersity index (PDI = M_w/M_n) of the arborescent polymers obtained as determined by SEC-MALLS analysis are provided in Table 3.4. A narrow MWD was achieved for all samples, with PDI $\leq$ 1.08 except for the samples synthesized using substrate RS128. It is not clear whether the comparatively higher PDI values obtained for the sample RS128 samples (PDI = 1.13-1.16) is linked to separation problems encountered in the SEC analysis of these very large molecules, to the higher PDI value obtained for the corresponding star-like precursor (PDI = 1.16), or to the lower coupling efficiencies achieved in these reactions.

3.4 Conclusions

A series of carbosilane dendritic macromolecules was synthesized from a tetravinylsilane central core, by hydrosilylation of the vinylsilane moieties with dichloromethylsilane and nucleophilic displacement of the chloride anions with vinylmagnesium chloride. The ^{1}H NMR spectra obtained were consistent with the structure of the molecules and the narrow, symmetrical SEC peaks obtained are consistent with a perfect structure. The carbosilane dendrimers, modified to contain 32, 64, or 128 peripheral Si-Cl sites served as coupling substrates for low molecular weight 1,2-polybutadienyllithium. The 1,2-polybutadiene star-like hybrids also had narrow

molecular weight distributions (PDI = 1.03-1.16). The star-like polymers were further hydrosilylated with dichloromethylsilane and used as coupling substrates for 1,4-polybutadienyllithium. Three series of dendrimer-arborescent hybrids were thus obtained containing 1,4-polybutadiene side chains with $M_n \approx 1500$, 5000, or 30000. The arborescent hybrids had narrow molecular weight distributions, with PDI $\leq$ 1.08 for all but two samples. The arborescent hybrids have branching functionalities reaching 10 times higher than for star-branched polybutadienes synthesized previously. The branching functionalities obtained were nonetheless lower than the nominal (theoretical) values, the deviations being largest for graft polymers with longer side chains.

Interesting physical properties are expected for these polybutadiene arborescent hybrids, due to their very high branching functionality and compact structure in combination with the very low entanglement molecular weight of the PBD segments (M_e = 1800 for 1,4-polybutadiene). The detailed rheological characterization of these materials will be the subject of future work.

3.5 References

1. Roovers, J. *Macromolecules* **1991**, *24*, 5895.
2. Roovers, J.; Toporowski, P. M. *Macromolecules* **1987**, *20*, 2300.
3. Masuda, T.; Ohta, Y.; Onogi, S. *Macromolecules* **1986**, *19*, 2524.
4. (a) Khadir, A.; Gauthier, M. *Polym. Mater. Sci. Eng*. **1997**, *77*, 174. (b) Schmaljohann, D.; Pötschke, P.; Hässler, R.; Voit, B. I.; Froehling, P. E.; Mostert, B.; Loontjens, J. A. *Macromolecules* **1999**, *32*, 6333. (c) Nunez, C. M.; Chiou, B.-S.; Andrady, A. L.; Khan, S. A. *Macromolecules* **2000**, *33*, 1720.

5. (a) Rempp, P.; Franta, E.; Herz, J.-E. *Adv*. *Polym*. *Sci*. **1988**, *86*, 145. (b) Hsieh, H. L.; Quirk, R. P. *Anionic Polymerization*: *Principles and Practical Applications*; Dekker: New York, 1996; Chapters 13.

6. Zhou, L.-L.; Hadjichristidis, N.; Toporowski, P. M.; Roovers, J. *Rubber Chem*. *Technol*. **1992**, *65*, 303.

7. Roovers, J.; Zhou, L.-L.; Toporowski, P. M.; Zwan, M.; Iatrou, H.; Hadjichristidis, N. *Macromolecules* **1993**, *26*, 4324.

8. Roovers, J.; Toporowski, P.; Martin, J. *Macromolecules* **1989**, *22*, 1897.

9. Comanita, B.; Noren, B.; Roovers, J. *Macromolecules* **1999**, *32*, 1069.

10. Heise, A.; Diamanti, S.; Hedrick, J. L.; Frank, C. W.; Miller, R. D. *Macromolecules* **2001**, *34*, 3798.

11. Teertstra, S. J.; Gauthier, M. *Prog*. *Polym*. *Sci*. **2004**, *29*, 277.

12. Lipton, M. F.; Sorensen, C. M.; Sadler, A. C.; Shapiro, R. H. *J. Organomet. Chem*. **1980**, *186*, 155.

13. Gauthier, M.; Tichagwa, L.; Downey, J. S.; Gao, S. *Macromolecules* **1996**, *29*, 519 and Supporting Information.

14. Zhou, L.-L.; Roovers, J. *Macromolecules* **1993**, *26*, 963.

15. Liu, W.-L.; Loveless, F. C. U.S. Patent 5 489 649, 1996.

16. Tanaka, Y.; Takeuchi, Y.; Kobayashi, M.; Tadokoro, H. *J*. *Polym*. *Sci*. *Part A-2, Polym*. *Phys*. **1971**, *9*, 43.

17. Young, R. N.; Quirk, R. P.; Fetters, L. J. *Adv*. *Polym*. *Sci*. **1984**, *56*, 1.

18. Carella, J. M.; Graessley, W. W.; Fetters, L. J. *Macromolecules* **1984**, *17*, 2775.

19. Halasa, A. F.; Lohr, D. F.; Hall, J. E. *J. Polym. Sci., Polym. Chem. Ed.* **1981**, *19*, 1357.

20. Uraneck, C. A. *J. Polym. Sci., Part A-1,* **1971**, *9*, 2273.

21. Bywater, S.; Firat, Y.; Black, P. E. *J. Polym. Sci., Polym. Chem. Ed.* **1984**, *22*, 669**.**

22. Hillmyer, M. A.; Bates, F. S. *Macromolecules* **1996**, *29,* 6994.

Chapter 4

Large-scale Synthesis of Arborescent Polystyrenes

4.0 Abstract

A method for the large (100-g) scale synthesis of arborescent polystyrenes based on acetyl coupling sites was developed. The acetyl functionalities were introduced randomly on the grafting substrate by reacting polystyrene with acetyl chloride in nitrobenzene in the presence of anhydrous $AlCl_3$. Styrene was polymerized with *sec*-butyllithium to yield polystyryllithium serving as side chains in the coupling reaction with the acetylated substrate. A grafting procedure developed previously for small-scale (10 – 15 g) reactions, based on end-capping of polystyryllithium with 2-vinylpyridine units in the presence of LiCl, led to a low grafting yield (75 % for a linear substrate) when scaled up to 100 g. The decreased yield was linked to side chain dimerization and deactivation of the macroanions. The modified 100-g scale procedure developed, using end-capping of the polystyryllithium with 1,1-diphenylethylene in the presence of LiCl, followed by the addition of 3 – 6 equivalents per side chain of dilute 2-vinylpyridine solution, eliminated side chain dimerization and led to grafting yields of up to 95 %. Successive acetylation and anionic grafting reaction cycles were used to synthesize arborescent polystyrenes of generations up to G2 with low polydispersity indices ($M_w/M_n \leq 1.04$) and molecular weights increasing in an approximately geometric fashion for each cycle.

4.1 Introduction

Arborescent polymers, along with dendrimers and hyperbranched polymers, are highly branched macromolecules belonging to the dendritic polymers family,[1] which is characterized by a cascade-branched structure. Numerous synthetic methods have been suggested for the preparation of these materials.

Dendrimers are generally synthesized from AB_n monomers (n = 2 or 3) according to divergent[2] or convergent[3] schemes. In the divergent strategy, the dendrimer is assembled stepwise from the central core to the periphery. In the convergent approach, in contrast, wedge-like dendrons are constructed from the periphery towards the center and assembled in a final step to yield the dendrimer. Both approaches allow strict control over the branching process and can lead to well-defined dendritic structures with very narrow molecular weight distributions ($M_w/M_n \leq 1.01$). In many cases, however, steric limitations can produce structural imperfections affecting the topology of the molecules, especially for higher generations. Since small molecules serve as building blocks in the syntheses, the increase in molecular weight per generation is generally low, and many reaction cycles are necessary to achieve a high molecular weight.

Hyperbranched polymers can be synthesized with a high molecular weight in a one-pot reaction from appropriately activated AB_n monomers.[4,5] Since these polymers are derived from random condensation reactions, they are generally characterized by an irregularly branched structure and a much broader molecular weight distribution than dendrimers. Nevertheless, significant progress has been achieved recently in terms of controlling the molecular weight, the molecular weight distribution, and the degree of branching in these syntheses.[6-8]

Arborescent graft polymers,[1] also referred to as Comb-burst[9] or dendrigraft polymers, have been synthesized using successive grafting reactions of polymeric building blocks, to minimize some of the problems encountered in dendrimer and hyperbranched polymer syntheses. The increases in branching functionality and molecular weight per generation thus attained are much higher than for dendrimer syntheses. Arborescent polymers with over 10^3 branches and molecular weights reaching $10^7 - 10^8$ are typically obtained in 3 to 4 reaction cycles. The structure of arborescent polymers is well-defined in terms of branching functionality, branch length, and molecular weight distribution (typically $M_w/M_n \approx 1.1$).

The synthesis of arborescent polymers is achieved using cycles of substrate functionalization and anionic grafting reactions.[10] Coupling sites are first introduced randomly on a linear substrate, and reacted with a 'living' polymer to yield a comb-branched or generation zero (G0) arborescent polymer. Repetition of the functionalization and grafting cycles leads to upper generation (G1, G2…) arborescent polymers, with molecular weights and branching functionalities increasing geometrically for successive generations. Both chloromethyl[1] and acetyl[11] functionalities have been used as coupling sites for the preparation of arborescent styrene homopolymers on a small (10 – 15 g) scale. Copolymers were also obtained on a small scale by grafting other macroanions onto arborescent polystyrene substrates.[12,13] Analogous reactions on a larger scale (100 g and over) based on the chloromethylation path are impractical because of the need for large amounts of chloromethyl methyl ether, a known carcinogen,[14] in the substrate functionalization procedure. The alternate grafting reactions based on acetylation,[11] when scaled to 100 g, are marred by much lower grafting yields than the

analogous small-scale reactions. The coupling reaction should ideally proceed in high yield, to minimize the need for purification of the products by time-consuming procedures such as precipitation fractionation.

We are now reporting on a modified procedure suitable for the large (100-g) scale synthesis of arborescent graft polystyrenes using acetyl coupling sites. The usefulness of the new method is demonstrated with the synthesis of successive generations of arborescent polystyrenes incorporating side chains with molecular weights of either 5000 or 30000.

4.2 Experimental Section

4.2.1 Solvent and Reagent Purification

Tetrahydrofuran (THF; Caledon, reagent grade) was purified by distillation from sodium-benzophenone ketyl under nitrogen. Toluene (Aldrich, 99 %) was purified by distillation from oligostyryllithium under nitrogen. The dry solvents were introduced directly from the stills into the polymerization reactor or ampule preparation manifolds through polytetrafluoroethylene (PTFE) tubing. Styrene (Aldrich, 99 %) and 2-vinylpyridine (2VP, Aldrich, 99 %) were purified by distillation after stirring over CaH_2 overnight. 1,1-Diphenylethylene (DPE, Aldrich, 97 %) was purified by adding enough *n*-butyllithium solution (Aldrich, 2.5 M in hexane) to obtain the deep red 1,1-diphenylhexyllithium coloration, and distillation under reduced pressure. The purified monomers were stored under nitrogen at -20 ^{o}C until a second purification step immediately before use. *sec*-Butyllithium (Aldrich, 1.3 M in cyclohexane) was used as received; the exact activity of the solution was determined by the method of

Lipton et al.[15] Acetyl chloride (Aldrich, 99 %), nitrobenzene (Aldrich, 99 %), and all other reagents were used as received. All the reagent ampules used in the polymerization and grafting procedures were prepared by high-vacuum techniques and filled with dry nitrogen.[16] The ampules were equipped with PTFE stopcocks and ground glass joints for mounting directly on the polymerization reactor.

4.2.2 Styrene Polymerization

Styrene (154 g, 1.48 mol) was further purified immediately before polymerization with phenylmagnesium chloride (Aldrich, 2.0 M solution in THF, 15 mL) using a high-vacuum purification technique.[16] A 2-L glass reactor equipped with a vacuum-tight mechanical stirrer was used to polymerize styrene. The reactor was first evacuated and flamed, filled with N_2, and then 1000 mL of toluene was added. Residual impurities were titrated by adding a few drops of styrene and enough *sec*-BuLi to obtain a persistent light yellow color at room temperature (23 °C). After cooling to 0 °C the calculated amount of *sec*-BuLi solution (22.8 mL, 30.8 mmol, for a target M_n = 5000) was added, followed by the styrene monomer over 10 min. The reaction mixture was then warmed to room temperature (23 °C) and stirred for 45 min. After cooling to -78 ^{o}C, dry THF (300 mL) was added slowly over a period of 5 min, to increase the rate of polymerization. After 15 min, the reaction was terminated with degassed methanol and the polymer was recovered by precipitation in methanol and drying under vacuum (yield 150 g).

4.2.3 Acetylation of Polystyrene

A 50.0 g sample of polystyrene (480 meq styrene units) was dried under vacuum in a 2-L round-bottomed flask, and dissolved in 650 mL of nitrobenzene. A catalyst solution was prepared by dissolving anhydrous $AlCl_3$ (22.4 g, 168 mmol) in 100 mL of nitrobenzene before adding acetyl chloride (14.4 mL, 202 mmol). The solution was added dropwise to the polymer solution over 30 min at room temperature (23 °C), and the reaction was allowed to proceed further for 30 min. Workup of the products first involved precipitation of the acetylated polymer in 2 L of methanol acidified with 100 mL of concentrated (11 M) HCl as a first step. The polymer was further purified by three cycles of dissolution in THF (200 mL) and precipitation in acidified methanol (1.5 L + 20 mL HCl), and two cycles of dissolution in THF (200 mL) and precipitation in methanol (1.5 L). The same procedure was used to purify the acetylated branched polystyrene substrates for the synthesis of the higher generation arborescent polymers.

4.2.4 Grafting Reaction

Arborescent polystyrenes were prepared by coupling living polystyryl anions with the acetylated polystyrene substrates. A typical 100-g scale grafting reaction is described in the following procedure for the synthesis of linear polystyrene grafted with M_n = 5000 side chains (PS-*g*-PS5) as an example. Styrene (105 g, 1.0 mol) was purified as described in Section 4.2.2. 2-Vinylpyridine (6.6 g, 63 mmol) was further purified on a high-vacuum manifold with three freezing – evacuation – thawing cycles in the presence of CaH_2 (~ 0.7 g) followed by slow distillation to a glass ampule. The monomer was diluted with ~ 60 mL of dry THF, and the ampule was filled with nitrogen. DPE (4.5 g, 25.2 mmol) was purified in an ampule by three cycles of azeotropic distillation with 10 mL of dry THF,

diluted by adding ~ 30 mL of dry THF, and the ampule was filled with nitrogen. All the monomer ampules were stored at -5 °C until needed. The partially (30 %) acetylated linear polystyrene substrate (10.1 g, 25.7 meq acetyl groups) was purified in an ampule by three cycles of azeotropic distillation using 100 mL of dry THF, dissolution in 100 mL of dry THF, and filling with nitrogen.

A 3-L glass reactor equipped with a vacuum-tight mechanical stirrer was fitted with the ampules containing the purified monomers, the acetylated polystyrene substrate, the dry toluene and THF inlets, and a septum. Solid LiCl (8.9 g, 210 mmol) was loaded in the reactor before it was evacuated, flamed, and purged with nitrogen. Toluene (500 mL) was then added, and residual impurities were titrated at room temperature (23 °C) with *sec*-BuLi after adding a few drops of styrene. After cooling the reactor to 0 °C the calculated amount of *sec*-BuLi solution (15.5 mL, 21.0 mmol for a target side chain M_n = 5000) was then added, followed by the styrene monomer over a period of 10 min. The reactor was then warmed to room temperature (23 °C) with stirring. After 45 min, the reactor was cooled to -78 ^{o}C and dry THF (1000 mL) was added over a period of 10 min, to increase the rate of polymerization. A sample of the polystyryl anions was removed from the reactor after 15 min and terminated with degassed methanol for the characterization of the side chains. The DPE solution was then added over 5 min, giving a color change from orange to red. A sample of the DPE-capped polystyryl anions was also removed from the reactor and terminated with degassed methanol after 15 min. The 2VP solution was then added over 10 min, giving a color change from red to dark red. After 15 min, a sample of the 2VP-capped chains was removed from the reactor and terminated with degassed methanol. The reactor was then warmed to room temperature

(23 °C) and the living polymer solution was slowly titrated with the acetylated polystyrene solution over 30 min to a pink color. Stirring was continued for 60 min at room temperature, and the residual coloration disappeared. The product was recovered by precipitation in methanol, dried under vacuum (crude product yield 120 g, grafting yield 95 %), and purified by precipitation fractionation in a toluene-methanol mixture to remove linear chain contaminant from the products.

Similar conditions were used for the synthesis of higher generation polymers, however 6 equiv of diluted 2-vinylpyridine solution per side chain were used to cap the 30K side chains.

4.2.5 Polymer Characterization

Size exclusion chromatography (SEC) analysis was performed for the substrates before and after acetylation, the side chains, the raw grafting products, and the fractionated graft polymers. The SEC instrument, operated at room temperature, consisted of a Waters 510 HPLC pump, a 500 mm × 10 mm Jordi DVB linear Mixed-Bed column (molecular weight range 10^2-10^7), and a Waters 410 differential refractometer detector. THF at a flow rate of 1 mL/min served as eluent for the analysis. Polystyrene-equivalent molecular weights (M_n, M_w) and polydispersity indices (PDI = M_w/M_n) were determined for the samples using a linear polystyrene standards calibration curve.

The absolute number-average molecular weight (M_n) and PDI of the graft polymers were determined by SEC-MALLS (multiangle laser light scattering) analysis using a Wyatt Dawn DSP-F instrument operating at 632.8 nm. The SEC-MALLS system consisted of a Waters 590 programmable HPLC pump coupled with Waters Ultrastyragel

columns (10^4, 10^5, and 10^6 Å pore sizes) using THF at a flow rate of 1 mL/min as eluent. Polymer concentration measurements were accomplished with a Waters 2410 DRI detector operating at 660 nm. The molecular weights were determined from the MALLS and the DRI signals, using the Astra Version 4.70.07 software package.

^{1}H NMR spectroscopy served to determine the acetylation level of the grafting substrates. A Bruker-300 (300 MHz) nuclear magnetic resonance spectrometer was used to obtain the spectra in $CDCl_3$ at a concentration of 5 % w/v.

4.3 Results and Discussion

The coupling reaction between polystyryllithium and acetylated polystyrene is described in Scheme 4.1. It involves nucleophilic addition on the carbonyl group of the capped macroanion (capping agent Z = 1 equiv DPE, and 3 equiv 2VP for M_n = 5000 side chains or 6 equiv 2VP for M_n = 30000 side chains). The synthesis comprises three steps: the substrate is acetylated to introduce coupling sites; the polymerization of styrene with *sec*-butyllithium generates living polystyryllithium, which is then end-capped to modify its reactivity; and titration of the living polymer with the acetylated polystyrene substrate produces the graft polymer. Specific aspects of each reaction step have been examined in detail elsewhere,[11] so the discussion will be limited to the modifications necessary to the procedure to optimize the grafting yield.

4.3.1 Linear Polystyrene Synthesis and Acetylation Procedure

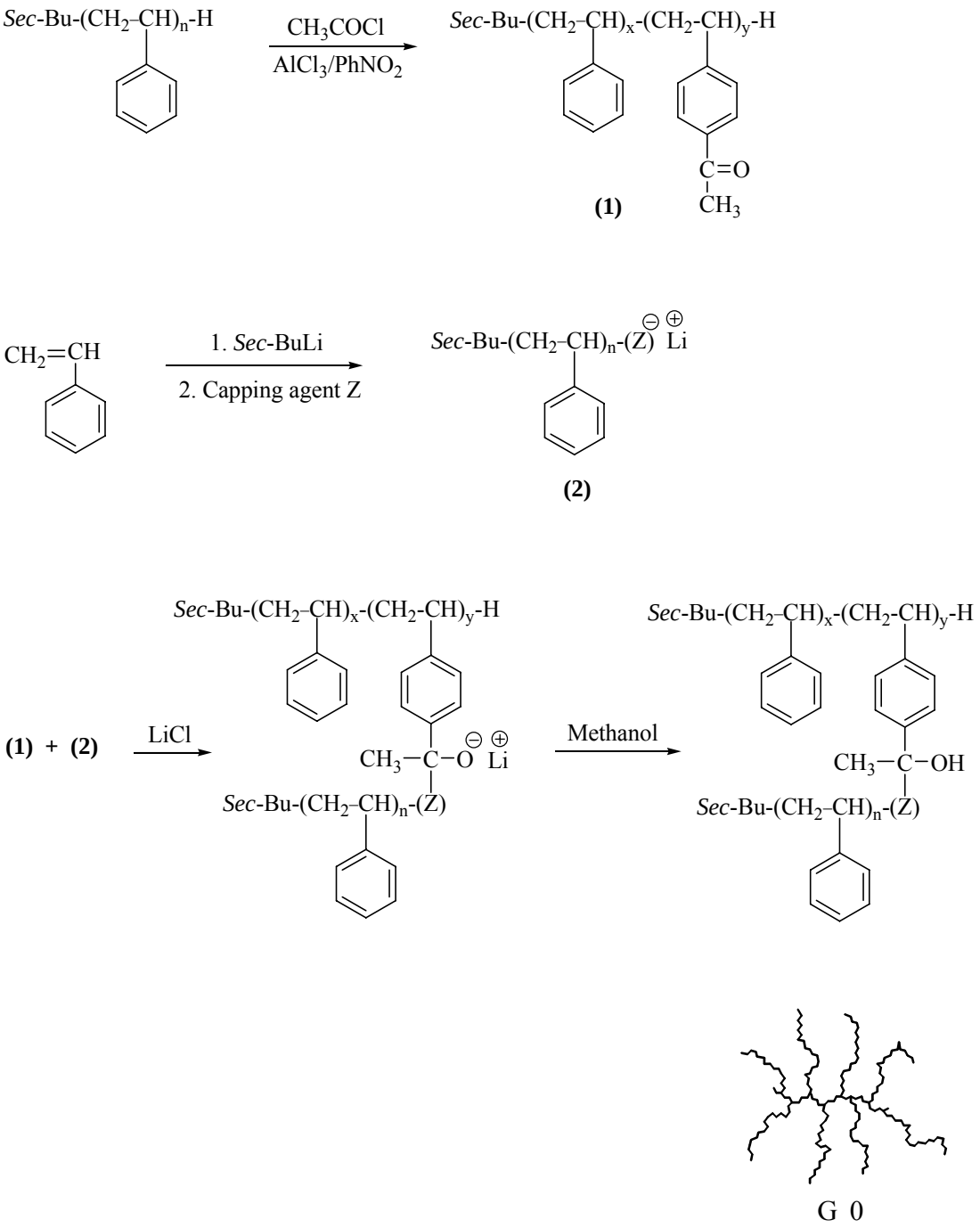

Scheme 4.1 Grafting reaction of acetylated polystyrene with capped polystyryllithium. The capping agents Z are DPE and 2VP.

The linear polymer obtained in a toluene/THF mixture had a number-average molecular weight M_n = 5200, close to the expected molecular weight, and a narrow molecular weight distribution (M_w/M_n = 1.06). The acetylation of polystyrene was performed with acetyl chloride in the presence of anhydrous $AlCl_3$ in nitrobenzene according to a known procedure.[11] Variation of the acetylation level provides control over the branching density along the backbone, and thus over the structural rigidity of the polymers.[17] The acetylation level can be controlled by adding nearly stoichiometric amounts of $AlCl_3$ and acetyl chloride in the reaction, but was maintained in the 20 – 30 mol % range for all generations in the present study to generate 10 – 15 grafting sites per $M_n \approx 5000$ polystyrene side chain. A substitution level of 30 mol % was attained for the linear substrate, as determined by ^{1}H NMR spectroscopy analysis. SEC analysis of the acetylated polymer yielded an apparent (polystyrene equivalent) M_n = 5500 and M_w/M_n = 1.06. While the SEC analysis results before and after acetylation cannot be compared directly, the low polydispersity index values obtained for both samples at least suggest that the acetylation reaction proceeded without cross-linking or chain cleavage reactions.

4.3.2 Grafting of Polystyryllithium and Reactivity Attenuation by End-capping

To maximize the grafting yield, defined as the fraction of living chains coupled to the substrate, the conditions of the 100-g scale reactions were first optimized for the coupling reaction with linear acetylated polystyrene. For the test reaction, $M_n \approx 5000$ polystyrene side chains were grafted onto the partially acetylated M_n = 5200 linear polystyrene substrate with an acetylation level of 30 mol % (15 coupling sites per chain). The grafting reactions were performed in a toluene/THF (1:2 v/v) mixture. The

polymerization of styrene was initiated in toluene at room temperature (23 ^{o}C) for 45 min, and THF was added to the reaction after cooling to -78 ^{o}C to increase the polymerization rate. After capping of the chains, the grafting reaction was performed at room temperature (23 °C).

In a previous study[11] it was shown that the solvent composition and the temperature had no significant influence on the grafting yield attained. The reported procedure for the small-scale synthesis of arborescent polymers,[11] using capping of the macroanions with 3 equiv of 2VP and LiCl, proceeded with 95 % yield. The SEC traces obtained for the polystyryl anions, the 2VP-capped polystyryl anions, and the crude grafting product in a 100-g reaction are compared in Figures 4.1. The grafting yield, calculated from the relative peak areas for the graft polymer and the other peaks in Figure 4.1c, was only 75 %. The SEC traces of Figures 4.1a and 4.1b show that the polystyrene side chains have a MWD that is unimodal and narrow before capping, but becomes bimodal after capping with 2VP. The elution volumes for the peaks in Figure 4.1b correspond to polystyrene-equivalent (apparent) molecular weights of 5300, 10400 for the rightmost and the leftmost peak, respectively, and are consistent with the occurrence of dimerization reactions in the capping step. The anionic polymerization of 2VP is known to be very fast in THF, among others due to the presence of "triple ions" at the chain ends.[18] The very quick consumption of 2VP as it is added to the reactor may leave some of the macroanions non-capped, simply as a result of mixing inhomogeneities. The residual, highly reactive polystyryl anions may attack the 2VP ring of another capped chain in the position alpha to the nitrogen atom, causing dimerization of the side chains, as shown in Scheme 4.2. A similar side reaction was indeed suggested to explain the

formation of branched products in the synthesis of polystyrene-*block*-poly(2-vinylpyridine) copolymers without capping of the polystyryl anions prior to addition of 2VP.[19]

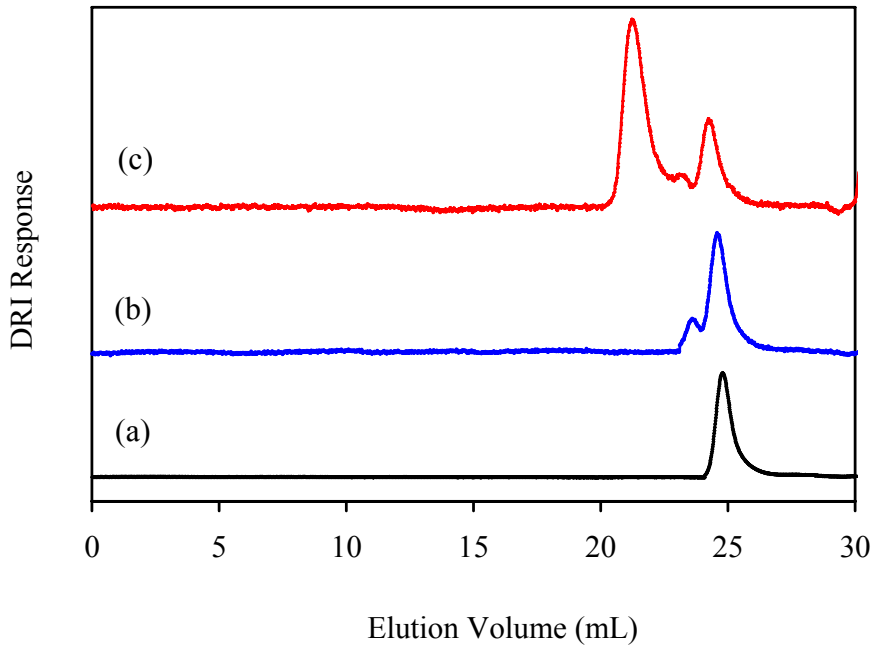

Figure 4.1 Synthesis of PS-*g*-PS5 before modification: SEC traces for (a) polystyryllithium before capping, (b) after capping with 3 equiv 2VP, and (c) crude product from the grafting reaction.

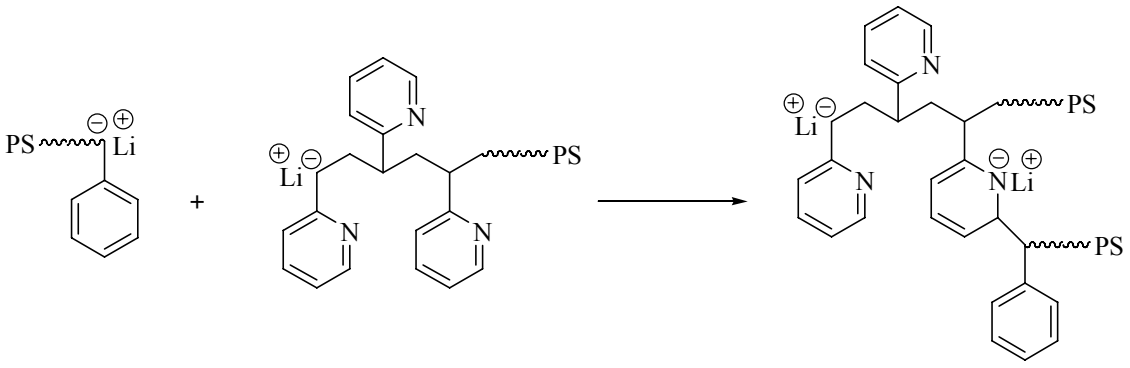

Scheme 4.2 Dimerization of the 2VP-capped polystyryllithium side chains

The carbonyl group is reactive towards nucleophilic addition, but it also makes the methyl protons on the acetyl functionality more acidic.[20] The highly reactive polystyryllithium anion of the non-capped chains can add to the carbonyl group and form the desired coupling product, but also add to the 2VP ring of another chain or undergo termination by abstraction of an acidic α-hydrogen. These competing side reactions are likely the major causes for the decreased grafting yield. Similar acidic hydrogen abstraction reactions have been observed, for example, in the sulfoalkylation reaction of polystyryllithium with 1,3-propane sultone, where abstraction by polystyryllithium of a proton α- to the sulfur atom decreased the functionalization yield.[21]

Considering the many uses of DPE as a capping agent reported in the literature,[1,22,23] the usefulness of DPE incorporation before the 2VP addition was also investigated. Because DPE does not homopolymerize, using ca. 1.2 equiv of DPE per living end ensures that all the chains are capped with one DPE unit, eliminating dimer formation upon 2VP addition (Figure 4.2a). It was previously shown that DPE capping of polystyryllithium is detrimental to the addition on acetyl coupling sites,[11] however, presumably due to the congested structure of the DPE-capped macroanions facilitating proton abstraction at the expense of nucleophilic addition. While DPE is not in itself a good capping agent for the coupling reaction of polystyryllithium with acetylated polystyrene, it is clearly useful to avoid dimer formation (Figure 4.2a). A grafting yield of 95 % was achieved after capping the polystyryllithium with DPE and 3 equiv of 2VP, to produce lower reactivity, less hindered macroanions than for DPE capping alone.

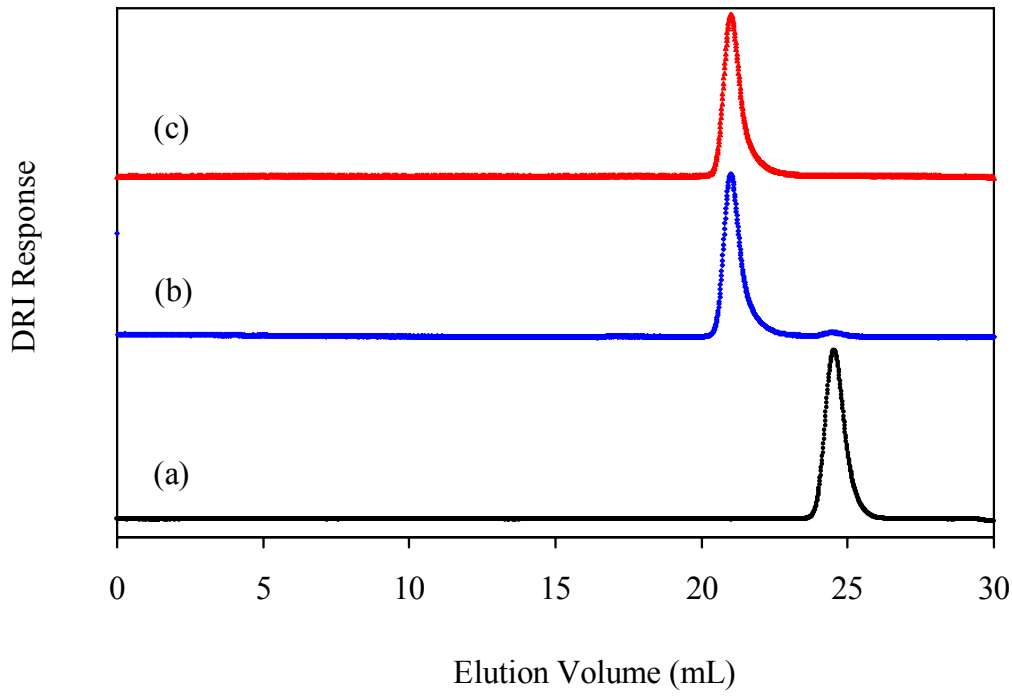

Figure 4.2 Large scale synthesis of PS-*g*-PS5 after modification: SEC traces for (a) polystyryllithium with DPE and 3 equiv 2VP addition, (b) crude product from the grafting reaction, and (c) fractionated graft polymer.

The yield of the arborescent polymer syntheses invariably decreased whenever the molecular weight of the macroanions used in the reaction was increased, and when grafting onto the higher generation, more congested substrates, irrespective of the type of macroanion and coupling site involved in the reaction.[10] Consequently, the large scale grafting reaction was also optimized for conditions more demanding than sample PS-*g*-PS5, based on short side chains and a very open, non-congested linear substrate structure. The synthesis of sample G0PS-*g*-PS30, using a more congested G0 substrate with an acetylation level of 24 mol % (223 coupling sites per substrate molecule) and $M_n \approx 30000$ polystyrene side chains was also investigated in more details. The 100-g scale reaction,

when performed with 1.2 equiv of DPE and 3 equiv of 2VP diluted 10-fold in the capping reaction, proceeded without side chain dimerization but with a grafting yield of only 17 %. The very low yield, even with DPE capping, is presumably linked to incomplete capping of the macroanions by 2VP as before. Another attempt was made by increasing the amount of 2VP used in the capping reaction to 6 equiv per living end after DPE capping. The grafting yield increased to 60 % under these conditions.

4.3.3 Arborescent Graft Polystyrenes

On the basis of the conditions optimized for the 100-g scale synthesis of samples PS-*g*-PS5 and G0PS-*g*-PS30, two series of arborescent polystyrenes with either short ($M_n \approx 5000$, PS5) or long ($M_n \approx 30000$, PS30) side chains grafted onto acetylated polystyrene substrates of different generations were synthesized, to examine the influence of the side chain size and the substrate generation number on the grafting yield. The characterization data obtained for the two sample series are summarized in Table 4.1. The substrates "G0PS" (PS-g-PS5) and "G1PS" (G0PS-g-PS5) were prepared by repetition of acetylation – grafting – fractionation reaction cycles using side chains with $M_n \approx 5000$ for each generation. Acetylation levels of 24 mol % (223 coupling sites) and 21 mol % (2220 coupling sites) were used for G0PS and G1PS substrates, respectively. Neither chain cleavage nor cross-linking was detected in the acetylation of the substrates prepared. Grafting in a toluene/THF (1:2 v/v) mixture at room temperature in the presence of LiCl was selected as a standard procedure for the preparation of the arborescent polystyrenes. The macroanions were capped with DPE, and 3 or 6 equiv of 2-vinylpyridine for $M_n \approx 5000$ and $M_n \approx$ 20-30000 side chains, respectively.

The nomenclature used to identify the arborescent polymers synthesized specifies the generation number of the substrate and the molecular weight of the side chains used in the last reaction. For example, G0PS-*g*-PS5 refers to a G0 polystyrene substrate grafted with $M_n \approx 5000$ side chains in the last reaction, while G0PS-*g*-PS30 refers to the same substrate grafted with $M_n \approx 30000$ side chains. It should be noted that sample PS-*g*-PS5 served as substrate G0PS after acetylation, and that G0PS-*g*-PS5 is the precursor for the G1PS substrate.

The results in Table 4.1 clearly demonstrate that when the branching functionality (generation) of the substrates or the molecular weight of the grafted side chains increase, the grafting yield decreases as expected. This effect is most pronounced when substrate G1PS is grafted with $M_n \approx 30000$ side chains. An important factor contributing to the deactivation of the living anions in the preparation of the higher generation polymers may be their reaction with residual protic impurities introduced with the substrate polymer solution: It is more difficult to purify these substrates after acetylation. To reach the end point (complete discoloration of the living anions) in the grafting procedure, an excess of substrate polymer must also be added for the preparation of the higher generation polymers. This approach, while maximizing the consumption of the anions (and the grafting yield), necessarily leads to the introduction of larger amounts of protic impurities in the reaction. Dependence of the grafting yield on the size of the polystyryl anions is also observed: The grafting yield for substrates of the same generation is always lower for the PS30 than for the PS5 sample series. The concentration of living ends in the reaction being lower for the higher molecular weight side chains, they are correspondingly more sensitive to deactivation by protic impurities.[11]

Table 4.1 Characteristics of Arborescent Polystyrenes of Successive Generations [a]

Sample [b]	Side Chains [c]		Grafting Yield (%) [e]	Graft Polymer				Coupling Efficiency (%) [i]
	M_n [d]	M_w/M_n [d]		M_n [f]	M_w/M_n [f]	M_n [g]	f_n [h]	
PS-*g*-PS5	5500	1.06	95	9.7×10^4	1.03	5.0×10^4	17	100
G0PS-*g*-PS5	4900	1.07	90	1.1×10^6	1.03	1.8×10^5	205	92
G1PS-*g*-PS5	5000	1.09	70	8.1×10^6	1.04	5.7×10^5	1400	63
PS-*g*-PS30	23000	1.10	86	4.2×10^5	1.03	1.6×10^5	18	100
G0PS-*g*-PS30	29000	1.08	60	3.6×10^6	1.03	5.2×10^5	121	54
G1PS-*g*-PS30	20700	1.05	30	9.4×10^6	1.04	5.4×10^5	401	18

a) All reactions in toluene/THF (1:2 v/v) at room temperature with 10 equiv LiCl. b) Acetylation level of the substrates for linear PS: 30 mol %, G0PS: 24 mol %; G1PS: 21 mol %. c) Short side chains capped with DPE and 3 equiv of 2VP, long side chains capped with DPE and 6 equiv of 2VP. d) Absolute values of the side chains determine by SEC analysis calibrated with linear polystyrene standards. e) Fraction of side chains generated attached to the substrate. f) Absolute values determined by SEC-MALLS analysis. g) Apparent values determined by SEC analysis using a linear polystyrene standards calibration curve. h) Number of branches added in the last grafting reaction. i) Fraction of available coupling sites on the substrate consumed in the reaction. The number of coupling sites on the PS, G0PS and G1PS substrates is 15, 223, and 2220, respectively.

The amount of linear and G0 acetylated polymers required in the titration of the living polymers is approximately as expected from the stoichiometry of the reaction. For the G1 substrate, however, a 30 – 50% excess of acetylated polymer was required to deactivate all the living ends. This suggests that the grafting reactions using the G1 acetylated substrate become diffusion-limited: Surface overcrowding can hinder the diffusion of the living chain ends to the acetyl sites, in analogy to the surface overcrowding effects reported in the synthesis of dendrimers.[2,24]

4.3.4 Sample Characterization

Size exclusion chromatography (SEC) characterization was performed for the grafting substrates before and after acetylation, the side chains, the crude grafting products, and to confirm the successful fractionation of the polymers. The SEC curves in Figure 4.2 illustrate the large scale synthesis of sample PS-*g*-PS5, starting with the chromatogram for the side chains capped with DPE and 2VP (M_n = 5500, M_w/M_n = 1.06, curve a). Two peaks, corresponding to the graft polymer and to linear contaminant, are observed in the SEC trace for the crude product in the absence of dimerization (curve b). The peak on the right has the same elution volume as the side chain sample removed before the grafting reaction (curve a). It corresponds to linear chains deactivated by residual protic impurities present in the acetylated polymer solution or the capping agent solution. The trace in Figure 4.2c confirms the complete removal of the linear polymer contaminant by fractionation.

The grafting yield (fraction of the living chains generated that is grafted on the substrate) can be calculated from the SEC trace for the crude product. The grafting yield

is calculated by comparing the peak area for the graft polymer to the total area of both peaks. For sample PS-*g*-PS5 (Figure 4.2), for example, a grafting yield of 95 % was obtained. The grafting yields reported in Tables 4.1 were obtained by the same method.

The absolute molecular weight of the graft polymers determined by SEC-MALLS analysis is reported in Table 4.1, along with the apparent values determined using a DRI detector. It is evident that the apparent M_n values are underestimated. This is due to the very compact (hard sphere-like) structure of arborescent polymers, as confirmed by static and dynamic light scattering,[17] and by viscosity measurements.[25] The polydispersity index remains low ($M_w/M_n \leq 1.04$) over successive generations of the graft polymers.

The number-average branching functionality (f_n) of the arborescent polymers, defined as the number of chains added in the last grafting reaction, was calculated from the equation

$$f_n = \frac{M_n(G) - M_n(G-1)}{M_n^{br}} \tag{4.1}$$

where $M_n(G)$, $M_n(G-1)$ and M_n^{br} are the absolute number-average molecular weight of graft polymers of generation G, of the preceding generation and of the side chains, respectively. The f_n values listed in Table 4.1 range from 17 to 1400 for the PS5 series, and from 18 to 401 for the PS30 series. Both sample series display a roughly geometrical increase in molecular weight and f_n with generation number.

The coupling efficiency, defined as the fraction (percentage) of acetyl coupling sites consumed in the reaction, can be calculated as the ratio of the branching functionality f_n to the number of coupling sites (C_s) on the substrate. The C_s were calculated according to the equation

$$C_s = \frac{(M_n)_{core}}{M_S} \times \%Acetylation \quad (4.2)$$

where $(M_n)_{core}$ represent absolute number-average molecular weight of the polymer used as a core (substrate), and M_S is the molecular weight of the styrene unit (104.16).

The coupling efficiency decreases as the length of the polystyrene side chains increases, and likewise as the number of coupling sites on the substrate increases (column 9 in Table 4.1). This decrease is attributed to increased congestion of the substrate leading to decreased accessibility of the coupling sites.

4.4 Conclusions

The results presented show that capping of polystyryllithium, first with a single DPE unit and then with 3-6 units of 2-vinylpyridine, provides a successful path for the large (100-g) scale synthesis of arborescent polystyrenes based on either M_n = 5000 or 30000 side chains. Cycles of acetylation and anionic grafting reactions led to well-defined arborescent polymers ($M_w/M_n \leq 1.04$) with a molecular weight and branching functionality increasing roughly geometrically for successive generations.

While these materials are useful as model weakly interacting branched polymers with a well-defined structure, there is also considerable interest in producing arborescent copolymers such as polystyrene-*graft*-poly(2-vinlypyridine), potentially useful as branched polyelectrolytes and microencapsulation agents. For this reason, the large (100-g) scale synthesis of arborescent copolymers based on acetyl coupling sites will be examined subsequently.

4.5 References

1. Gauthier, M.; Möller, M. *Macromolecules* **1991**, *24*, 4548.

2. (a) Tomalia, D. A.; Baker, H.; Dewald, J.; Hall, M.; Kallos, G.; Martin, S.; Roeck, J.; Ryder, J.; Smith, P. *Polym. J. (Tokyo)* **1985**, *17*, 117. (b) Tomalia, D. A.; Baker, H.; Dewald, J.; Hall, M.; Kallos, G.; Martin, S.; Roeck, J.; Ryder, J.; Smith, P. *Macromolecules* **1986**, *19*, 2466.

3. Hawker, C. J.; Fréchet, J. M. J. *J. Am. Chem. Soc*. **1990**, *112*, 7638.

4. Kim, Y. H. *Adv. Mater*. **1992**, *4*, 764.

5. Voit, B. I. *Acta Polym*. **1995**, *46*, 87.

6. Radke, W.; Litvinenko, G.; Müller, A. H. E. *Macromolecules* **1998**, *31*, 239.

7. Yan, D.; Zhou, Z. *Macromolecules* **1999**, *32*, 819.

8. Bharathi, P.; Moore, J. S. *Macromolecules* **2000**, *33*, 3212.

9. Tomalia, D. A.; Hedstrand, D. M.; Ferritto, M. S. *Macromolecules* **1991**, *24*, 1435.

10. For a recent review on arborescent and other dendrigraft polymers see Teertstra, S. J.; Gauthier, M. *Prog. Polym. Sci*. **2004**, *29*, 277.

11. Li, J.; Gauthier, M. *Macromolecules* **2001**, *34*, 8918.

12. (a) Kee, R. A.; Gauthier, M. *Macromolecules* **1999**, *32*, 6478. (b) Kee, R. A.; Gauthier, M. *Macromolecules* **2002**, *35*, 6526.

13. (a) Li, J.; Gauthier, M.; Teertstra, S. J.; Xu, H.; Sheiko, S. S. *Macromolecules* **2004**, *37*, 795. (b) Gauthier, M.; Li, J.; Dockendorff, J. *Macromolecules* **2003**, *36*, 2642.

14. (a) Figueroa, W. G.; Raszkowski, R.; Weiss, W. *New Engl. J. Med.* **1973**, 288, 1096. (b) Laskin, S.; Drew, R. T.; Cappiello, V.; Kuschner, M.; Nelson, N. *Arch. Envir. Health.* **1975**, *30*, 70.

15. Lipton, M. F.; Sorensen, C. M.; Sadler, A. C.; Shapiro, R. H. *J. Organomet. Chem.* **1980**, *186*, 155.

16. Gauthier, M.; Tichagwa, L.; Downey, J. S.; Gao, S. *Macromolecules* **1996**, *29*, 519.

17. Gauthier, M; Möller, M.; Burchard, W. *Macromol. Symp.* **1994**, *77*, 43.

18. Müller, A. H. E. In *Comprehensive Polymer Science*; Vol. 3; Allen, G.; Bevington, J. C. Eds.; Pergamon: New York, 1989; p 387.

19. Fontanille, M.; Sigwalt, P. *Bull. Soc. Chim. France* **1967**, 4095.

20. Gutsche, C. D. *The Chemistry of Carbonyl Compounds*; Prentice-Hall: Englewood Cliffs, 1967; p 17.

21. Quirk, R. P.; Kim, J. *Macromolecules* **1991**, *24*, 4541.

22. Freyss, D.; Leng, M.; Rempp, P. *Bull. Soc. Chim. France* **1964**, 221.

23. Quirk, R. P. In *Comprehensive Polymer Science, First Supplement*; Allen, G. Ed.; Pergamon: Oxford, 1992; p 83.

24. Tomalia, D. A.; Hall, M.; Hedstrand, D. M. *J. Am. Chem. Soc.* **1987**, *109*, 1601.

25. Gauthier, M.; Li, W.; Tichagwa, L. *Polymer* **1997**, *38*, 6363.

Chapter 5

Arborescent Polystyrene-*graft*-poly(2-vinylpyridine) Copolymers:

Large-scale Synthesis and Solution Polyelectrolyte Behavior

5.0 Abstract

A method was developed for the 100-g scale synthesis of arborescent (dendrigraft) copolymers with poly(2-vinylpyridine) (P2VP) segments. The branched polyelectrolyte precursors were obtained in up to 96 % yield by coupling 'living' P2VP macroanions with linear polystyrene and arborescent polystyrene substrates of generations G0 or G1, randomly functionalized with acetyl groups. Arborescent copolymers with $M_n \approx 5000$ or 30000 side chains and containing 87-98 mol % P2VP were thus synthesized. These materials are characterized by a very compact structure, a narrow molecular weight distribution (M_w/M_n = 1.08-1.10), and a roughly geometric increase in branching functionality and molecular weight for successive generations. The copolymers are freely soluble in water and in polar organic solvents such as methanol and N,N-dimethylformamide (DMF) upon protonation by trifluoroacetic acid (TFA). The solutions obtained display properties typical of polyelectrolytes, including strong curvature in plots of reduced viscosity (η_{sp}/C) *versus* concentration (C) at both low and high concentrations. The copolymers exhibit larger reduced viscosity increases in methanol than in DMF, and coil expansion apparently varies in the order G1 > G0 > G2. The reduced viscosity of the arborescent polyelectrolyte solutions is much lower than for linear P2VP samples of comparable molecular weights, however, due to the small dimensions and increased structural rigidity of the molecules. The addition of salts to the branched polyelectrolyte solutions further decreases their viscosity and suppresses the curvature of the reduced viscosity plots, presumably as a result of charge screening.

5.1 Introduction

Polyelectrolytes exhibit properties in solution very distinct from both neutral macromolecules and low molecular weight electrolytes.[1] This is due to the combination of properties derived from long-chain macromolecules with those arising from electrostatic interactions. These properties are not simply superimposed, as there is a mutual influence of the characteristics of both components. Bound charges on the polyelectrolyte chains lead to intra- and intermolecular interactions that are stronger and of much longer range than for neutral macromolecules. A direct consequence of the charge interactions is the expansion of the polymer coil due to strong electrostatic repulsion of the ionic groups. The properties of these polymers in solution depend on different parameters including the degree of dissociation of the ionic groups, the solvent quality for the polymer backbone, the dielectric constant of the solvent, and the presence of salts.[2] One major factor controlling the solution properties of polyelectrolytes is the balance between intramolecular and intermolecular interactions. Intramolecular interactions typically dominate at low concentrations, while intermolecular interactions dominate at higher concentrations.[3] The polyelectrolyte effect is well-documented for linear polyelectrolytes, but it is poorly understood for branched polymers.

Arborescent polymers[4] provide an excellent opportunity to investigate the effects of branching in polyelectrolytes systematically, because they can be prepared with a wide range of structures, incorporating different side chain sizes and branching functionalities. Arborescent polymers are derived from successive grafting reactions of well-defined polymeric building blocks. This “graft upon graft” approach makes it possible to obtain macromolecules with high branching functionalities and molecular weights in a few

reaction steps, while maintaining a narrow molecular weight distribution ($M_w/M_n \approx 1.1$). The synthesis of arborescent polymers starts with the random introduction of coupling sites along a linear polymer chain. 'Living' anionic polymer chains are then coupled with the linear substrate to generate a comb-branched (generation 0 or G0) polymer. Repetition of the functionalization and coupling reactions cycle leads to higher generation (G1, G2, etc.) arborescent polymers.

This grafting strategy has been used for the synthesis of arborescent polystyrenes using cycles of acetylation and coupling with polystyryl anions, on both small (10 to 20-g)[5] and large (100-g) scales (as described in Chapter 4). A modified small-scale procedure to graft poly(2-vinylpyridine) (P2VP) side chains onto acetylated polystyrene substrates was also developed to generate polystyrene-*graft*-poly(2-vinylpyridine) copolymers, useful as dendritic polyelectrolyte precursors.[6]

We are now reporting on the large (100-g) scale synthesis of a series of arborescent 2-vinylpyridine copolymers incorporating P2VP segments grafted onto acetylated linear, comb-branched (G0), and G1 polystyrene substrates by adapting the reported small-scale procedure.[6] Two arborescent copolymer series, containing either $M_n \approx 5000$ (P2VP5 series) or $M_n \approx 30000$ side chains (P2VP30 series) were synthesized. Characterization results for the copolymers by size exclusion chromatography and ^{1}H NMR spectroscopy are discussed. The P2VP copolymers are easily converted to polyelectrolytes upon protonation by a strong acid such as trifluoroacetic acid (TFA), and are freely soluble in water and in polar organic solvents such as methanol and N,N-dimethylformamide (DMF). The reduced viscosity (η_{sp}/C) of arborescent polyelectrolyte

solutions was investigated as a function of concentration (C) and structure for the two families of P2VP copolymers synthesized.

5.2 Experimental Section

5.2.1 Solvent and Reagent Purification

Tetrahydrofuran (THF; Caledon, reagent grade) was purified by refluxing and distillation over sodium-benzophenone ketyl under dry nitrogen atmosphere. The dry solvent was introduced directly from the purification still into the reactor or ampule preparation manifolds through polytetrafluoroethylene (PTFE) tubing. 2-Vinylpyridine (2VP, Aldrich, 99 %) was purified by distillation at reduced pressure after stirring over CaH_2 overnight. The purified reagents were stored under nitrogen at -20 ^oC until needed. *sec*-Butyllithium (*sec*-BuLi; Aldrich, 1.3 M in cyclohexane) was used as received. The exact concentration of the solution was determined by the procedure of Lipton et al.[7] Lithium chloride (99.99+ %, Aldrich), acetyl chloride (Aldrich, 99 %), nitrobenzene (Aldrich, 99 %) and all other reagents were used as received. The reagent ampules used in the polymerization and grafting procedures were prepared with the help of high-vacuum techniques and then filled with nitrogen.[8] The ampules were equipped with high-vacuum PTFE stopcocks and ground glass joints, so they could be mounted directly on the polymerization reactor.

5.2.2 Arborescent Polystyrene-*graft*-poly(2-vinylpyridine) Copolymers

The synthesis of arborescent graft copolymers by coupling P2VP chains with polystyrene substrates bearing either chloromethyl[9,10] or acetyl[6] functional groups was

reported previously. Acetyl groups were used as coupling sites for the current study and only procedures differing significantly from those reported previously are described.

Linear, G0, and G1 partially acetylated polystyrene substrates were prepared by cycles of acetylation, grafting, and fractionation as described in Chapter 4. The branched substrates were synthesized from a polystyrene core and side chains with $M_n \approx 5000$. The copolymers were obtained by grafting P2VP macroanions with $M_n \approx 5000$ or 30000 onto the acetylated substrates. The polymerization of 2VP was performed in THF at -78 °C using *sec*-BuLi as initiator. The synthesis of PS-*g*-P2VP5 (G0 copolymer) from a $M_n \approx 5000$ linear acetylated polystyrene substrate and $M_n \approx 5000$ poly(2-vinylpyridine) side chains is provided as an example of a graft copolymer synthesis.

2-Vinylpyridine was purified further prior to polymerization on a high-vacuum manifold using three freezing-evacuation-thawing cycles in the presence of CaH_2, followed by slow condensation to a glass ampule. The monomer was then diluted 10-fold with dry THF, the ampule was purged with purified nitrogen, and stored at -5 °C until needed. The partially (30 mole %) acetylated linear polystyrene substrate (10.1 g, 25.7 meq acetyl groups) was purified in an ampule with three azeotropic distillation cycles using dry THF before redissolution in 100 mL of the solvent. Ampules containing purified 2VP (105 g, 1.00 mol in 1 L of THF), the acetylated substrate, the THF line from the drying still, and a septum inlet were mounted on a 3-L glass reactor equipped with a vacuum-tight mechanical stirrer. Solid LiCl (8.9 g, 210 mmol) was added to the reactor before it was evacuated, flamed, and purged with purified N_2. Dry THF (1 L) was then added directly from the drying still. After cooling the reactor to -78 °C a few drops of monomer and *sec*-butyllithium were added to scavenge impurities until a persistent faint

red color was observed, followed by the required amount of *sec*-BuLi (15.5 mL, 21.0 mmol) for a target side chain M_n = 5000. After 5 min the slow addition of 2VP was started, resulting in an immediate color change from faint to dark red. The 2VP addition was completed in 5 min. After 45 min, a sample of the side chains was removed with a syringe and terminated with degassed methanol. The remaining solution was warmed to room temperature (23 °C) and titrated with the acetylated polystyrene solution over ca. 30 min, until a residual pale red coloration was observed. Stirring was continued for 60 min at room temperature, leading to further fading of the color, and the remaining polymer chains were deactivated by injecting ~1 mL of degassed methanol in the reactor. The non-grafted P2VP side chains were removed from the crude product by precipitation fractionation using THF/methanol (4/1 v/v) as solvent and *n*-hexane as non-solvent. The purified copolymer was recovered by precipitation in *n*-hexane and dried under vacuum.

5.2.3 Linear Poly(2-vinylpyridine)

Linear poly(2-vinylpyridine) samples with $M_n \approx$ 65000, 230000, and 430000 were synthesized as a reference materials for comparison of their polyelectrolyte behavior with the arborescent copolymers. The conditions used were the same as for the side chains in the copolymer syntheses.

5.2.4 Polymer Characterization

A size exclusion chromatography (SEC) system calibrated with linear polystyrene standards was used for routine analysis of the polystyrene substrates, the P2VP side chains, the raw grafting products, and the fractionated graft copolymers. The instrument,

operated at room temperature, consisted of a Waters 510 HPLC pump, a 500 × 10 mm^2 Jordi DVB linear Mixed-Bed column (linear polystyrene molecular weight range 10^2-10^7), and a Waters 410 differential refractometer detector. THF at a flow rate of 1 mL/min served as eluent for the analysis of the polystyrene samples. N,N,N',N'-Tetramethylethylenediamine (Aldrich, 99 %; 5 % v/v) was added for the analysis of the P2VP side chains and the graft copolymers, to minimize their adsorption on the column.[11]

The absolute number-average molecular weight (M_n) and molecular weight distribution of the linear P2VP samples (reference materials) and the P2VP side chains were determined by SEC analysis with a laser light scattering (MALLS) detector using a MiniDawn (3-angle) detector from Wyatt Technology operating at 632.8 nm. The SEC-MALLS system consisted of a Waters 510 HPLC pump coupled with a 500 × 10 mm^2 Jordi DVB linear Mixed-Bed column (linear polystyrene molecular weight range 10^2-10^7) operated at room temperature. THF at a flow rate of 1 mL/min served as eluent, and polymer concentration measurements were accomplished with a Waters 410 DRI detector. The molecular weights were obtained from the MALLS and DRI signals using the Astra Version 4.70.07 software package.

Since the SEC-MALLS system used was dedicated exclusively to measurements in THF, absolute molecular weight measurements were not attempted for the graft copolymers. An alternate method was used to estimate the number-average molecular weight (M_n) of the copolymers, by combining the absolute M_n of the substrate (from SEC-MALLS analysis in pure THF) with the copolymer composition determined by ^1H NMR analysis. The composition was determined using a Bruker-300 (300 MHz) nuclear magnetic resonance spectrometer in $CDCl_3$ at a concentration of 5 %.

5.2.5 Viscosity Measurements

Flow times were determined for the pure solvents and the polymer solutions using a Cannon-Ubbelohde Size 75 viscometer immersed in a water bath at (25.0 ± 0.2) °C. The polymer solutions were prepared by dissolving 0.2-0.4 g of vacuum-dried polymer (depending on the sample) at room temperature in 10 mL of solvent (DMF, methanol, or water) with stirring for one day. The maximum concentration of the solutions was adjusted to either 2 or 4 % w/v, depending on the viscosity of the sample. The solutions and the solvents were filtered through 5 μm PTFE membrane filters before adding the protonating agent, trifluoroacetic acid (TFA), within a range of 0.1 to 3 equiv TFA per 2VP unit. The solutions were subsequently stirred for 30 days to ensure homogeneity. For aqueous solutions the filtration was accomplished only after addition of the protonating agent and stirring for one month. Series of five consistent (± 0.05 s) flow times were obtained for up to eleven different concentrations, using successive additions of solvent to the solution reservoir of the viscometer. Lithium chloride (LiCl) solutions at concentrations of 0.05 and 0.25 M in methanol and DMF were also added to the polyelectrolyte solutions protonated with 1.0 equiv TFA/2VP unit in some cases, to study the effect of added salt. In that case, a LiCl solution of identical concentration was used to dilute the polymer solution in the successive dilution procedure, to maintain a constant ionic strength at the different polymer concentrations. The reduced viscosity (η_{sp}/C) was determined as a function of concentration (C) for the linear P2VP homopolymers and for copolymers of different generations (G0-G2) with $M_n \approx 5000$ or 30000 P2VP side chains.

5.3 Results and Discussion

5.3.1 Synthesis

The arborescent polystyrene-*graft*-poly(2-vinylpyridine) copolymers synthesized in a previous study were obtained on a small (10- to 20-g) scale in up to 96 % yield.[6] The procedure used to couple P2VP anions with an acetylated linear polystyrene substrate as provided in Scheme 5.1 comprises three steps. The grafting substrate is acetylated to introduce coupling sites; 2-vinylpyridine is polymerized to generate 'living' poly(2-vinylpyridinyl)lithium; and the living polymer is titrated with the acetylated polystyrene substrate to yield the graft copolymer.

The characteristics of the linear and branched polystyrene substrates used in the preparation of the graft copolymers are summarized in Table 5.1. The substrates were obtained from cycles of acetylation, grafting, and fractionation as described in Chapter 4, using $M_n \approx 5000$ polystyrene core and side chains with a narrow molecular weight distribution.

The large (100-g) scale synthesis of P2VP arborescent copolymers is based on the procedure reported in reference 6 with some changes. In the initiation reaction, *sec*-BuLi served as initiator instead of 1,1-diphenyl-3-methylpentyllithium (generated in situ from *sec*-BuLi and DPE), as *sec*-BuLi was found to work equally well in the presence of LiCl. Dilution of the monomer (10-fold) was used to ensure homogeneity of the reaction mixture and a narrow molecular weight distribution, since 2VP is very reactive. Two series of arborescent copolymers incorporating either short ($M_n \approx 5000$, P2VP5) or long ($M_n \approx 30000$, P2VP30) P2VP side chains were derived from different acetylated polystyrene substrates. Characterization results for these copolymers are provided in Table 5.2. The graft copolymer sample nomenclature used in Table 5.2 specifies their

composition and structure. For example, G0PS-*g*-P2VP5 refers to a graft copolymer with $M_n \approx 5000$ P2VP side chains grafted onto a G0 (once-grafted) arborescent polystyrene substrate, while G0PS-*g*-P2VP30 refers to the same substrate grafted with $M_n \approx 30000$ P2VP side chains.

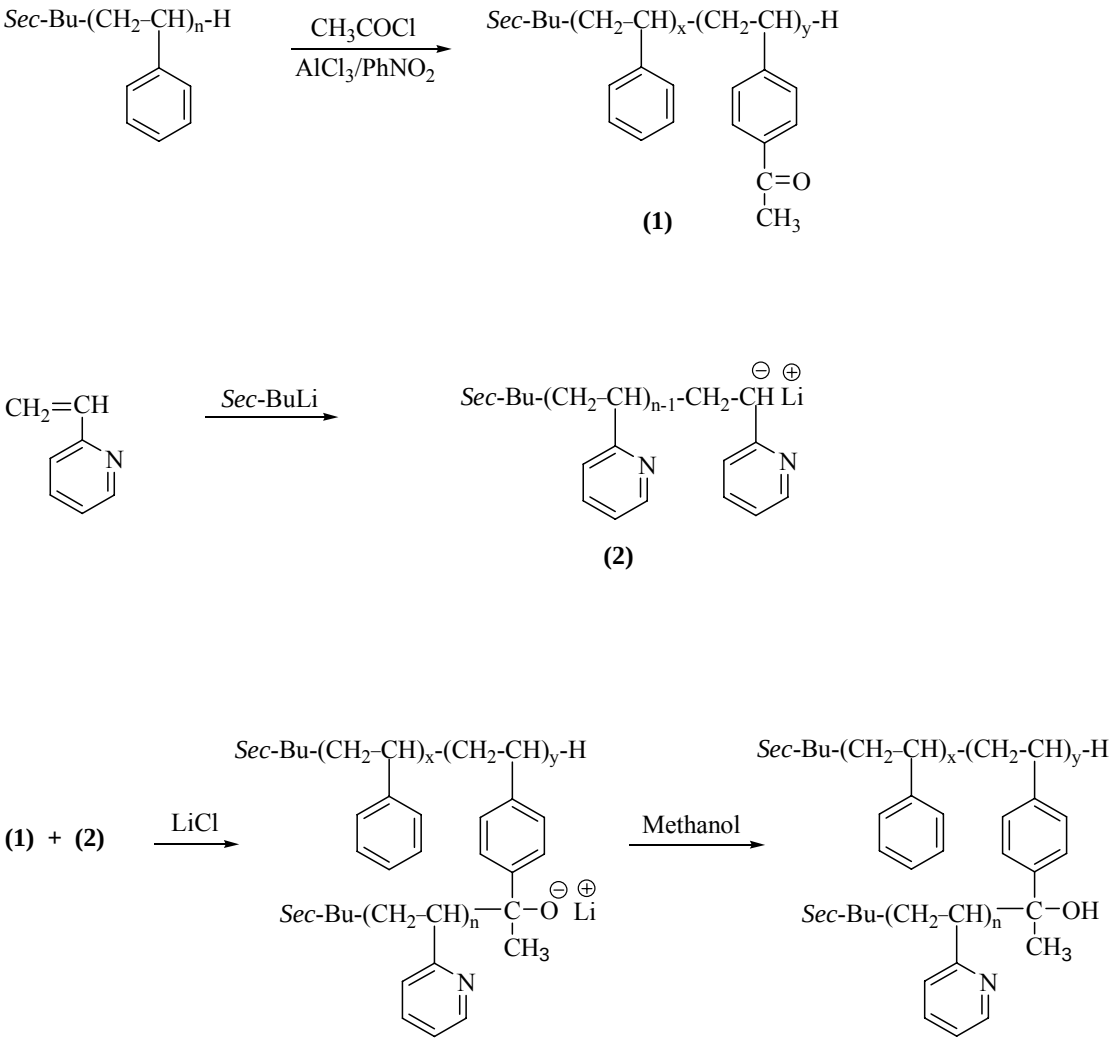

Scheme 5.1 Synthesis of polystyrene-*graft*-poly(2-vinylpyridine) copolymer.

Table 5.1 Characteristics of Polystyrene Substrates [a]

Polymer	Side Chains [b]		Substrate				
	M_n [c]	M_w/M_n [c]	M_n [d]	M_w/M_n [d]	f_n [e]	CH_3CO-/mole % [f]	Coupling sites
PS (linear)			5.2×10^3 [c]	1.06 [c]		30	15
G0PS	5500	1.06	9.7×10^4	1.03	17	24	223
G1PS	4900	1.07	1.1×10^6	1.03	205	21	2220

a) Substrates obtained by cycles of acetylation, grafting, and fractionation using $M_n \approx$ 5000 polystyrene core and side chains. b) Polystyrene branches end-capped with DPE and 3 equiv of 2VP. c) Absolute values determined by SEC analysis with a linear polystyrene standards calibration curve. d) Absolute values determined by SEC-MALLS analysis. e) Number of branches added in the last grafting reaction. f) Acetylation level determined by ^{1}H NMR spectroscopy analysis.

The grafting yield, defined as the fraction of the side chains generated becoming linked to the substrate, decreases significantly for higher generation substrates and for longer P2VP side chains, in agreement with a previous study.[6] Within each series, the grafting yield decreases as the generation (or branching functionality) of the coupling substrate increases (Table 5.2, Column 4). An important factor contributing to the deactivation of the living anions in the preparation of the higher generation copolymers may be their reaction with residual protic impurities introduced with the substrate

Table 5.2 Characteristics of Arborescent Poly(2-vinylpyridine) Copolymers of Successive Generations [a]

Sample	P2VP Side Chains		Grafting Yield (%) [c]	Graft Copolymer				Mol % P2VP [g]	Coupling Efficiency (%) [h]
	M_n [b]	M_w/M_n [b]		M_n [d]	M_w/M_n [e]	M_n [e]	f_n [f]		
PS-*g*-P2VP5	5100	1.15	96	7.4×10^4	1.08	4.1×10^4	13	93	90
G0PS-*g*-P2VP5	5500	1.15	90	1.1×10^6	1.08	1.1×10^5	182	91	82
G1PS-*g*-P2VP5	6200	1.10	70	8.4×10^6	1.09	1.6×10^5	1177	87	53
PS-*g*-P2VP30	31500	1.08	80	2.6×10^5	1.08	1.1×10^5	8	98	54
G0PS-*g*-P2VP30	27700	1.08	71	2.4×10^6	1.10	2.3×10^5	83	96	37
G1PS-g-P2VP30	32700	1.07	25	1.1×10^7	–	–	303	90	14

a) 2VP polymerization in THF at -78 °C and grafting at room temperature (23 °C) with 10 equiv LiCl added. b) Absolute values determined by SEC-MALLS c) Fraction of side chains generated becoming attached to the substrate. d) Estimated values determined by combining the absolute M_n of the substrate with the copolymer composition from ^{1}HNMR analysis. e) Apparent values determined by SEC analysis using a linear polystyrene standards calibration curve; G1PS-*g*-P2VP30 not eluted from the column in SEC analysis. f) Number of branches added in the last grafting reaction. g) P2VP content determined by ^{1}H NMR spectroscopy analysis. h) Fraction of coupling sites on the substrate consumed.

polymer solution: It is more difficult to purify these substrates after acetylation. To reach the end point (complete discoloration of the living polymer solution) in the grafting procedure, an excess of substrate (beyond the expected 1:1 acetyl to P2VP anion stoichiometry) is necessary for the preparation of higher generation copolymers.[6] This approach, while maximizing the consumption of the macroanions (and the grafting yield), necessarily leads to the introduction of a larger amount of protic impurities in the reaction. Comparison of the grafting yield for substrates of the same generation shows that the yield is always lower for the P2VP30 than the P2VP5 side chains. This effect is most noticeable for the G1 substrates, with a decrease from 70 % for G1PS-*g*-P2VP5 to 25 % for G1PS-g-P2VP30 (Table 5.2, Column 4). The concentration of living ends decreases when the molecular weight of the side chains increases, making the reaction that much more susceptible to deactivation by impurities. Similar variations were observed for the preparation of arborescent polystyrenes[12] and poly(2-vinylpyridine) copolymers[10] using chloromethyl functionalities.

The composition of the copolymers was determined by ^{1}H NMR spectroscopy analysis after removal of the linear (non-grafted) P2VP contaminant from the crude product. The results obtained (Table 5.2, Column 9) indicate P2VP contents of 87-93 mol % for the P2VP5 series copolymers, and 90-98 mol % for the P2VP30 series.

The absolute number-average molecular weight (M_n) and polydispersity index (M_w/M_n) of the graft copolymers could not be determined by SEC-MALLS analysis, because the instrument was dedicated exclusively to analysis in pure THF. Consequently, an alternate method was used to estimate the absolute molecular weight of the copolymer by combining the absolute M_n of the substrate with the copolymer composition from

^{1}H NMR spectroscopy analysis. The absolute M_n values for the graft copolymers estimated by that method are reported in Table 5.2, Column 6. Considering the significant errors involved in NMR analysis for copolymers with high (> 90 mol %) P2VP contents, the errors on the M_n values for these graft copolymers are also likely large. The apparent values determined by SEC analysis using a DRI detector are reported along with the estimated values for comparison, and it is clear that the apparent molecular weights are underestimated. This is due to the very compact structure of arborescent polymers, as confirmed by light scattering[13] and viscosity[14] measurements. The polydispersity index remains low ($M_w/M_n \leq 1.10$) for successive generations of the graft polymers.

The number-average branching functionality (f_n) of the arborescent polymers, defined as the number of chains added in the last grafting reaction, was calculated from the equation

$$f_n = \frac{M_n(G) - M_n(G-1)}{M_n^{br}} \tag{5.1}$$

where $M_n(G)$ is the estimated number-average molecular weight of the graft copolymer of generation G, whereas $M_n(G-1)$ and M_n^{br} are the absolute number-average molecular weights of the polystyrene substrate and the side chains, respectively. The f_n values listed in Table 5.2 range from 13 to 1177 for the P2VP5 series, and from 8 to 303 for the P2VP30 series. Both sample series display a roughly geometric increase in M_n and f_n for successive generations.

The coupling efficiency, defined as the fraction (percentage) of acetyl coupling sites consumed in the reaction, was calculated as the ratio of the branching functionality f_n to the number of coupling sites on the substrate. The coupling efficiency decreases with the length of the P2VP side chains and as the number of coupling sites on the substrate

increases (Table 5.2, Column 10). This decrease was attributed to increased congestion of the grafting substrate leading to decreased accessibility of the coupling sites. In an investigation of the morphology of arborescent polystyrenes using fluorescence quenching techniques, it was indeed demonstrated that the inner portion of the molecules was less accessible to quencher molecules than chains in the outer layer.[15] The fraction of less accessible material was found to increase for higher generation polymers. This differential accessibility effect explains the decrease in coupling efficiency observed for higher generation acetylated polystyrene substrates. Since polystyrene and P2VP are immiscible, it is also possible that the grafting sites were even less accessible to the larger macroanions, resulting in an even lower coupling efficiency for the higher molecular weight (P2VP30) side chains.

5.3.2 Viscosity of Arborescent Copolymer Polyelectrolyte Solutions

Branched polymers are attractive because many of their physical properties, including solution viscosity, differ from their linear counterparts. It was thus reported that the dilute solution viscosity of branched polyelectrolytes with approximately eight side chains, obtained by partial acetalization of the corresponding poly(vinyl alcohol)s with glyoxylic acid or *o*-phthalaldehydic acid, was much lower than for a linear polymer with the same degree of polymerization (X_n = 7000).[16] Polyelectrolytes prepared by sulfonation of star-branched polystyrenes with 13-18 arms were also used to investigate the effect of branching. The hydrodynamic radius increased by only 20 – 40 % on decreasing the ionic strength of the solutions, while ca. 100 % expansion was observed for the corresponding linear material. The difference in behavior was attributed to the

topology constraints present in the high branching functionality star polymers.[17] The intrinsic viscosity of the branched polyelectrolytes was investigated further in salt-free aqueous solutions by preparing a series of cross-linked polystyrenesulfonates with molecular weights in the range 4.96×10^5 – 3.07×10^6. In contrast to linear chains, the viscosity of the cross-linked materials was molecular weight-independent below their overlap concentration.[18] More recently, a pH-dependent study of dilute solutions of branched poly(methacrylic acid) (PMAA) was conducted in 10 vol % MeOH/H_2O.[19] In comparison with linear PMAA the influence of pH on viscosity was minimal in these branched polymers, with the almost complete suppression of the polyelectrolyte effect attributed to the branched architecture of the molecules. The reduced viscosity of the branched polymers was also lower than for linear PMAA, the branched architecture precluding significant expansion of the molecules. Similar suppression of the polyelectrolyte effect was also reported for hyperbranched polyesters with terminal carboxylic acid groups at high added salt concentrations.[20]

These results provide some hints of the trends to be expected with arborescent polyelectrolytes. The excellent control attained over the structure of arborescent polymers and their wide range of branching functionalities provide further opportunities to investigate the influence of branching in polyelectrolytes in a systematic fashion.

Variations in the structure of arborescent copolymers can provide materials with a wide range of physical properties. Thus copolymers with short P2VP segments should be equivalent to a branched block copolymer with spherical symmetry (Figure 5.1a). When long P2VP segments are grafted onto the polystyrene substrates, in contrast, the small dimensions of the substrate relative to the outer branches yields a structure approximating

that of star-branched molecules (Figure 5.1b). The compact structure of these copolymers should lead to interesting polyelectrolyte behavior upon protonation by a strong acid such as trifluoroacetic acid (TFA). On the one hand, expansion of the molecules may be favored when compared with linear poly(2-vinylpyridine) samples, due to the close proximity of ionic groups within the molecules. On the other hand, branching also increases the structural rigidity of the macromolecules, which may hinder conformation changes and oppose the electrostatic repulsion forces. The relative importance of these two contributions was probed by examining the solution properties of arborescent polyelectrolytes as a function of molecular structure, protonation level, solvent type, and salt addition. The reduced viscosity (η_{sp}/C) of arborescent polyelectrolyte solutions was compared as a function of polyelectrolyte concentration (C) for the two families of P2VP copolymers synthesized and for linear P2VP samples under the same conditions.

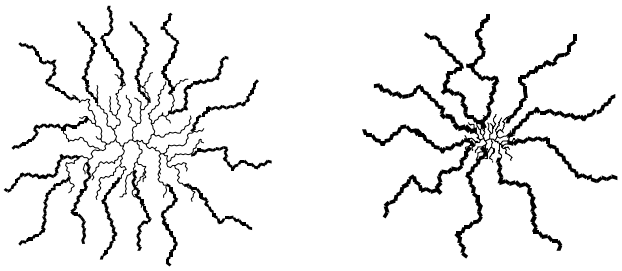

Figure 5.1 Comparison of structures obtained when a G1 polystyrene substrate is grafted with (a) short and (b) long P2VP side chains.

Polyelectrolytes are characterized by a high density of ionic groups covalently bonded along the polymer chain. Because of these charges, polyelectrolyte solutions exhibit distinct behaviors from neutral polymers. The solution properties depend on different parameters including the degree of dissociation of the ionic groups, the solvent

quality for the polymer backbone, the dielectric constant of the solvent, and the presence of salts.[2] One major factor affecting the properties of polyelectrolyte solutions is the balance between intramolecular and intermolecular interactions. The former typically dominate at low concentrations, while the latter dominate at higher concentrations.[3]

A polyelectrolyte solution may be considered to contain a single polymer species (although the influence of polydispersity may be significant) and one species of counterion, with a charge opposite to the polymer chain and present in equivalent amount for electroneutrality. The solution may also contain a low-molar-mass electrolyte (an "added salt", that may also be a strong acid or base), having a common ion with the polyelectrolyte but otherwise assumed not to interact with the polyelectrolyte. The discussion will be restricted to solutions containing monovalent ions and not take explicitly into account charge fluctuations along the macromolecular chain, although not necessarily every repeat may carry a charge. The total charge of the macromolecules is assumed to be distributed uniformly along the chain and to depend on the experimental conditions (solvent, pH, temperature, etc.) used.

The variation in the reduced viscosity (η_{sp}/C) of a neutral polymer solution as a function of concentration (C) usually yields a straight line corresponding to the Huggins equation[21]

$$\eta_{sp}/C = [\eta] + k'[\eta]^2 C \qquad (5.2)$$

with $\eta_{sp} = (\eta-\eta_0)/\eta_0$, where η and η_0 are the viscosity of the solution and the solvent, respectively, $[\eta]$ being the limiting (intrinsic) viscosity and k', the Huggins constant. The solution viscosity of neutral polymers is generally lower than that of polyelectrolytes of comparable molecular weight. The $[\eta]$ term is related to the hydrodynamic volume of the

molecules and k' is a measure of solvent quality. In contrast, the following characteristics are typical for "salt-free" polyeletrolyte solutions:

(1) A plot of (η_{sp}/C) versus C displays strong upwards (concave) curvature;

(2) The upturn of the viscosity curve at low polymer concentrations is larger for higher dielectric constant solvents;

(3) The reduced viscosity of polyelectrolytes in polar solvents is much higher than that of the parent (neutral) polymer.

The upturn in the reduced viscosity (η_{sp}/C) curve at low polymer concentrations in 'salt-free' polyelectrolyte solutions represents an 'abnormal behavior'[22] with respect to diluted neutral polymer solutions, for which the intrinsic viscosity [η] can be determined simply by extrapolation to C = 0 according to Equation (5.2). The existence of an upturn for polyelectrolyte solutions makes such an extrapolation meaningless.[23] Expansion of the polyion chains[24] in solution is at the origin of the increase. The charge screening effect due to the counterions becomes weaker as the polymer concentration decreases, causing the expansion of the polyion chains due to increased intramolecular repulsive forces. This phenomenon describes qualitatively the increase in (η_{sp}/C) at low C. Alternate explanations for this phenomenon have also been suggested,[23,25] and this peculiar behavior still remains an open issue.

The arborescent polystyrene-*graft*-poly(2-vinylpyridine) copolymers are soluble in polar solvents (DMF, methanol) and act as a weak base able to acquire a net charge by protonation of the pyridine ring. The copolymers are soluble in acidic aqueous solutions for the same reason, even though the neutral copolymers are insoluble in pure water. The apparent pK_a of such a polymer is difficult to define,[26] because it depends on factors such

as the degree of protonation of the chains and the background electrolyte concentration. It was shown previously that linear P2VP, when dissolved in water with an equivalent concentration of a strong acid (HCl), had a protonation level of at least 70 %.[27] Due to charge repulsions between neighboring groups it appeared unlikely that this protonation level could be exceeded, however.

5.3.2.1 Influence of Protonation Level and Solvent Type

The properties of the copolymer solutions in methanol will be considered as a starting point, using sample G0PS-*g*-P2VP5 as an example. Methanol is a polar protic solvent with a dielectric constant ($\varepsilon = 33$) sufficient to induce significant dissociation of the counterions from the protonated P2VP chains. As a result, the arborescent P2VP copolymers display classical polyelectrolyte behavior even at low protonation levels (0.1 equiv TFA/2VP unit). The influence of the protonation level on solution viscosity, depicted in Figure 5.2, is characterized by a marked polyelectrolyte effect due to chain expansion at low concentrations. The upswing is accentuated at 1.0 equiv TFA/2VP unit, but becomes less pronounced when excess TFA (3.0 equiv TFA/2VP unit) is added. Chain expansion is presumably suppressed with excess TFA due to charge screening, because of partial ionization of the excess TFA.

An upturn is also observed in the high concentration range, as the viscosity is much larger than for the neutral copolymer due to dominant intermolecular association of the ion pairs along the chains. The upwards curvature in Figure 5.2 therefore reflects increasing aggregation at higher polymer concentrations. Intermolecular association is

also partly suppressed by excess TFA, presumably as a result of charge screening due to partial ionization of the non-bonded TFA molecules.

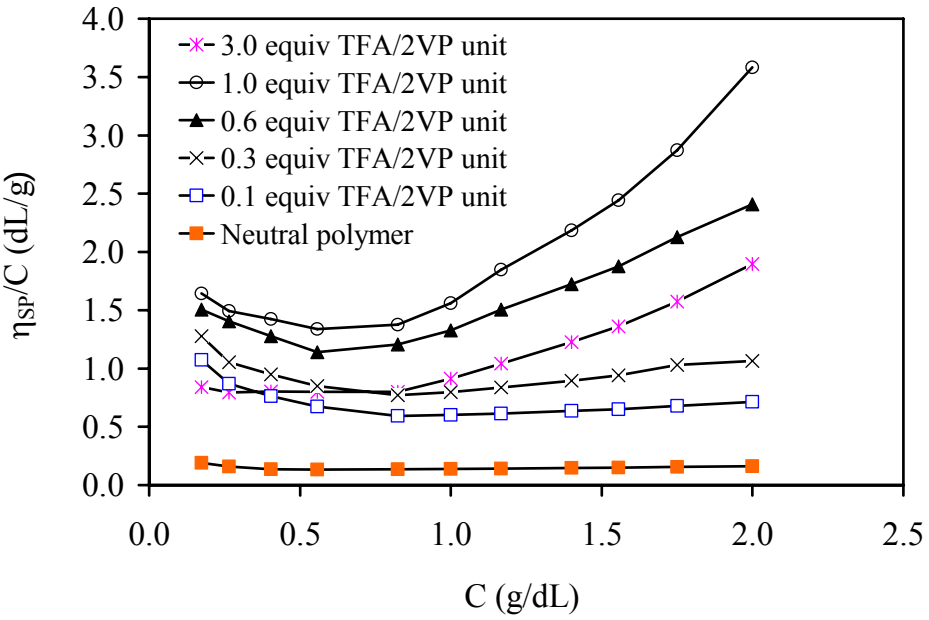

Figure 5.2 Reduced viscosity of G1 copolymer {G0PS-*g*-P2VP5} solutions protonated by TFA in methanol at 25 °C.

The reduced viscosity of the same copolymer of overall generation 1 (G0PS-*g*-P2VP5) is compared in Figure 5.3 for three different solvents (methanol, DMF, and water) with 1.0 equiv TFA/2VP unit. These solvents differ in terms of dielectric constant and character: Polarity increases within the series methanol ($\varepsilon = 33$) < DMF ($\varepsilon = 37$) < water ($\varepsilon = 80$), DMF being aprotic while the other two are protic solvents. It can be seen that viscosity enhancement (particularly in the high concentration range) correlates with solvent polarity (methanol > DMF > water), intermolecular association being most significant in the least polar solvents. The upturn in the low concentration range, linked to

coil expansion, is only visible in the two protic solvents due to their stronger ionizing power. The lack of upturn in DMF can be explained by the stronger counterion/polyion interactions and smaller electrostatic repulsive interactions due to the counterions, the latter "shielding" the polyion charges. Electrostatic repulsive interactions between the charges on the chain decrease under these conditions and lead to an overall decrease in chain size, inducing in turn a decrease in reduced viscosity. The interactions between the counterions and the polyion are thus stronger due to the lower ionizing power of DMF.

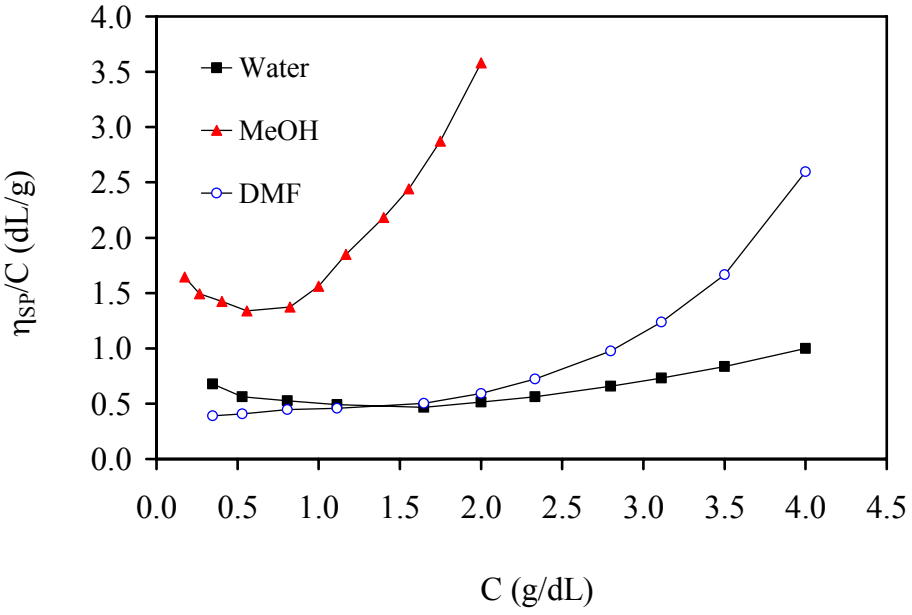

Figure 5.3 Reduced viscosity of G1 copolymer {G0PS-*g*-P2VP5} in different solvents with 1.0 equiv TFA/2VP unit at 25 °C.

5.3.2.2 Influence of Polymer Structure

After investigating the influence of the protonation level and solvent type on the dilute solution behavior of an arborescent copolymer of overall generation 1 (G0PS-*g*-P2VP5), the influence of the copolymer structure on the solution properties will be

examined by comparing the behaviors of the two families of P2VP copolymers in DMF and in methanol at constant protonation level (1.0 equiv TFA/2VP unit). The trends observed will also be compared with measurements on linear P2VP samples of different molecular weights under the same conditions.

The reduced viscosity of arborescent polyelectrolytes with short P2VP side chains ($M_n \approx 5000$, P2VP5 sample series) of different generations in DMF and in methanol are compared in Figures 5.4a and 5.4b, respectively. The corresponding curves for copolymers with long P2VP side chains ($M_n \approx 30000$, P2VP30 sample series) are displayed in Figures 5.4c and 5.4d, respectively.

The reduced viscosity of all arborescent polyelectrolyte samples is systematically higher in methanol than in DMF over the whole concentration range investigated. The low-concentration upturn, linked to coil expansion, is also more pronounced in methanol due to its higher ionizing power. The viscosity enhancement in the high concentration range, when present, correlates with the solvent polarity as before [methanol ($\varepsilon = 33$) > DMF ($\varepsilon = 37$)], intermolecular association being most favored in the less polar solvents and at higher polymer concentrations. Interestingly, the behavior of copolymers based on the G0PS substrate (G0PS-*g*-P2VP5 and G0PS-*g*-P2VP30; G1 generation overall) is very different from copolymers based on linear PS (PS-*g*-P2VP5, PS-*g*-P2VP30) and G1PS substrates (G1PS-*g*-P2VP5, G1PS-*g*-P2VP30) in both solvents. The G1 copolymers generally display the largest upturn in the low concentration range (except for G0PS-*g*-P2VP5 in DMF), and the strongest association in the high concentration range (except for G0PS-*g*-P2VP30 in methanol). The viscosity enhancement at low concentrations, linked to molecular expansion under the influence of electrostatic repulsive forces along the

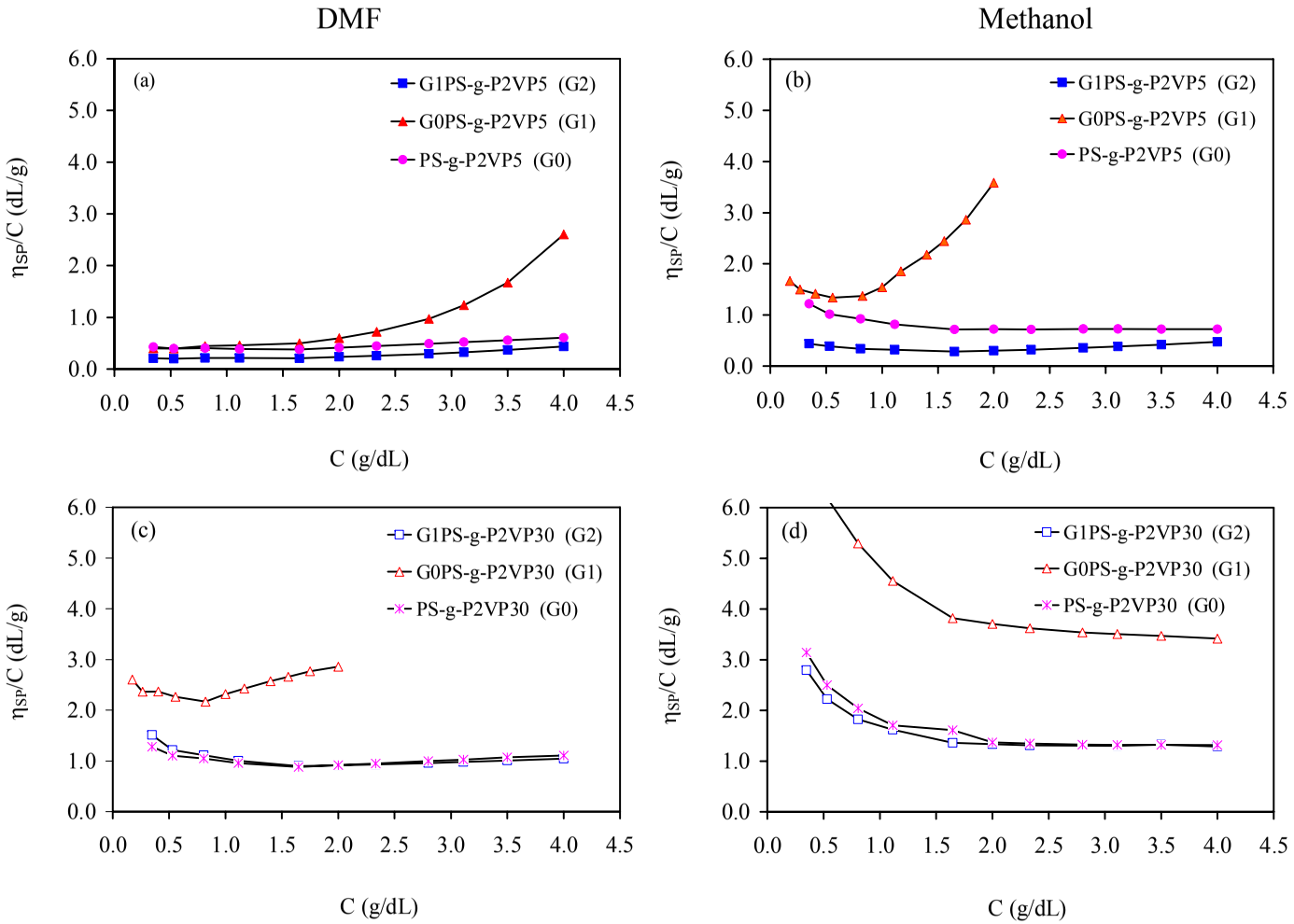

Figure 5.4 Comparison of the reduced viscosity of arborescent copolymers with 5K P2VP side chains in (a) DMF, (b) methanol, and 30K P2VP side chains in (c) DMF, (d) methanol, with 1.0 equiv TFA/2VP unit at 25 °C.

chain, is clearly most significant for the G1 copolymers. The repulsive electrostatic forces are opposed by the elastic forces due to the loss of entropy as the chains are forced to stretch. Conformation changes and chain deformation should be more difficult for branched molecules than for linear polymers, due to increased steric crowding and possibly to initial partial stretching of the chains. On the other hand, the charge density per unit volume of the molecules should be higher for branched polyelectrolytes than for linear polyelectrolytes, due to their more compact structure. This could either enhance electrostatic repulsions and molecular expansion, or else favor counterion condensation, enhancing ion pair formation and intramolecular association. The extent of chain expansion and intermolecular association must, therefore, depend on the delicate balance of polymer-solvent interactions, the extent of ionic group dissociation, and intramolecular elastic forces. On the basis of the results obtained, it appears that molecular expansion and intermolecular association are most favored for copolymers of generation G1 overall (G0PS-*g*-P2VP5 and G0PS-*g*-P2VP30). The other copolymers apparently have very little ability to associate intermolecularly over the concentration range examined (the reduced viscosity curves being remarkably flat in the high concentration range), possibly as a result of enhanced intramolecular association. All copolymer molecules with P2VP30 side chains nonetheless have a higher tendency to expand at low concentrations (under the influence of electrostatic repulsions) than their P2VP5 analogues, presumably due to the higher flexibility of the longer side chains.

In comparing the two copolymer series in the same solvent, the reduced viscosity is always higher for the P2VP30 series with the long, flexible side chains than the P2VP5 series with shorter, stiffer side chains. This is in agreement with a study of the solution

properties of star-branched polyelectrolytes,[28] sodium polyacrylate stars with the same branching functionality (same number of arms) always displaying enhanced molecular expansion for increasing branch molecular weights.

With the exception of the P2VP5 sample series in DMF, the reduced viscosity increases to different extents when the polyelectrolyte concentration decreases. The lack of upturn observed in the low concentration range for the P2VP5 series copolymers in DMF (Figure 5.4a), a solvent with a comparatively lower ionizing power than methanol, suggests a more collapsed chain conformation due to enhanced counterion condensation. Stronger counterion-polyion interactions lead to lower electrostatic repulsive forces and less pronounced chain expansion. Since the copolymers in the P2VP30 series have more flexible side chains than the P2VP5 series, the upturn due to coil expansion is more clearly visible (Figure 5.4c). The reduced viscosity enhancement within each series is found to vary in the order (G1 > G0 > G2) for the P2VP5 series in DMF in the higher concentration range, whereas it varies in the order (G1 ≈ G0 > G2) in the lower concentration range (Figure 5.4a), and (G1 > G0 > G2) in methanol over the entire concentration range examined (Figure 5.4b). For the P2VP30 series it varies in the order (G1 > G0 ≥ G2) in DMF (Figure 5.4c) and (G1 >> G0 ≥ G2) in methanol (Figure 5.4d) over the whole concentration range investigated. Within each sample series coil expansion is most pronounced for the G1 samples as compared to G0 and G2. This is presumably due to the relatively low steric crowding level experienced by the G1 molecules, in combination with a compact molecular size.

Within each series of arborescent copolymers, the reduced viscosity is lowest for the G2 samples. This effect is again attributed to the enhanced structural rigidity of these

molecules. Previous investigations of arborescent polymers[6,9,10,13] confirmed the very compact structure of these graft polymers, with hydrodynamic volumes over 10 times lower than linear polymers of comparable molecular weight. In a morphology investigation of arborescent polystyrenes using fluorescence quenching techniques, it was demonstrated that the inner portion of the molecules was less accessible to quencher molecules than chains in the outer layer.[15] The fraction of less accessible material was found to increase for higher generation polymers. Small-angle neutron scattering measurement on arborescent polystyrene[29] also confirmed the high chain density in the core portion of the molecules relative to the outer layer. This enhanced structural rigidity explains the low reduced viscosity increases observed for the G2 samples.

5.3.2.3 Comparison with Linear P2VP Samples and Added Salt Effects

Three linear poly(2-vinylpyridine) samples P2VP65, P2VP230, and P2VP430, with target $M_n \approx 70000$, 250000, and 450000, respectively, were synthesized as reference materials for comparison of their polyelectrolyte behavior with the arborescent copolymers. Molecular weights close to the target values and narrow molecular weight distributions were attained in all cases, as determined by SEC-MALLS analysis (P2VP65: $M_n = 65000$, $M_w/M_n = 1.06$; P2VP230: $M_n = 230000$, $M_w/M_n = 1.08$; P2VP430: $M_n = 430000$, $M_w/M_n = 1.09$).

Comparisons with linear P2VP samples in DMF and in methanol are provided in Figures 5.5a and 5.5b for the P2VP5 samples, respectively, and in Figures 5.5c and 5.5d for the P2VP30 samples, respectively, using different scales to take into account the higher reduced viscosity of the linear P2VP samples. Irrespective of the solvent type

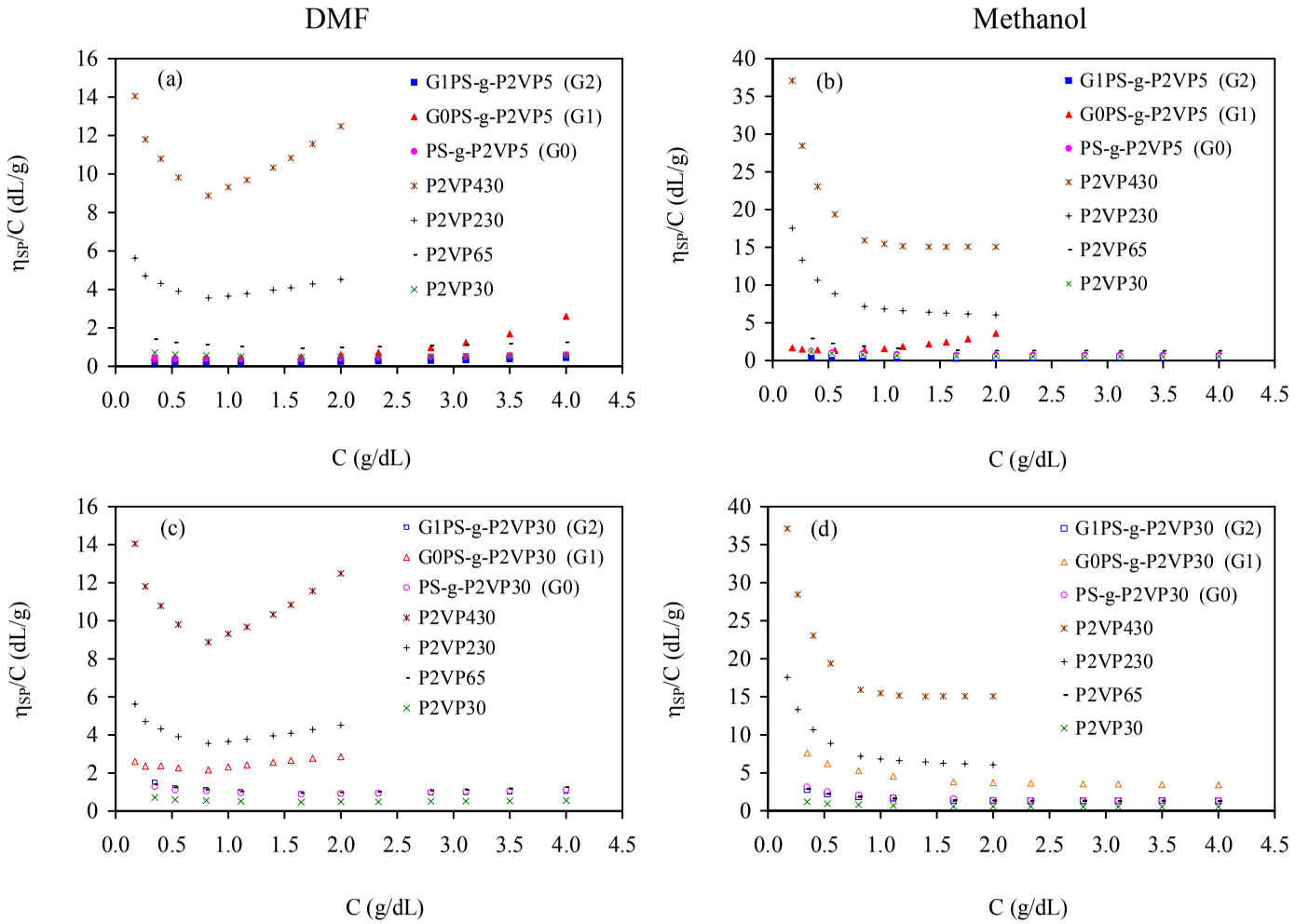

Figure 5.5 Comparison of the reduced viscosity of linear P2VP and arborescent copolymer generations based on 5K P2VP side chains (a) DMF, (b) methanol, and 30 K P2VP side chains (c) DMF, (d) methanol, with 1.0 equiv TFA/2VP unit at 25 °C.

used, it is clear that the reduced viscosity of the arborescent copolymers is only comparable to linear P2VP for samples of relatively low molecular weights (P2VP30, P2VP65), while it is much lower than for linear samples with M_n = 230K (P2VP230) and 430K (P2VP430). This is particularly interesting when considering that the graft copolymers have absolute molecular weights ranging from $M_n = 7.4\times10^4 - 1.1\times10^7$. The upturn in the reduced viscosity at low concentrations is also much more important for the P2VP230 and P2VP430 linear samples than for any of the arborescent polyelectrolytes. This confirms the strong suppression of molecular expansion for the branched polyelectrolytes, presumably due to their more rigid structure. These results are again consistent with findings reported for four- and six-arm star-branched sodium polyacrylate solutions:[28] Molecular expansion was invariably more important for linear sodium polyacrylate samples with molecular weights comparable to the star-branched systems, and decreased as the branching functionality of the stars increased. This was explained by the lower degrees of freedom available for the chains in star polymers of higher branching functionality. It is interesting to note the similar trends observed among the arborescent polyelectrolytes, in spite of their molecular weight up to 27 times larger than the linear P2VP samples used in the comparison.

Finally, the influence of added salts on the viscosity of arborescent polyelectrolyte solutions is depicted in Figures 5.6a and 5.6b for DMF and methanol, respectively. This behavior is characteristic of polyelectrolyte solutions in general: The concave curves revert to straight lines in the presence of a salt, becoming similar to neutral polymer solutions. It is well-known that for polyelectrolytes, counterion binding (condensation) within the polymer coil is enhanced in the presence of salts.[30] According to

Le Châtelier's principle, counterion binding should be favored as the concentration of salt is increased. This leads to decreased repulsive interactions between the ionic moieties along the polymer chains, a smaller molecular size, and a lower reduced viscosity.

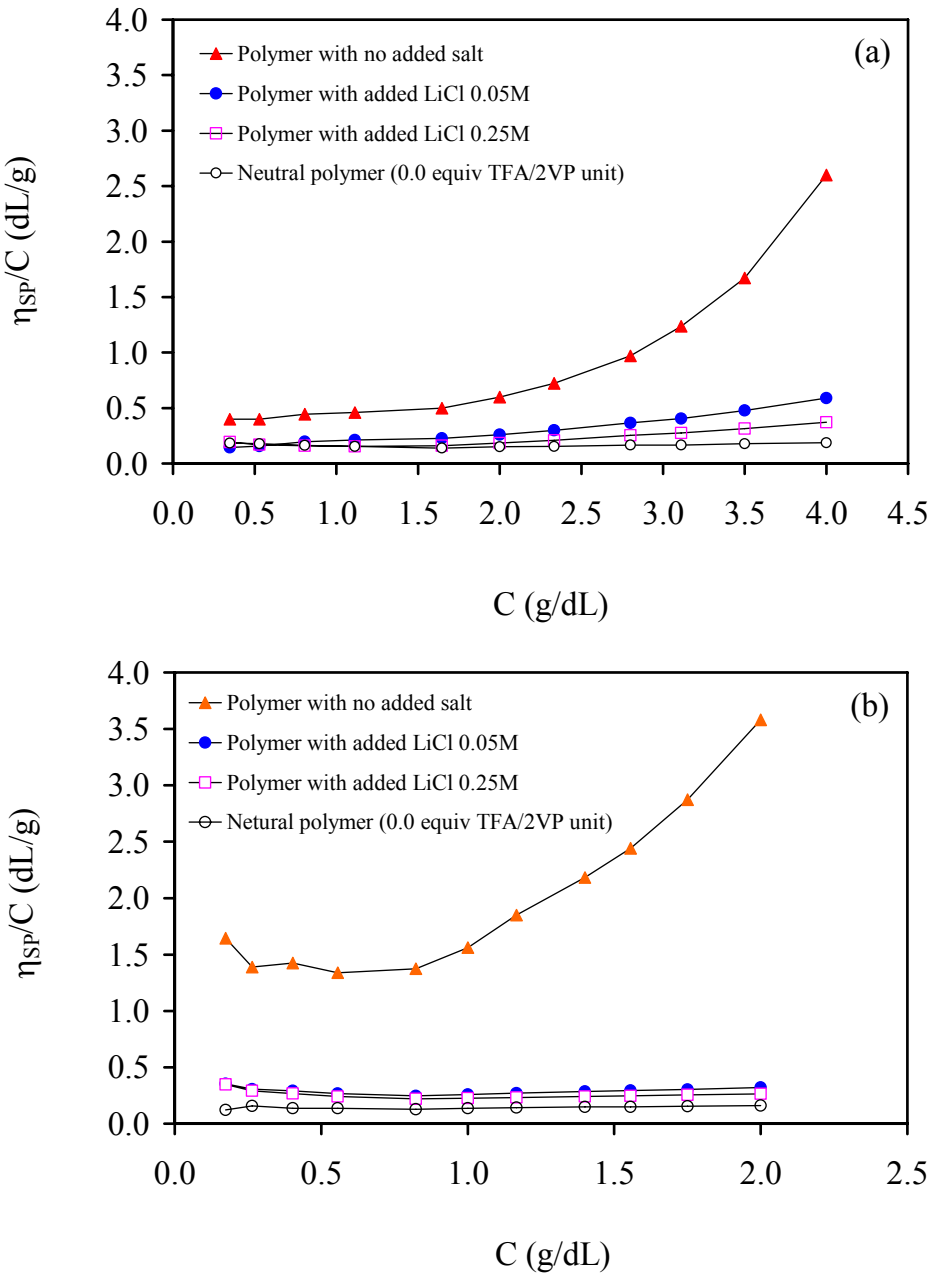

Figure 5.6 Effect of LiCl on the viscosity of an arborescent copolymer of generation G1 overall {G0PS-g-P2VP5} with 1.0 equiv TFA/2VP unit at 25 °C: (a) DMF, (b) methanol.

5.4 Conclusions

The large (100-g) scale synthesis of dendritic polyelectrolyte precursors in up to 96 % yield was demonstrated by grafting living poly(2-vinylpyridinyl)lithium onto linear and branched polystyrene substrates randomly functionalized with acetyl groups. Two arborescent copolymer families with $M_n \approx 5000$ or 30000 P2VP side chains and containing 87-98 mol % P2VP were thus synthesized. A narrow molecular weight distribution (M_w/M_n = 1.08-1.10) was maintained for graft copolymers of successive generations. These materials are characterized by a very compact structure and a roughly geometric increase in branching functionality and molecular weight for each generation.

The polyelectrolyte behavior of the arborescent polystyrene-*graft*-poly(2-vinylpyridine) copolymers was investigated. These materials are freely soluble in polar solvents including methanol, DMF, and water upon protonation by strong acids such as trifluoroacetic acid. The copolymer solutions display properties typical of polyelectrolytes, including strong curvature in plots of reduced viscosity (η_{sp}/C) versus concentration (C) at both low and high concentrations. In comparing the influence of the solvent type used, the reduced viscosity of both copolymer series (P2VP5 and P2VP30) was always higher in methanol than in DMF, due its stronger ionizing power. In the same solvent, the reduced viscosity was also higher for copolymers with the long, flexible P2VP30 side chains as compared to the stiffer P2VP5 copolymers. The reduced viscosity was found to decrease within each sample series in the order G1 > G0 > G2. Molecular expansion is apparently more pronounced for the G1 copolymers as compared to the G0 and G2 copolymers, presumably due to the balance of enhanced charge repulsions and increased structural rigidity within the compact molecules. In comparison with linear

P2VP samples, however, the reduced viscosity of arborescent polyelectrolyte solutions is much lower, in spite of their much higher molecular weights. The addition of salt to the branched polyelectrolyte solutions decreases their viscosity and suppresses the curvature of the reduced viscosity plots, presumably due to charge screening effects of the type observed in linear polyelectrolyte systems.

5.5 References

1. For an overview of the properties of polyelectrolytes, see for example: (a) *Polyelectrolytes: Science and Technology*; Hara, M., Ed.; Marcel Dekker: New York, 1993. (b) Gray, F. M. *Polymer Electrolytes*; RSC Materials Monographs, Royal Society of Chemistry: London, 1997.
2. Dobrynin, A. V.; Rubinstein, M. *Prog. Polym. Sci.* **2005**, *30,* 1049.
3. Hara, M.; Wu, J.-L.; Lee, A. H. *Macromolecules* **1988**, *21*, 2214.
4. Gauthier, M. In *Ionic Polymerizations and Related Processes*; Puskas, J. E., Ed.; NATO ASI Series E359; Kluwer Academic: Dordrecht, 1999; p 239.
5. Li, J.; Gauthier, M. *Macromolecules* **2001**, *34*, 8918.
6. Gauthier, M.; Li, J.; Dockendorff, J. *Macromolecules* **2003**, *36*, 2642.
7. Lipton, M. F.; Sorensen, C. M.; Sadler, A. C.; Shapiro, R. H. *J. Organomet. Chem.* **1980**, *186*, 155.
8. Gauthier, M.; Tichagwa, L.; Downey, J. S.; Gao, S. *Macromolecules* **1996**, *29*, 519.
9. Kee, R. A.; Gauthier, M. *Polym. Prepr., Am. Chem. Soc., Div. Polym. Chem.* **1999**, *40(2)*, 165.

10. Kee, R. A.; Gauthier, M. *Macromolecules* **2002**, *35*, 6525.

11. Matsushita, Y.; Nakao, Y.; Saguchi, R.; Choshi, H.; Nagasawa, M. *Polym. J.* **1986**, *18*, 493.

12. Gauthier, M.; Möller, M. *Macromolecules* **1991**, *24*, 4548.

13. Gauthier, M.; Möller, M.; Burchard, W. *Macromol. Symp.* **1994**, *77*, 43.

14. Gauthier, M.; Li, W.; Tichagwa, L. *Polymer* **1997**, *38*, 6363.

15. Frank, R. S.; Merkle, G.; Gauthier, M. *Macromolecules* **1997**, *30*, 5397.

16. Ichiro, S.; Yasuyoshi, S.; Shizuo, T. *Kobunshi Kagaku* **1962**, *19*, 663.

17. Mays, J. W. *Polymer Commun.* **1990**, *31*, 170.

18. Antonietti, M.; Briel, A.; Förster, S. *Macromolecules* **1997**, *30*, 2700.

19. Graham, S.; Cormack, P. A. G.; Sherrington, D. C. *Macromolecules* **2005**, *38*, 86.

20. Turner, S. R.; Walter, F.; Voit, B. I.; Mourey, T. H. *Macromolecules* **1994**, *27*, 1611.

21. Huggins, M. L. *J. Am. Chem. Soc.* **1942**, *64*, 2716.

22. Fuoss, R. M. *J. Polym. Sci., Part B* **1948**, *3*, 603.

23. Eisenberg, H.; Pouyet, J. *J. Polym. Sci.* **1954**, *13,* 85.

24. Hodgson, D. F.; Amis, E. J. In *Polyelectrolytes Science and Technology*, Hara, M. Ed.; Marcel Dekker: New York, 1993; p 127.

25. Cohen, J.; Priel, Z.; Rabin, Y. *J. Chem. Phys.* **1998**, *88,* 7111.

26. Bekturov, E. A.; Bakauova, Z. Kh. *Synthetic Water-Soluble Polymers in Solution*, Huethhig and Wepf: Basel, 1986; Chapter 2.

27. Muller, G.; Ripoll, C.; Selegny, E. *Eur. Polym. J.* **1971**, *7*, 1373.

28. Moinard, D.; Borsali, R.; Taton, D.; Gnanou, Y. *Macromolecules* **2005**, *38*, 7105

29. Choi, S.; Briber, R. M.; Bauer, B. J.; Topp, A.; Gauthier, M.; Tichagwa, L. *Macromolecules* **1999**, *32*, 7879.

30. Oosawa, F. *Polyelectrolytes*, Dekker: New York, 1971; Chapter 7.

Chapter 6

Grafting Polyisoprene onto Cross-linked Latex Particles for the Preparation of Model Rubber-compatible Fillers

6.0 Abstract

Model filler particles were obtained by grafting polyisoprene (PIP) chains onto spherical latex particles of polystyrene (PS) cross-linked with 12 mol % divinylbenzene (DVB). These particles, with a narrow size distribution and a diameter of ca. 400 nm, were synthesized by starved-feed emulsion polymerization without emulsifier. Acetyl coupling sites were introduced randomly at either low (5 mole %) or high (30 mole %) substitution levels on the latex particles by Friedel-Crafts acylation with acetyl chloride and $AlCl_3$ in nitrobenzene. The acetylation reaction was monitored by Fourier Transform Infrared (FT-IR) analysis of the particles. 'Living' polyisoprenyllithium chains, generated from isoprene and *sec*-butyllithium (*sec*-BuLi), were then coupled with the acetylated PS latex particles. The PIP side chains had a high *cis*-1,4-polyisoprene microstructure content and a number-average molecular weight (M_n) of either 2×10^3 (2K), 5×10^3 (5K), or 3×10^4 (30K). The PIP content of the grafted particles was determined from the yield of isolated particles and by ^{1}H NMR spectroscopy analysis. The grafted latex particles were blended in solution with linear polyisoprene ($M_n = 3.95 \times10^5$, 395K) as a rubber matrix. The influence of the filler-matrix interactions on the rheological behavior of the blends was determined by dynamic mechanical analysis for the different filler structures generated. All the blends exhibited increases in complex viscosity and storage modulus, and decreased damping factors relatively to the pure matrix polymer. The enhancements observed, decreasing in the order 30 mol % > 5 mol % acetylation, and in terms of the grafted PIP chain length as 30K > 5K ≈ 2K, are deemed to reflect the extent of interactions between the filler particles and the polymer matrix.

6.1 Introduction

Commercial plastics and rubbers are often filled with solid particles, either to enhance their mechanical properties or to reduce the cost of the materials.[1] The properties of these materials depend primarily on the interactions between the matrix and the filler particles, although interparticle interactions are also important in some cases.[2] Thus carbon black-filled rubber belongs to the first category, but silica-filled hydrocarbon rubber to the latter. Consequently, the influence of physical interactions on the rheology of polymers can be very complex.[3,4] Strong interactions between the matrix polymer and the filler particles tend to increase the viscosity and the dynamic moduli, since strong adsorption of the polymer on the filler surface restricts chain mobility within the matrix. The nature and surface composition of the particles, as well as matrix properties such as the polarity and the molecular weight influence the rheology of the mixtures.[3] While much effort has been devoted to investigating the effect of filler surface treatment on the rheological behavior of filled polymers, most studies have used commercial fillers such as carbon black, calcium carbonate, mica, and talc.[5-7] These fillers often have a complex structure and generally form aggregated suspensions with poorly characterized particle-matrix interactions that impedes the interpretation of the rheological results.

The influence on melt rheology of model cross-linked fillers obtained by emulsion polymerization has been investigated to some extent, by simple dispersion of the particles in different matrices,[8-11] by incorporation of the particles into the matrix network through covalent bonding,[12] or by using core-shell particles to enhance filler compatibility with the matrix.[13] Terminal grafting of well-defined chain segments as a mean to control the

interactions between model filler particles and the matrix has, to the best of our knowledge, has only been reported in one case.[14]

In this research, we sought to elucidate the rheological implications of particle-matrix interactions in a polyisoprene rubber matrix filled with low-density rubber-compatible model particles. The particles have a core-shell morphology, with a core derived from cross-linked PS latex particles of uniform size, and a shell of terminally grafted PIP chains. The addition of PIP chains on the surface of the filler particles provides control over the interactions or adhesion between the filler particles and the rubber matrix. More favorable interactions should facilitate the dispersion of the filler and facilitate agglomerate break up under the influence of shear forces.[15]

The synthesis of the model filler was based on essentially monodispersed spherical PS latex particles, crosslinked with 12 mole % DVB, obtained by starved-feed emulsifier-free emulsion polymerization.[16] The particles were functionalized by acetylation[17] and reacted with 'living' polyisoprenyllithium chains with a high *cis*-1,4-microstructure content and a uniform size (M_w/M_n = 1.05-1.12).[17] Two series of model filler samples were generated based on different acetylation levels for the latex particles (~ 5 mol % vs. ~ 30 mol %), and PIP side chains with a high *cis*-1,4-polyisoprene (PIP) content and a molecular weight of either 2K, 5K, or 30K. A rubber matrix of linear polyisoprene (LPIP395, M_n = 395K) with a high *cis*-1,4-microstructure content was synthesized anionically and blended in solution with the model fillers. Freeze fracture scanning electron microscopy (SEM) was performed to characterize the degree of dispersion of the filler particles within the matrix. The rheological properties of the blends were then investigated to clarify the influence of particle-matrix interactions in term of

the length and the weight fraction of the PIP chains in the filler on the frequency-dependent complex viscosity, storage modulus, and loss tangent curves.

6.2 Experimental Section

6.2.1 Solvent and Reagent Purification

Tetrahydrofuran (THF; Caledon, reagent grade) was purified by distillation from sodium-benzophenone ketyl under nitrogen. Cyclohexane (BDH, HPLC grade) was purified by refluxing with oligostyryllithium under nitrogen. The dry solvents were introduced directly from the purification stills into the polymerization reactor or ampule preparation manifolds through polytetrafluoroethylene (PTFE) tubing. Isoprene (Aldrich, 99 %, inhibited with 100 ppm 4-*tert*-butylcatechol, TBC) was purified by distillation after stirring with CaH_2 overnight. Styrene (Aldrich, 99 %, inhibited with 10-15 ppm TBC), and the cross-linker divinylbenzene (DVB, Aldrich, 55 % meta and para isomers, 42 % ethylvinylbenzene, and 3 % diethylbenzene, inhibited with 1000 ppm TBC) were first washed in a separatory funnel with three aliquots of 2 M sodium hydroxide solution and with deionized water to remove the TBC. All monomers were stored at -20 °C until further use. Ammonium persulfate (Fisher), *n*-butyllithium (*n*-BuLi, Aldrich, 2.5 M in hexane), and *sec*-butyllithium (*sec*-BuLi, Aldrich, 1.3 M in cyclohexane) were used as received. The exact activity of the organolithium compound solutions was determined by the method of Lipton et al.[18] 2,2′-Bipyridyl (Aldrich, 99+%) was dissolved in dry cyclohexane to give a 0.10 M solution. All other reagents were used as received from the suppliers. The reagent ampules used in the polymerization and grafting procedures were prepared by high-vacuum purification techniques and filled with dry

nitrogen.[19] The ampules were equipped with PTFE stopcocks and ground glass joints for mounting on the polymerization reactor.

6.2.2 Synthesis of Emulsifier-free Poly(styrene-*co*-divinylbenzene) Latex Particles

A typical procedure for the preparation of PS latex particles cross-linked with 12 mol % DVB was carried out as follows. Deionized water (1800 mL) was added to a 3-L resin kettle (glass reactor) immersed in a water bath at (70 ± 1) °C as shown in Figure 6.1.

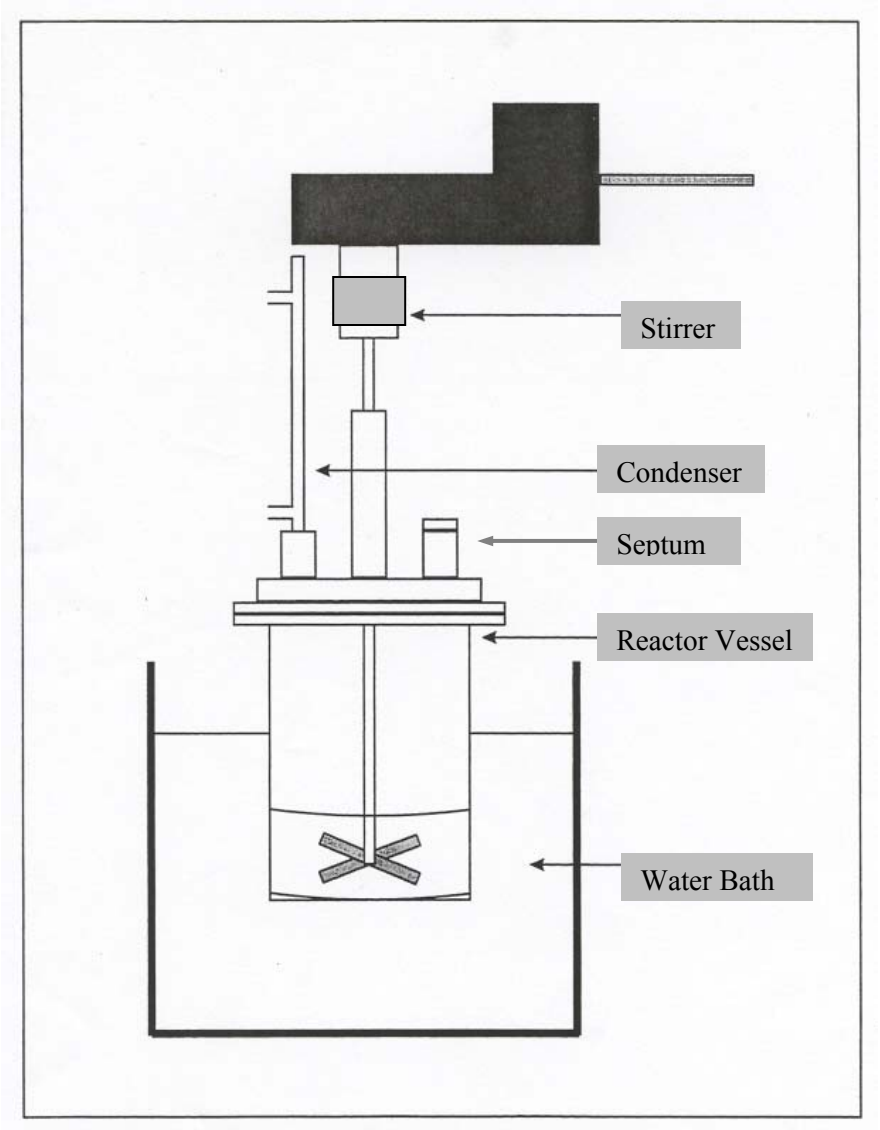

Figure 6.1 Schematic illustration of the reactor configuration for latex production.

Dissolved oxygen was chased from the reactor by bubbling nitrogen through the water for 60 min while stirring at 400 rpm. Purified styrene (80 mL, 0.70 mol) and DVB (6 mL, 0.04 mol) were then added to the reactor, which was left to stir for 20 min before adding ammonium persulfate (676 mg, 3.0 mmol, dissolved in 30 mL of deionized and deoxygenated water) to give a total initiator concentration of 1.64×10^{-3} M. The polymerization began (as indicated by an opalescent coloration) after 10 min and the reaction was allowed to proceed for 75 min. Nitrogen flow was continued throughout the reaction at a lower rate (ca. 1 bubble / sec) to minimize evaporation. After the 75-min nucleation period, the addition to the reactor of equal increments of a mixture of styrene and DVB in a volume ratio of 1:1 was started with a syringe through the septum (Figure 6.1) according to the addition scheme described in Table 6.1.

Table 6.1 Addition Sequence for Styrene and DVB Monomers in Starved-feed System.

Time of Addition (min)	Volume of DVB/Styrene (mL)
75	3.6
110	3.0
140	2.8
175	2.2
200	2.2
225	2.2
255	2.0
295	2.0

There was a minimum of 20 min between each addition, to avoid pooling of monomer at the surface and destabilization of the emulsion. The reaction was allowed to proceed for a

total of 8 h since the beginning of initiator addition. The particles were isolated by flocculation of the aqueous latex with a minimum amount (ca. 10 mL) of concentrated (12 M) HCl, suction filtration, and drying under vacuum. Further purification of the particles involved their redispersion in THF, flocculation with a mixture of methanol and HCl (10:1 v/v), and drying under vacuum to constant weight.

6.2.3 Acetylation of the Latex Particles

A sample of latex particles with a diameter of 400 ± 6 nm (64.0 g, 615 meq styrene units) was dried under vacuum in a 2-L round-bottomed flask, and dispersed in 600 mL of nitrobenzene. For a target acetylation level of ~ 30 mol %, a catalyst solution was prepared by dissolving anhydrous $AlCl_3$ (Aldrich, 99.99 %, 27.0 g, 202 mmol) in 150 mL of nitrobenzene, and adding acetyl chloride (16.0 mL, 225 mmol). The acetyl chloride-$AlCl_3$ solution was added dropwise to the particle dispersion over 60 min at room temperature (23 °C), and the reaction was allowed to proceed for 60 min. Workup of the products involved precipitation of the acetylated particles in 3 L of methanol acidified with 100 mL of concentrated (12 M) HCl, and recovery of the particles by suction filtration as a first step. They were further purified by two cycles of redissolution in 200 mL of THF, precipitation in 2 L of methanol acidified with 40 mL of concentrated HCl, and suction filtration. The isolated particles were then redispersed in 200 mL of chloroform and precipitated one last time in 2 L of methanol, and recovered by suction filtration before drying under vacuum to constant weight. The same procedure was used to achieve an acetylation level of ~ 5 mol %, by reducing the quantity of acetyl chloride-$AlCl_3$ solution used (4.5 g, 34 mmol of $AlCl_3$ in 25 mL of nitrobenzene, and 2.7 mL, 37.5 mmol of acetyl chloride).

6.2.4 Synthesis of Polyisoprene-grafted Latex Particles

Two series of grafted latex particle samples were generated from polystyrene particles with an acetylation level of either 5 or 30 mol %, and side chains with a number-average molecular weight $M_n \approx$ 2K, 5K, or 30K.

The polymerization of isoprene was performed in cyclohexane at room temperature, to obtain a microstructure with a high *cis*-1,4-units content. The synthesis of latex particles with a 30 mol % acetylation level and grafted with $M_n \approx 5000$ polyisoprene chains is provided as an example. The acetylated latex substrate (12 g, 30 % acetylation, 31 mequiv acetyl units) was purified in an ampule by three cycles of azeotropic distillation with 100 mL of dry THF and redispersion in 100 mL of THF. Isoprene was further purified on a high-vacuum manifold immediately before polymerization by three freezing – evacuation – thawing cycles in the presence of *n*-BuLi solution (1 mL for 20 mL monomer), and slow distillation to a glass ampule. A five-neck 3-L glass reactor equipped with a mechanical stirrer was fitted with two ampules containing purified isoprene (54.5 g, 0.801 mol) and the acetylated latex substrate, dry THF and cyclohexane inlets, and a septum. Solid LiCl (2.31 g, 54.5 mmol) was loaded in the reactor before it was evacuated, flamed, and purged with purified nitrogen. Cyclohexane (500 mL) and 0.5 mL of 0.10 M 2,2′-bipyridyl solution were added to the reactor, and the solvent was titrated with *sec*-butyllithium solution to give a persistent light orange color.[20] The reactor was then cooled to 0 °C before the calculated amount of *sec*-BuLi (9.90 mL, 10.9 mmol, for a target M_n = 5000) was added. The isoprene was added dropwise from the ampule and the reactor was warmed to room temperature after complete addition of the monomer. The polymerization was allowed to proceed for 5 h before cooling to 0 °C and adding 1 L of THF. A sample of the side chains was removed for characterization and terminated with degassed

isopropanol acidified with few drops of HCl. The reactor was cooled to -96 °C with a toluene/liquid nitrogen bath. The acetylated polystyrene latex particles dispersion was then added at once. The reactor was warmed to room temperature (23 ^{o}C) in a water bath and stirred for 2 h, the color of the reaction mixture fading completely over that time. Residual macroanions were terminated by injecting 1 mL of degassed, acidified isopropanol in the reactor. The raw product (65 g) was recovered by precipitation in methanol and dried under vacuum. The grafted latex particles were isolated from linear PIP contaminant (after redispersion of the raw product in hexane at a concentration of 10 % by weight) by centrifugation for 90 min at 6000 rpm. Successful separation was confirmed by the lack of a peak corresponding to the polyisoprene side chains in SEC analysis of the purified sample. The purified grafted particles (14.9 g) were then recovered by redispersion in THF, precipitation in methanol, suction filtration, and drying under vacuum to constant weight.

6.2.5 Synthesis of Linear Polyisoprene

The polymerization of isoprene was performed in cyclohexane at room temperature to yield a microstructure with a high *cis*-1,4-unit content as before. The purified isoprene monomer ampule (185 g, 2.72 mol), the dry cyclohexane inlet, and a rubber septum were mounted on the 3-L glass reactor with a vacuum-tight mechanical stirrer. The reactor was evacuated, flamed, filled with purified N_2, and cyclohexane (1.5 L) and 1.5 mL of 0.10 M 2,2′-bipyridyl solution in cyclohexane were added. The solvent was titrated with *sec*-butyllithium solution to give a persistent light orange color,[20] the reactor was than cooled to 0 °C before the calculated amount of *sec*-BuLi (0.96 mL, 1.06 mmol, for a target M_n = 175000) was added. The isoprene was added from the ampule slowly over 15 min, and the reactor was

warmed to room temperature (23 ^{o}C) in a water bath after the complete addition of the monomer. After 72 h, the reaction was terminated by injecting 1 mL of degassed, acidified isopropanol in the reactor. The crude product (180 g) was recovered by precipitation in methanol and drying under vacuum for 24 h. The polymer had an absolute M_n = 395000 (M_w/M_n = 1.09), as determined by SEC analysis with a multi-angle laser light scattering (MALLS) detector, and a microstructure with 94 % 1,4-*cis*-and -*trans*-isomers combined and 6 % 3,4-units as determined by ^{1}H NMR spectroscopy analysis by the method of Tanaka et al.[21]

6.2.6 Blending

The polyisoprene-grafted latex particle samples and the linear polyisoprene matrix used for the blends were first stabilized with 0.25 % w/w *N*-*N*'-diphenyl-1,4-phenylenediamine by dissolution in THF. The stabilized samples were recovered by evaporation of the solution to constant mass over several days under vacuum.

Solution blending was achieved at room temperature (23 °C) by dispersing the polyisoprene-grafted latex particles and dissolving the high *cis*-1,4 linear polyisoprene matrix sample (LPIP395, 1.0 g) separately in 50 mL of THF with sonication for 60 min. Different amounts of grafted latex particles were used as reported in Table 6.4, depending on their polyisoprene weight fraction. The two components were then mixed and sonicated further for 30 min. The mixture was poured into a 150 mL PTFE beaker with a magnetic stirring bar, and left to evaporate with stirring in a fume hood at room temperature. The blends were dried further under vacuum and stored at -78 °C.

6.2.7 Sample Characterization

The size of the latex particles before and after grafting was assessed by SEM analysis. A drop of diluted latex in THF was evaporated on a SEM specimen pin mount (aluminum stud), coated with gold using a Potaron sputter coater, and examined in a Hitachi S-570 scanning electron microscope with an acceleration voltage of 10-15 kV. The dispersion state of the particles within the polyisoprene matrix was examined by freeze fracture SEM microscopy in the Department of Food Sciences, University of Guelph, Ontario. Blend samples were mounted on a copper holder designed for the Emscope SP2000A Cryo-preparation unit (Ashford, Kent, UK) using Tissue-Tek®, a cryo-mounting gel. The copper holders were plunged into liquid nitrogen slush (-207 ^{0}C), withdrawn from the freezing chamber under argon to prevent condensation on the surface of the samples, and were put under vacuum for fracturing to provide a fresh surface. The samples were coated with gold (30 nm) in the Emscope cryo-preparation system below -135 °C. The holder was then transferred, frozen and under vacuum, onto the cold stage in the Hitachi S-570 SEM instrument and the temperature was maintained below -135 °C at all times. The SEM images were captured digitally using the Quartz PCI imaging software (Quartz Imaging Corp., Vancouver, BC).

FT-IR spectroscopy was used to monitor the acetylation reaction. Samples for analysis were prepared by sonication of 15 mg of latex particles in 5 mL of chloroform for 15 min. The dispersion was cast on a NaCl plate and allowed to dry slowly under an inverted beaker. The spectrum was recorded on a Perkin Elmer FT-IR spectrometer at a resolution of 4 cm^{-1} using 4 scans.

Routine SEC characterization was performed for the linear polyisoprene matrix sample, the polyisoprene side chains, the raw grafting products, and the purified grafting products

using a Waters 510 HPLC pump equipped with a Jordi 500 mm DVB linear mixed-bed column and a Waters 410 differential refractometer (DRI) detector. The polymers were analyzed in THF at a flow rate of 1 mL/min. Apparent polydispersity indices (M_w/M_n) for the M_n ~ 2K PIP side chains were determined using a linear polystyrene standards calibration curve.

The absolute number-average molecular weight (M_n) and polydispersity index (M_w/M_n) of the linear polyisoprene matrix and the ~ 5K and ~ 30K PIP side chains were determined by SEC-MALLS (multiangle laser light scattering) analysis using a Wyatt Dawn DSP-F instrument operating at 632.8 nm. The SEC-MALLS system used consists of a Waters 590 programmable HPLC pump coupled with Waters Ultrastyragel columns (10^4, 10^5, and 10^6 Å pore sizes) using THF at a flow rate of 1 mL/min. Polymer concentration measurements in the eluent were accomplished with a Waters 2410 DRI detector operating at 660 nm. Molecular weights were obtained from the MALLS and DRI signals, using the Astra Version 4.70.07 software package.

^{1}H NMR spectroscopy was used to determine the absolute M_n for the ~ 2K PIP side chain samples. The microstructure of the PIP linear matrix and side chains, and the composition of the grafted latex particles were analyzed by ^{1}H NMR spectroscopy on a Bruker-300 (300 MHz) nuclear magnetic resonance spectrometer instrument in $CDCl_3$ at a concentration of 5 %. The microstructure of the PIP samples was analyzed by the method of Tanaka et al.[21] For the composition analysis of the grafted latex particle, ^{1}H NMR spectra were obtained under the same conditions for a known concentration of the fractionated particles (after the removal of non-grafted PIP chains) and in the presence of a known amount of the same side chains as an internal standard. The areas of the integrated PIP peaks in the two

samples were compared to calculate the weight percentage of PIP in the product. The PIP contents were also determined from the yield of purified grafted particles.

6.2.8 Rheology

The blends of the stabilized linear polyisoprene matrix with the grafted latex particles were characterized on a Paar Physica US-200 Rheometer using a parallel-plate geometry with a diameter of 25 mm and a plate gap of 1 mm at 25 °C. The blends were compression-molded at room temperature (23 °C) to ca. 1 mm thick and 25 mm diameter disks. The samples were loaded between the plates and allowed to equilibrate for 1 h at 25 °C. Dynamic mechanical analysis (complex viscosity, storage modulus, and damping factor) was performed with a frequency sweep from 60 to 1×10^{-4} Hz at 25 °C. The strain amplitude was controlled at 15 % for all the samples, based on dynamic strain sweeps performed to determine the regime of linear viscoelasticity, using strains of 1 – 20 % with different fixed frequencies (1, 10, 40, 60, and 80 Hz).

6.3 Results and Discussion

6.3.1 Emulsifier-free Synthesis of Poly(styrene-co-divinylbenzene) Latex Particles

Surfactants are used most of the time in emulsion polymerization, to facilitate the emulsification of the monomer and to impart colloidal stability to the particles. This approach is disadvantageous for certain applications such as in the current study, not only because of the risk of contamination of the polymer blends by the surfactant, but also due to its potential interference with the anionic grafting reaction. For these reasons, a surfactant-free emulsion polymerization technique was developed to produce the cross-linked model filler particles. In

this approach the initiator concentration, solids content, temperature, and stirring rate must be carefully controlled to obtain stable emulsions.[22] These parameters also dictate the size and uniformity of the particles obtained. Styrene was polymerized by free radicals generated from ammonium persulfate according to Scheme 6.1. In the emulsifier-free method, the polar groups introduced as chain ends on the polymer stabilize the growing particles in the aqueous phase. The stabilizing surface groups for persulfate-initiated systems have been characterized as a combination of sulfate, hydroxyl, and carboxyl functionalities, the proportion of each species depending on the reaction conditions.[23]

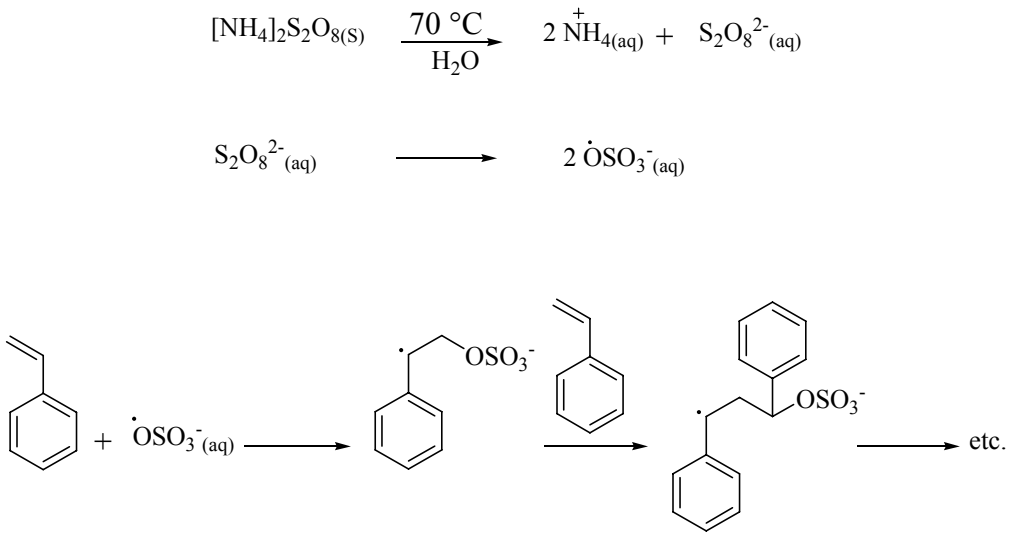

Scheme 6.1 Free radical polymerization of styrene with ammonium persulfate.

The addition of a cross-linking agent complicates the polymerization procedure because it can destabilize the emulsion and lead to coagulation of the reaction. Furthermore, the commercial DVB cross-linking agent used is a mixture containing mainly the *para*- and *meta*- isomers. Both isomers have copolymerization reactivity ratios favoring the incorporation of DVB over styrene in the composition range used ($r_1 = 0.260$, $r_2 = 1.18$ for styrene and *p*-divinylbenzene, respectively, and $r_1 = r_2 = 0.58$ for styrene and *m*-divinylbenzene,

respectively). Simple combination of the two monomers in a batch polymerization reaction would result in non-homogenous cross-linking of the particles. For that reason, a starved-feed emulsifier-free emulsion polymerization technique[16] was preferred. The latex obtained had a solids content of 4.4 % and a spherical shape (Figure 6.2). Distinct particles were observed in the SEM pictures after coagulation and redispersion of the product in a good solvent for polystyrene, as expected for cross-linked particles. The particle diameter determined from the SEM images using the ImageJ 1.36b image processing and analysis program is 400 ± 6 nm. This substrate was used in the subsequent acetylation and grafting reactions.

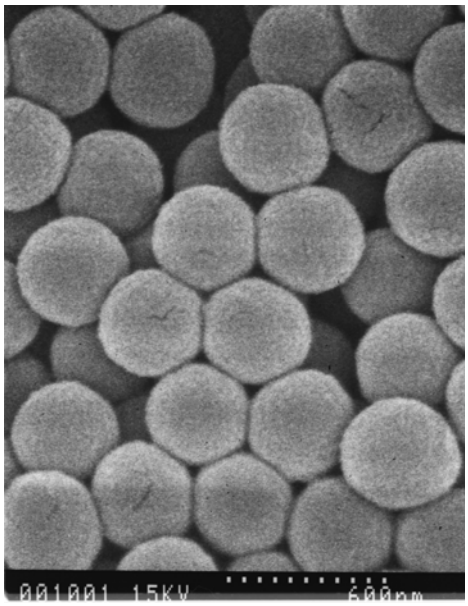

Figure 6.2 SEM image for 400 nm spherical PS particles cross-linked with 12 mol % DVB.

6.3.2 Acetylation of Poly(styrene-co-divinylbenzene) Latex Particles

The acetyl groups serving as coupling sites were incorporated in the latex particles by Friedel-Crafts acylation. Chloromethylation was used previously to introduce chloromethyl

coupling sites on polystyrene substrates,[24] but the acetylation path used in the current study presents some important advantages. Acetyl chloride is much more innocuous than chloromethyl methyl ether (CMME) serving in the chloromethylation reaction.[25] It is easier to control the functionalization level attained by acetylation than by chloromethylation: A large excess of CMME is typically used in chloromethylation to minimize side reactions,[26,24a] which leads to the deactivation of variable amounts of catalyst depending on the purity level of the CMME. In contrast, the acetylation level attained is determined by nearly stoichiometric amounts of $AlCl_3$ and acetyl chloride.[17] Variation in the acetylation level provides control over the density of coupling sites on the substrate, and thus the density of grafted polymer chains at the surface of the particles.[27] The acetylation level was set at ~ 5 mol % and ~ 30 mol %, to obtain two different grafting site densities on the PS latex particles.

The acetylation of the cross-linked polystyrene latex particles was performed by adding a mixture of acetyl chloride and anhydrous $AlCl_3$ to the particles dispersed in nitrobenzene.[17] The acetylation level of linear polystyrene substrates is conveniently quantified by ^1H NMR spectroscopy analysis.[17] The acetylated latex particles are insoluble, however, and cannot be characterized by that technique. Acetylation of the substrate was rather confirmed by FT-IR spectroscopy analysis, by the presence of an intense and well-resolved characteristic carbonyl stretching vibration at 1684 cm^{-1} as shown in Figure 6.3b. For comparison, the FT-IR spectrum for a non-acetylated PS latex particle is shown in Figure 6.3a. Unfortunately, FT-IR analysis cannot provide the precise acetylation level attained, because it is not clear whether acetylation takes place evenly throughout the whole volume of the particles or preferentially on their surf-

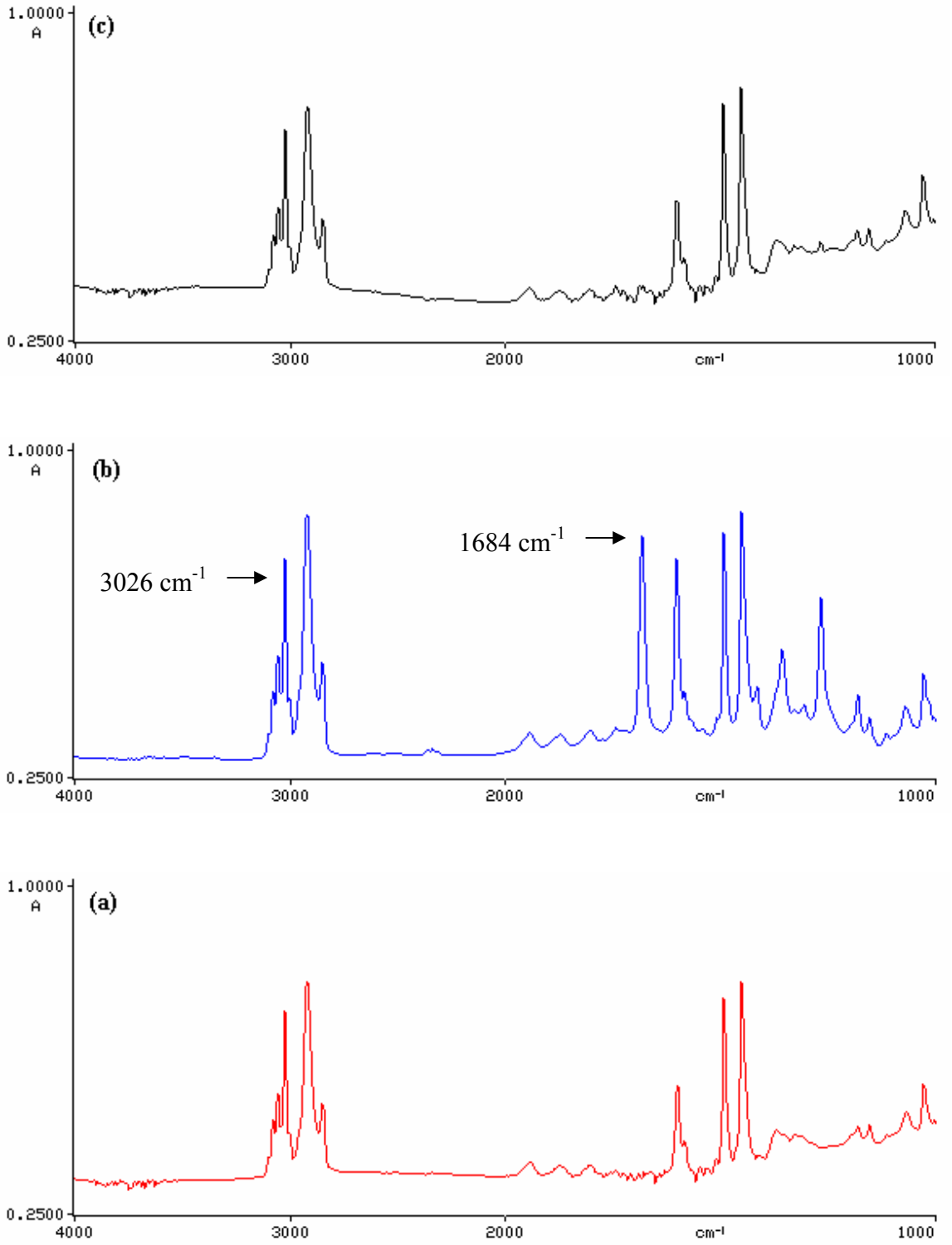

Figure 6.3 FT-IR spectra for (a) latex particles, (b) ~ 30 mol % acetylated latex particles, and (c) latex particles after grafting with M_n = 5000 PIP side chains {PS[30]-*g*-PIP5}

ace. Another problem is that the penetration depth of the IR beam is unknown, making it impossible to use integrated absorbance peak intensities for quantitative analysis.

In a previous study, a calibration curve correlating peak height ratios (in the absorbance mode) of FT-IR spectra with the acetylation level determined by ^{1}H NMR analysis was generated using linear polystyrene samples.[28] This calibration technique assumes that the width of all the peaks remains constant, or that the peak area is proportional to the peak height. The peaks compared were at 1684 cm^{-1} and 3026 cm^{-1}, corresponding to carbonyl and alkyl (C-H) stretches, respectively (identified on Figure 6.3b). If the calibration curve is assumed to be valid for the acetylated latex particle samples, a substitution level of 17 mol % can be determined for the targeted ~ 30 mol % acetylation level. No calculation was attempted for the ~ 5 mol % acetylated PS latex, as the peak ratio for that sample falls outside the limits of the calibration curve. In spite of these limitations, the presence of the absorbance peak at 1684 cm^{-1} is used as a semi-quantitative indication of the acetylation level attained.

6.3.3 Polymerization of Isoprene

The microstructure of polyisoprene chains is strongly dependent on the polarity of the solvent used[29] and, to a lesser extent, on the initiator and monomer concentrations in the reaction.[30] In non-polar (hydrocarbon) solvents a predominantly *cis*-1,4-microstructure resembling natural rubber is obtained, while more polar solvents (e.g. THF) lead to a mixed microstructure with 1,4-, 1,2-, and 3,4-isoprene units. To achieve good mixing in the blends, *cis*-1,4-polyisoprene chains obtained by polymerization in cyclohexane were used in the present study for the side chains grafted on the latex particles. The ^{1}H NMR spectrum for LPIP395 (matrix polymer) is shown in Figure 6.4.

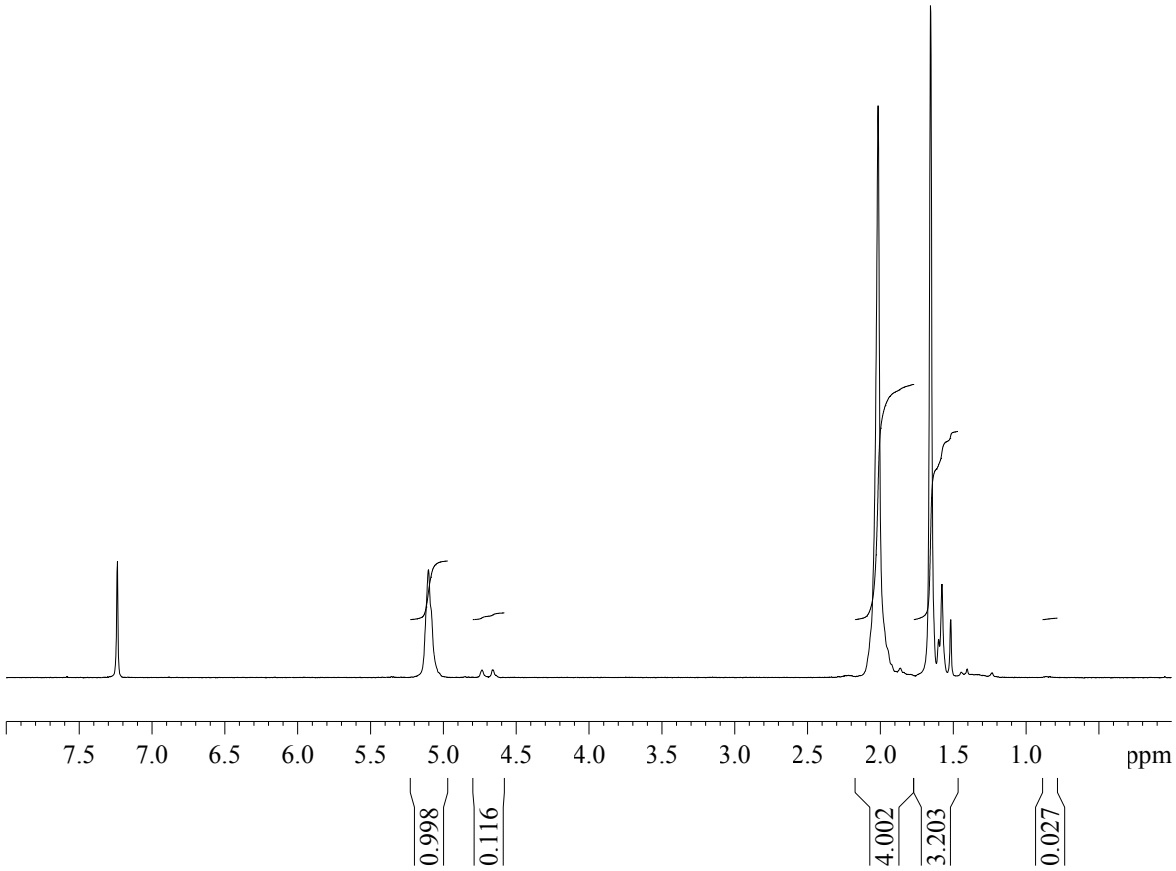

Figure 6.4 300 MHz ^{1}H NMR spectrum for linear high *cis*-1,4-polyisoprene (matrix polymer) in $CDCl_3$.

By comparing the area of the peaks at 5.10 ppm (olefinic protons of the *cis*- and *trans*-1,4-microstructures combined) and the doublet at 4.73 and 4.66 ppm (two vinylic protons of the 3,4-microstructure),[21] the content of 1,4- and 3,4-units was estimated to be 94 % and 6 %, respectively. The linear polyisoprene matrix (LPIP395) had an absolute number-average molecular weight M_n = 395000 and M_w/M_n = 1.09. A high *cis*-1,4-microstructure content was also obtained for the side chain samples removed from the reactor before the latex particle grafting reactions, and the analysis results are summarized in Table 6.2 The microstructure of the polyisoprene chains varied from 88-94 mol % for the combined *cis*- and *trans*-1,4-

microstructures, and from 6-13 mol % for 3,4-units. The microstructure variations observed among the samples are consistent with the different initiator and monomer concentrations used in the polymerization reactions. An increase in initiator concentration or a decrease in monomer concentration should both lead to a decrease in 1,4-units content.[30] A lower 1,4-units content is indeed observed for shorter ($M_n \approx 2000$ and 5000) side chains, prepared at higher initiator concentrations and lower monomer concentrations as compared with $M_n \approx 30000$ side chains and the LPIP395 matrix polymer (Table 6.2).

Table 6.2 Microstructure of Polyisoprene Side Chains and Linear Polyisoprene Matrix Determined from ^{1}H NMR Spectroscopy Analysis.

Sample	Microstructure / mol %	
	1,4-*cis*-and -*trans*-isomers combined	3,4-units
PS[5]-*g*-PIP2	88	12
PS[5]-*g*-PIP5	88	12
PS[5]-*g*-PIP30	94	6
PS[30]-*g*-PIP2	87	13
PS[30]-*g*-PIP5	88	12
PS[30]-*g*-PIP30	94	6
LPIP395	94	6

6.3.4 Grafting Reaction

The latex particles were grafted with polyisoprene side chains with a microstructure similar to the matrix polymer, to study the influence of filler particle-matrix interactions on the rheological behavior of the blends. The grafting reaction involves nucleophilic attack on the

carbonyl functionalities of the acetylated polystyrene latex substrate by the polyisoprenyl anions as shown in Scheme 6.2.

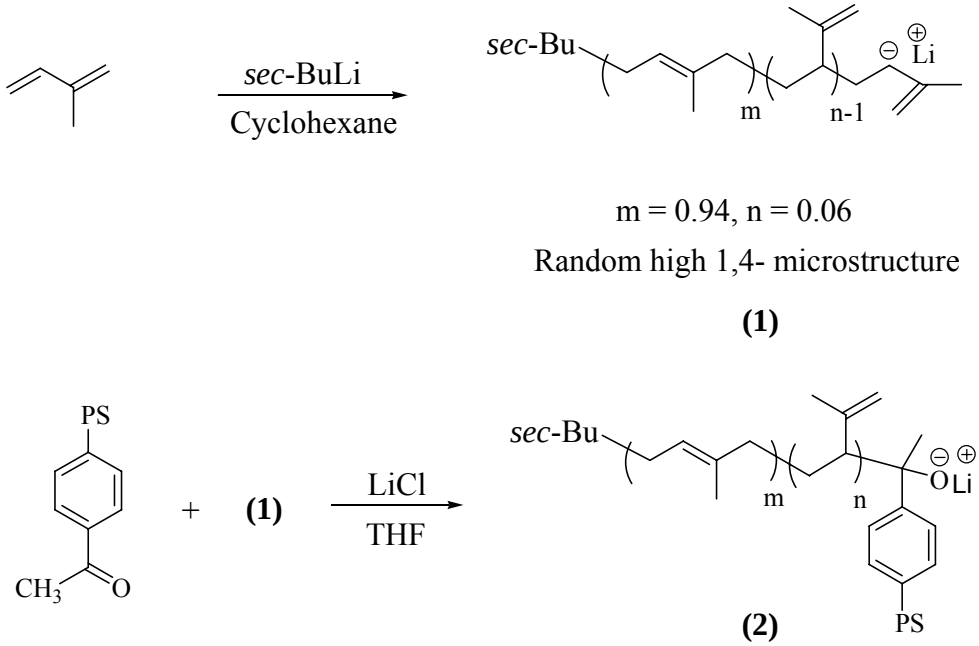

Scheme 6.2 Grafting reaction of polyisoprenyl anions onto acetylated particles.

The FT-IR spectrum of the 30 % acetylated latex particles grafted with M_n = 5000 side chains, after removal of the linear PIP contaminant, is shown in Figure 6.3c. The carbonyl stretch present at 1684 cm^{-1} in the acetylated latex particle (Figure 6.3b) is absent in the

product, indicating the essentially complete consumption of the carbonyl groups by the polyisoprenyl anions in the reaction. SEM imaging also provides evidence for the success of the grafting reaction: In Figures 6.5 and 6.6, some of the grafted particles appear "sticky" after grafting, due to the interpenetration of the grafted chains within the PIP shell. This effect is more prominent for the longer (M_n = 30000) PIP side chains and the PS substrates with a higher (~ 30 mol %) acetylation level, presumably due to the increased density of PIP chains within the PIP shell. Some smaller particles (secondary population) can also be seen in Figures 6.5 and 6.6, even though they were not seen in the SEM of the original latex substrate (Figure 6.2). These particles, presumably also present in the substrate, are termed secondary particles because of their smaller size and are due to active oligomers formed in the water phase not being captured by the existing particles.[31]

The characteristics of the grafted latex particles obtained are summarized in Table 6.3. The sample nomenclature used for the grafted particles reflects their composition and structure. For example, PS[5]-*g*-PIP2 refers to latex particles with an acetylation level of ~ 5 mol % and grafted with $M_n \approx 2000$ polyisoprene side chains. Side chains with a high *cis*-1,4-isoprene units content were prepared by polymerization in cyclohexane, but a large volume of THF was introduced in the reactor to increase the polarity of the reaction mixture prior to grafting. This was done to increase the yield of the coupling reaction, found to be negatively influenced by low polarity solvents.[32] This approach was also found to be beneficial when grafting polyisoprene side chains onto both chloromethylated and acetylated linear polystyrene substrates.[33] The grafting yield, defined as the fraction of side chains generated in the reaction that becomes coupled with the substrate, was found to decrease when grafting longer side chains onto the latex particles (Table 6.3). The inaccessibility to the macroanions of coupling

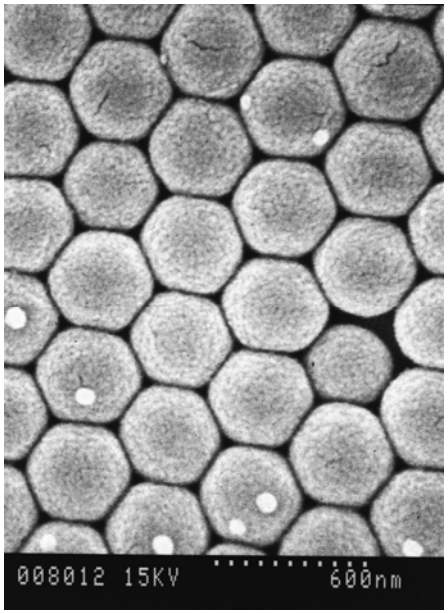

(a)

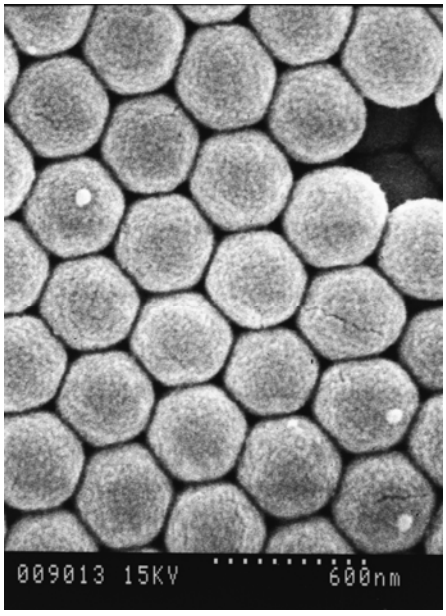

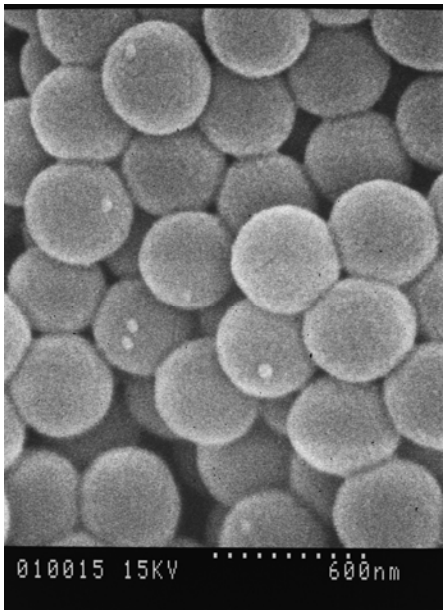

(b) **(c)**

Figure 6.5 SEM images for ~ 5 mol % acetylated latex particles grafted with PIP: (a) PS[5]-*g*-PIP2, (b) PS[5]-*g*-PIP5, and (c) PS[5]-*g*-PIP30.

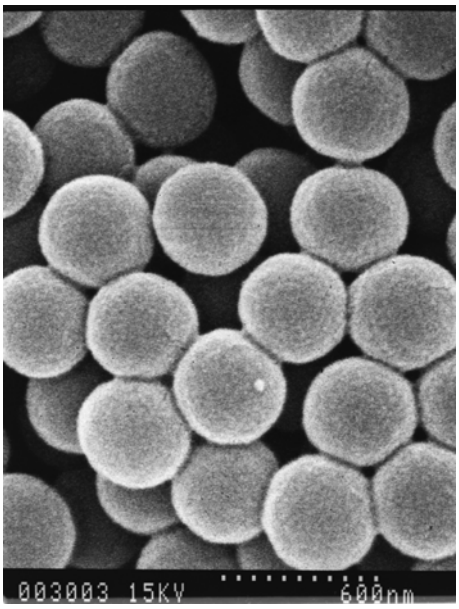

(a)

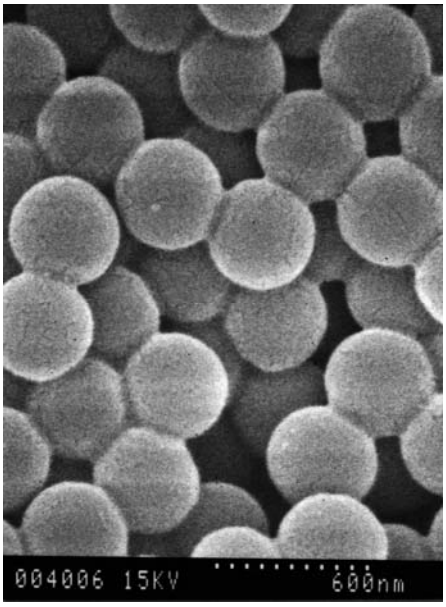

(b)

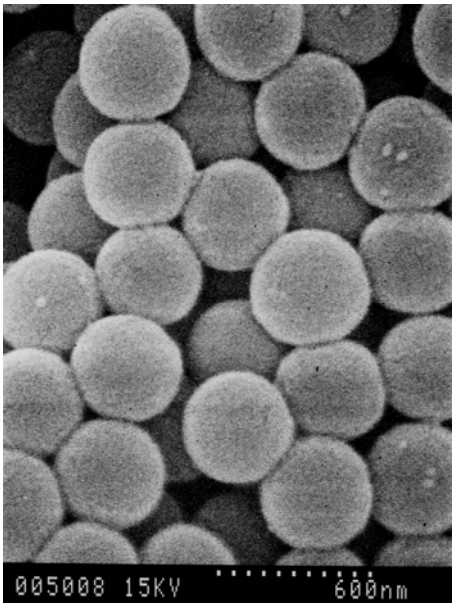

(c)

Figure 6.6 SEM images for ~ 30 mol % acetylated latex particles grafted with PIP: (a) PS[30]-*g*-PIP2, (b) PS[30]-*g*-PIP5, and (c) PS[30]-*g*-PIP30.

sites buried within the substrate, and the presence of residual protic impurities difficult to remove from the rigid particle substrate, are suggested to explain the low (21 – 33 %) grafting efficiencies obtained. Another factor potentially significant is the inherent immiscibility of the polystyrene and polyisoprene phases, further hindering the diffusion of the macroanions to the coupling sites.

The thickness of the PIP shell (Table 6.3, column 5) was obtained by subtracting the core size (400 ± 6 nm) from the diameters determined from the SEM micrographs of Figures 6.2, 6.5, and 6.6 using the ImageJ 1.36b image processing and analysis program. The shell thickness is ca. 25-30 nm and comparable for most samples with the exception of PS[5]-*g*-PIP2 and PS[5]-*g*-PIP5. The shell thickness obtained for these two samples is insignificant, considering the large standard deviations on the measurements. For the composition analysis of the grafted latex particles, ^{1}H NMR spectra were obtained under the same conditions for the fractionated particles (after the removal of non-grafted PIP chains) and after addition of a known amount of side chain material as an internal standard. Composition analysis of the grafted particles by ^{1}H NMR spectroscopy yielded polyisoprene contents varying from 5.5 % to 17 % by weight (Table 6.3, column 8). The polyisoprene contents were also estimated from the mass of particles isolated after the grafting reaction in comparison to the mass of the acetylated particles used in the reaction (Table 6.3, column 9). The weight fraction of polyisoprene obtained by the two methods is significantly different. Composition analysis of the grafted particles by ^{1}H NMR spectroscopy based on the peak area for the PIP chains depends strongly on chain mobility. The PIP contents determined by that method are invariably lower than for the gravimetric method, in particular for shorter PIP chains. This is attributed to the restricted

Table 6.3 Characteristics of Polyisoprene-grafted Latex Particles and PIP Side Chains

Sample	PIP Side Chains		PS [d]	Graft PS			% w/w PIP		ϕ_{PS}
	M_n [c]	M_w/M_n [c]	(g)	PIP Shell Thickness [e] (nm)	Yield [f] (g)	Grafting Efficiency (%) [g]	NMR [h]	Yield [i]	Yield [j]
PS[5]-*g*-PIP2	1500[a]	1.08[b]	15	5 ± 21	15.9	33	-	5.66	0.93
PS[5]-*g*-PIP5	4900	1.09	15	4 ± 18	16.3	32	-	7.98	0.91
PS[5]-*g*-PIP30	26800	1.12	15	27 ± 19	16.6	21	8.00	9.64	0.89
PS[30]-*g*-PIP2	1700[a]	1.10[b]	12	31 ± 14	14.8	31	5.50	18.9	0.79
PS[30]-*g*-PIP5	5400	1.05	12	24 ± 12	14.9	29	14.5	19.5	0.78
PS[30]-*g*-PIP30	28600	1.12	14	29 ± 10	17.6	22	17.0	20.5	0.77

a) M_n from ^{1}H NMR analysis. b) Apparent values from SEC analysis with a linear polystyrene standards calibration curve. c) Absolute values from SEC-MALLS analysis. d) Mass of acetylated latex particles used in the grafting reaction. e) Determined by SEM analysis. f) Yield of purified grafted particles. g) Fraction of side chains attached to the substrate. h) PIP content from ^{1}H NMR spectroscopy; no signal detected for PS[5]-*g*-PIP2 and PS[5]-*g*-PIP5. i) PIP content calculated from purified grafted particles yield. j) Volume fraction of polystyrene determined from the yield.

mobility of the portion of the PIP chains attached to the particles, making these side chains difficult to detect by NMR spectroscopy. In fact no NMR signal was observed for particles grafted with very short (M_n = 2000) PIP side chains, presumably for the same reason.

6.3.5 Blending

The composition of the blends investigated, provided in Table 6.4, was set to maintain a constant polystyrene core volume fraction ϕ = 0.35 after mixing with the LPIP395 matrix. The distribution of the filler particles within the polyisoprene matrix was examined by the freeze fracture SEM technique. The SEM micrographs for the blends, provided in Figures 6.7a-c and 6.8a-c, show that even though some particle aggregation was present, the distribution of particles achieved within the matrix by solution blending was fairly homogeneous.

Table 6.4 Composition of the Blends

Sample	Grafted Latex (g)	LPIP395 (g)
PS[5]-*g*-PIP2	0.68	1.00
PS[5]-*g*-PIP5	0.71	1.00
PS[5]-*g*-PIP30	0.46	1.00
PS[30]-*g*-PIP2	0.89	1.00
PS[30]-*g*-PIP5	0.90	1.00
PS[30]-*g*-PIP30	0.93	1.00

It should be noted that while the particles are uniformly dispersed within the matrix polymer, the particles in the blend incorporating sample PS[30]-*g*-PIP30 (Figure 6.8c) look significantly larger than for the other blends. This effect is attributed to enhanced entanglement of the grafted side chains with the matrix polymer. In contrast, no significant increase in apparent diameter (and presumably in entanglement level) is observed for blends based on the ~ 5 mol % acetylated particles, even for M_n = 30000 side chains (Figure 6.7a-c).

6.3.6 Rheology

Dynamic mechanical measurements were performed on the blends to study the influence of the polyisoprene side chain length and the composition of the particles on the viscoelastic properties of the filled polyisoprene matrix. Two distinct regions are generally observed in modulus-frequency curves above the glass transition temperature (T_g) for linear, high molecular weight polymers.[34] These are present for the linear polyisoprene matrix and for all the blends. The relatively flat plateau at high and intermediate frequencies is associated with localized motions of polymer segments restricted by entanglements. The low-frequency or terminal region is associated with viscous flow of the polymer, involving motions of the entire molecules. This terminal relaxation process is most effectively described by reptation motions of a chain along its entangled length.[35] The rheology of filled polymers depends on the structure and the composition of the filler and the matrix, because of variations in the particle-matrix interactions. Strong interactions tend to increase the viscosity and the dynamic modulus, as polymer chains bonded or strongly adsorbed onto the filler surface restrict the mobility

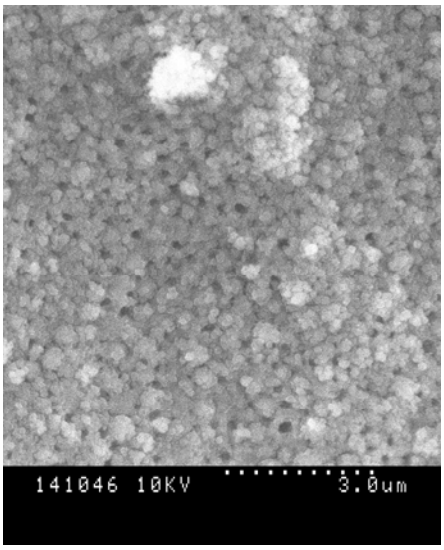

(a)

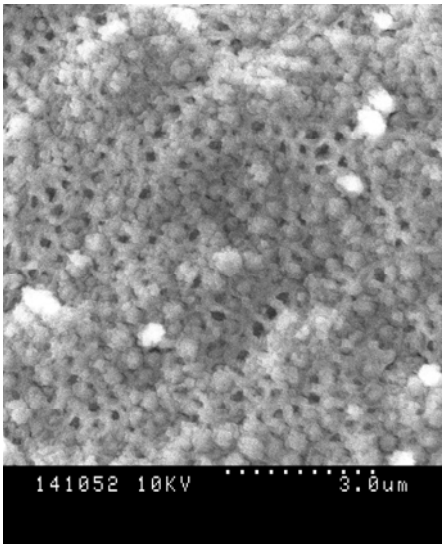

(b)

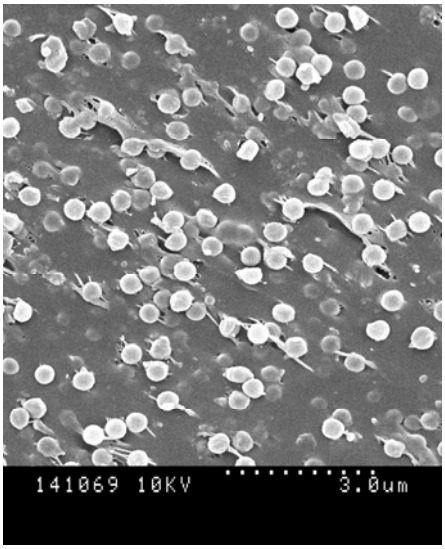

(c)

Figure 6.7 SEM images for blends of ~ 5 mol % acetylated particles grafted with PIP for (a) PS[5]-*g*-PIP2, (b) PS[5]-*g*-PIP5, and (c) PS[5]-*g*-PIP30.

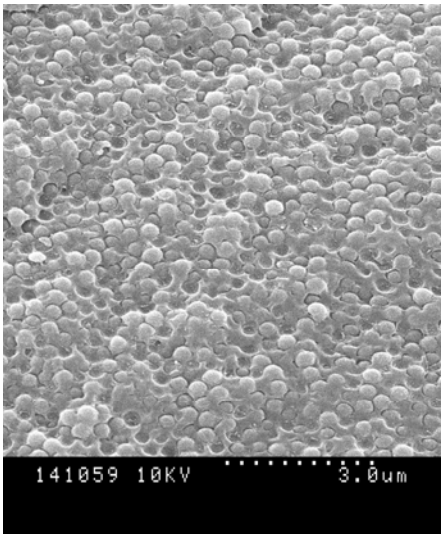

(a)

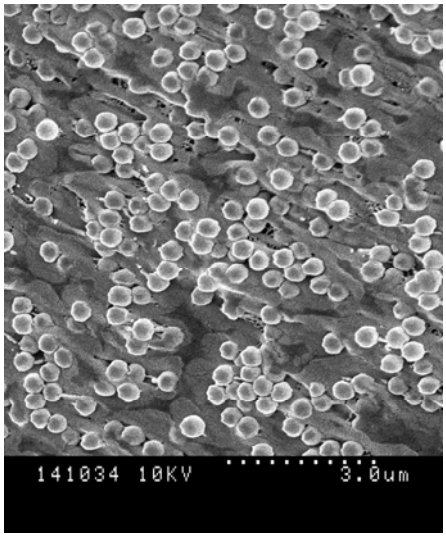

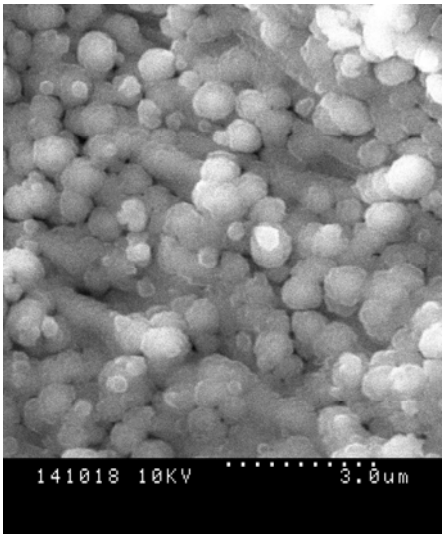

(b) **(c)**

Figure 6.8 SEM images for blends of ~ 30 mol % acetylated particles grafted with PIP for (a) PS[30]-*g*-PIP2, (b) PS[30]-*g*-PIP5, and (c) PS[30]-*g*-PIP30.

of the matrix polymer chains.[3,4] A number of investigations indeed reported significant increases in viscosity and dynamic modulus after the surface treatment of fillers with a binding or coupling agent to increase the interactions between the polymer matrix and the fillers.[12,13, 36-38] Dynamic mechanical measurements were also performed on blends of a low molecular weight polysulfide matrix with fillers of different chemical compositions. The authors argued that fillers which were "chemically compatible" with the matrix due to better particle-matrix interactions were better dispersed within the matrix, and led to larger increases in dynamic modulus and viscosity[11] (this was also discussed in Chapter 2, Section 2.5.4). On the basis of these trends a similar influence of the grafted PIP chains was expected, due to the influence of the grafted PIP chains on the degree of entanglement and compatibilization of the particles with the PIP matrix.

The complex viscosity (η^*), storage modulus (G'), and damping factor (tan δ) curves, obtained as a function of frequency from 1×10^{-4} to 60 Hz, are shown in Figures 6.9a-b, 6.9c-d, and 6.9e-f, respectively. It is clear that the rheology of the filled polymers is significantly affected by the grafted particles. Favorable particle-matrix interactions due to the grafted polyisoprene shell increases the complex viscosity, and the storage modulus for all the blends in the high frequency range (1 – 60 Hz) corresponding to the plateau region of the modulus curves, as well as in the low frequency range (10^{-4} – 1 Hz) related to terminal relaxation. The increases are more important for particles based on an acetylation level of ~ 30 mol % (Figure 6.9b, 6.9d), containing a larger number of compatibilizing polyisoprene chains at their surface, than for particles based on an acetylation level of ~ 5 mol % (Figure 6.9a, 6.9c). For sample PS[30]-*g*-PIP30 (Figure 6.9d), the storage modulus of the blend is almost 4-fold larger than for the non-filled

LPIP395 matrix, in agreement with the Guth-Smallwood equation, $G = G_0 (1 + 2.5\phi + 14.1\phi^2)$, where G, G_0, and $\phi = 0.26$ represent the modulus of the filled polymer, the modulus of the non-filled polymer matrix, and the volume fraction of the filler, respectively. In comparison, samples PS[30]-*g*-PIP2 and PS[30]-*g*-PIP5 displayed somewhat lower increases, i.e. 2.3-fold and 2.5-fold, respectively. For samples PS[5]-*g*-PIP2, PS[5]-*g*-PIP5, and PS[5]-*g*-PIP30, based on ~ 5 mol % acetylated particles, the storage modulus of the blends is 2.7-fold, 2.0-fold, and 3.0-fold larger than for the non-filled LPIP395 matrix, respectively (Figure 6.9c). Since the particles were shown to be uniformly distributed in all the blends, this effect is attributed to a higher degree of entanglement for the longer (M_n = 30000) polyisoprene side chains with the matrix. This should increase the frictional resistance of the polymer chains, and thus the viscosity of the blends. A similar mechanism was suggested to explain the behavior of carbon black-filled rubbers for which filler-matrix interactions dominated.[2] Another study suggested an identical mechanism to explain the behavior of SBR filled with core-shell particles (PMMA core and polystyrene shell) and carbon black, by showing that the interactions of the matrix with the core-shell particles dominated over those with carbon black.[13]

The ratio of the loss and storage moduli (G"/G'), also called the damping factor or tan δ, corresponds to the ratio of energy dissipated to energy stored in one deformation cycle. At high frequencies (~ 1-60 Hz) the PIP matrix and all blends are within the rubbery plateau region, where energy storage and loss are determined by the local motions of the polymer chain segments. Since the relaxation time for the rigid filler particles is much longer than for the chain segments in the matrix, tan δ is determined mainly by the PIP matrix and is not strongly affected by the filler particles. Consequently,

tan δ appears to be relatively insensitive to composition over that frequency range. In the low frequency range (~ 0.0001-0.1 Hz), since the whole polymer molecules can move, the non-filled PIP matrix behaves like a viscous liquid and tan δ increases. Comparatively lower tan δ values are observed for all the blends in the low frequency range (Figure 6.9e-f), the change being most prominent for particles based on ~ 30 mol % acetylation. This result suggests that favorable particle-matrix interactions due to the grafted shell of polyisoprene chains increase the elasticity of the blends. The high density of grafted PIP chains on the particles favors chain entanglement and the formation of an elastic network with the PIP matrix chains that restricts the flow of the whole molecules. Indeed, the largest decreases in tan δ are observed for the blends of the particles grafted with longer PIP chains (M_n = 30000), presumably due to their more extensive entanglement with the matrix chains.

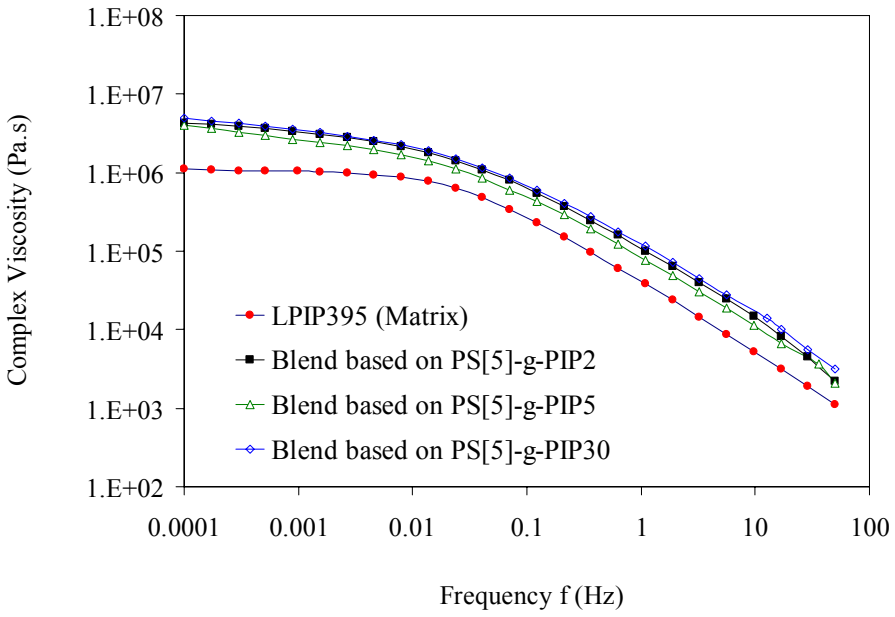

Figure 6.9a Complex viscosity of LPIP395 matrix non-filled and filled with PS[5] particles grafted with polyisoprene side chains as indicated.

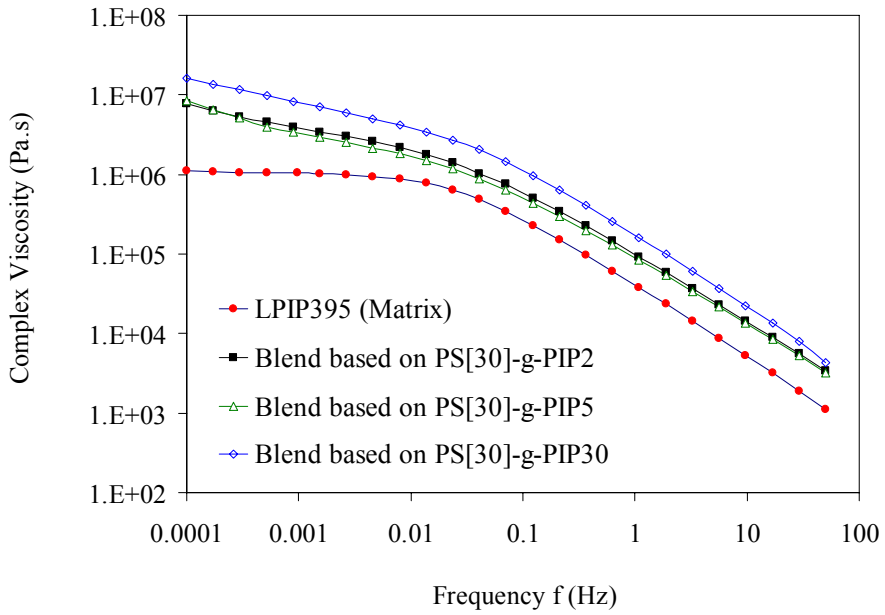

Figure 6.9b Complex viscosity of LPIP395 matrix non-filled and filled with PS[30] particles grafted with polyisoprene side chains as indicated.

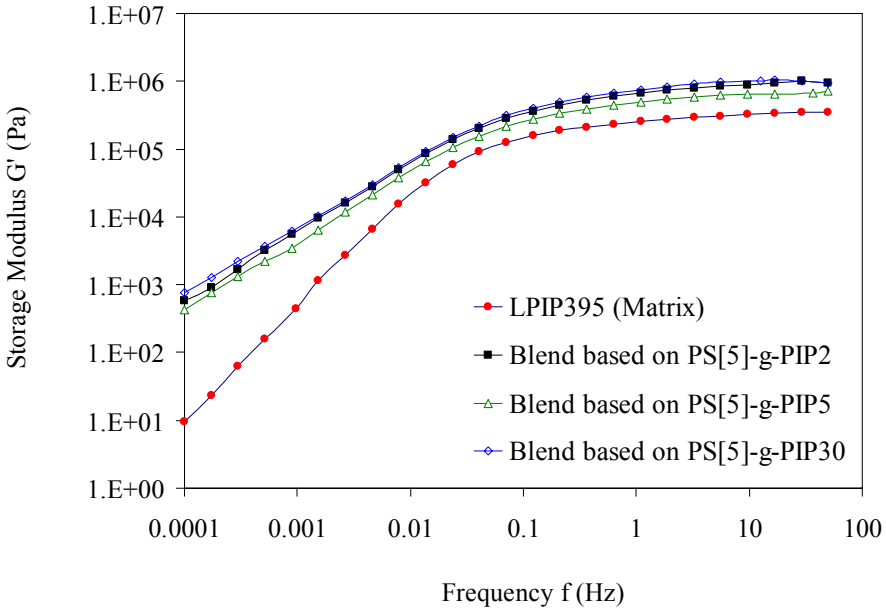

Figure 6.9c Storage modulus of LPIP395 matrix non-filled and filled with PS[5] particles grafted with polyisoprene side chains as indicated.

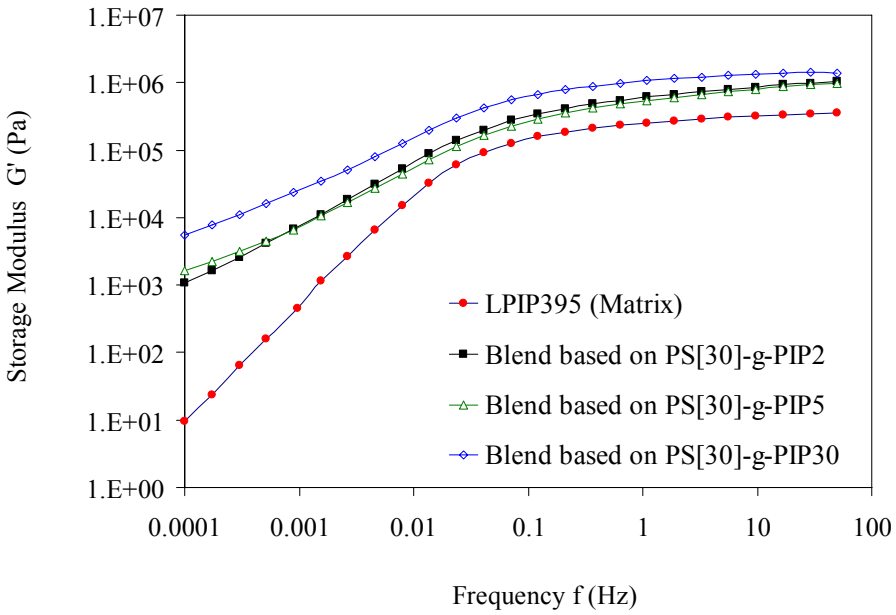

Figure 6.9d Storage modulus of LPIP395 matrix non-filled and filled with PS[30] particles grafted with polyisoprene side chains as indicated.

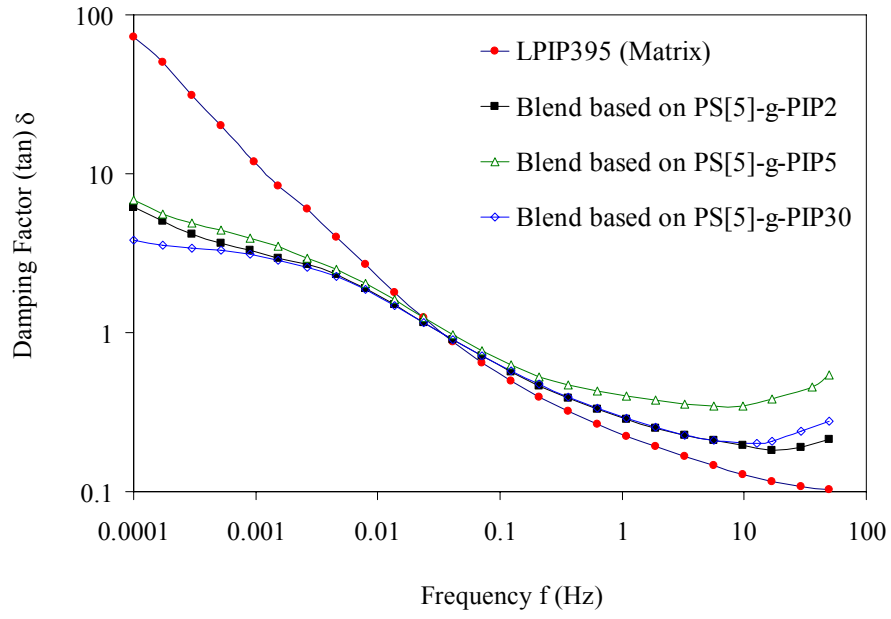

Figure 6.9e Damping factor of LPIP395 matrix non-filled and filled with PS[5] particles grafted with polyisoprene side chains as indicated.

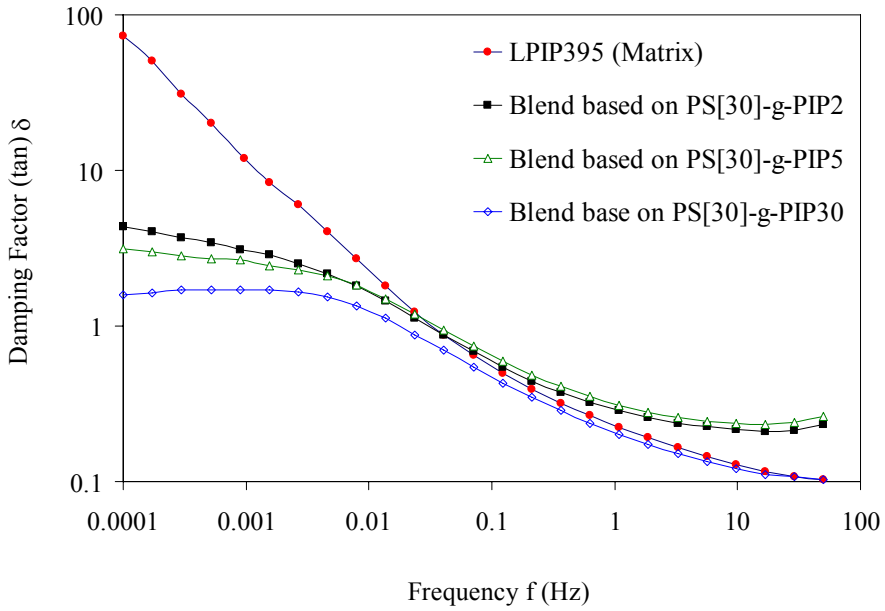

Figure 6.9f Damping factor of LPIP395 matrix non-filled and filled with PS[30] particles grafted with polyisoprene side chains as indicated.

6.4 Conclusions

Monodispersed polystyrene latex particles cross-linked with 12 mol % DVB were prepared by starved-feed emulsion polymerization in the absence of emulsifier. The particles obtained were of uniform, spherical shape with a diameter of 400 ± 6 nm as determined by SEM analysis. Activation of the particles was achieved by acetylation to target levels of ~ 5 mol % and ~ 30 mol % prior to grafting with *cis*-1,4-polyisoprene side chains with a molecular weight of either 2000, 5000, or 30000. The weight fraction of polyisoprene in the grafted particles was determined from the recovery yield of purified product and by NMR spectroscopy. Freeze fracture SEM imaging of blends of the linear PIP with the modified filler particles confirmed that the particles were uniformly distributed within the polyisoprene matrix in most cases.

The influence of filler structure on the rheological behavior of the blends was examined by dynamic mechanical analysis in terms of frequency-dependent complex viscosity, storage modulus, and damping factors over a frequency range of 10^{-4} to 60 Hz. All the blends exhibited enhanced complex viscosity, storage modulus, and decreased damping factor values relative to the matrix polymer. On that basis, it appears that the interactions between the filler particles and the polymer matrix decreased in the order ~ 30 mol % > ~ 5 mol % acetylation, and in terms of the M_n of the grafted PIP chain length, 30000 > 5000 ≈ 2000. The tan δ of the blends appears to be relatively insensitive to filler composition in the rubbery plateau (~ 1-60 Hz) region, but it is lower in comparison to the non-filled polymer matrix in the low frequency (flow) region. The decreased damping factors, indicative of lower heat dissipation, could be interesting for applications where the generation of heat is undesirable such as tires.

6.5 References

1. Byers, J. T.; Wayner, M. P. In *Rubber Technology*, *3rd Ed*; M. Morton, ed.; Van Nostrand Reinhold: New York, 1987. Chapter 3.
2. Wolff, S.; Wang, M.-J. *Rubber Chem. Technol*. **1992**, *65*, 329.
3. Agarwal, S.; Salovey, R. *Polym. Eng. Sci*. **1995**, *35*, 1241.
4. Zhu, J.; Ou, Y.-C.; Feng, Y.-P. *Polym. Int*. **1995**, *37*, 105.
5. Metzner, A. B. *J. Rheol*. **1985**, *29*, 739.
6. Kamal, M. R.; Mutel, A. *J. Polym. Eng*. **1985**, 5, 293.
7. Yilmazer, U.; Farris, R. J. *J. Appl. Polym. Sci*. **1983**, *28*, 3369.

8. Park, M.; Gandhi, K.; Sun, L.; Salovey, R.; Aklonis, J. J. *Polym. Eng. Sci.* **1990**, *30*, 1158.

9. (a) Sun, L.; Park, M.; Salovey, R.; Aklonis, J. J. *Polym. Eng. Sci.* **1992**, *32*, 777. (b) Sun, L.; Park, M.; Aklonis, J. J.; Salovey, R. *Polym. Eng. Sci.* **1992**, *32*, 1418.

10. Sun, L.; Aklonis, J. J.; Salovey, R. *Polym. Eng. Sci.* **1993**, *33*, 1308.

11. Cai, J. J.; Salovey, R. *J. Polym. Sci., Part B: Polym. Phys.* **1999**, *37*, 815.

12. Nuyken, O.; Bayer, R. *Kautsch. Gummi Kunstst.* **1995**, *48*, 704.

13. Nuyken, O.; Ko, S.-K.; Voit, B.; Yang, D. *Kautsch. Gummi Kunstst.* **1995**, *48*, 784.

14. (a) Merrington, A.; Yang, Z.; Meier, D. J. Proc. *1st Int. Particle Technol. Forum, Amer. Inst. Chem. Eng.* 1994. (b) Yang, Z.; Merrington, A.; Meier, D. J. *Polym. Mater. Sci. Eng.* **1994**, *73*, 438.

15. Todd, D. B. *Adv. Polym. Tech.* **2000,** *19*, 54.

16. Ding, Z.-Y.; Ma, S.; Kriz, D.; Aklonis, J. J.; Salovey, R. *J. Polym. Sci., Part B: Polym. Phys.* **1992**, *30*, 1189.

17. Li, J.; Gauthier, M. *Macromolecules* **2001**, *34*, 8918.

18. Lipton, M. F.; Sorensen, C. M.; Sadler, A. C.; Shapiro, R. H. *J. Organomet. Chem.* **1980**, *186*, 155.

19. Gauthier, M.; Tichagwa, L.; Downey, J. S.; Gao, S. *Macromolecules* **1996**, *29*, 519.

20. Liu, W.-L.; Loveless, F. C. U.S. Patent 5 489 649, 1996.

21. Tanaka, Y.; Takeuchi, Y.; Kobayashi, M.; Tadokoro, H. *J. Polym. Sci. Part A-2, Polym. Phys.* **1971**, *9*, 43.

22. For a review of emulsifier-free emulsion polymerization see for example Shouldice, G. T. D.; Vandezande, G. A.; Rudin, A. *Eur. Polym. J.* **1994**, 30, 179.

23. Goodwin, J. W.; Hearn, J.; Ho, C. C.; Ottewill, R. H. *Br. Polym. J.* **1973**, 5, 347.

24. (a) Gauthier, M.; Möller, M. *Macromolecules* **1991**, *24*, 4548. (b) Gauthier, M.; Frank, P. C. *React. Funct. Polym.* **1996**, *31*, 67.

25. (a) Figueroa, W. G.; Raszkowski, R.; Weiss, W. *New Engl. J. Med.* **1973**, *288*, 1096. (b) Laskin, S.; Drew, R. T.; Cappiello, V.; Kuschner, M.; Nelson, N. *Arch. Envir. Health.* **1975**, *30*, 70.

26. Altares, T., Jr.; Wyman, D. P.; Allen, V. R.; Meyersen, K. *J. Polym. Sci., Part A* **1965**, *3*, 4131.

27. Gauthier, M.; Möller, M.; Burchard, W. *Macromol. Symp.* **1994**, *77*, 43.

28. Frank, P. C. *M. Sc. Thesis*, University of Waterloo, Waterloo, **1995**.

29. Worsfold, D. J.; Bywater, S. *Can. J. Chem.* **1964**, *42*, 2884.

30. Worsfold, D. J.; Bywater, S. *Macromolecules* **1978**, *11*, 582.

31. (a) Morrison, B. R.; Gilbert, R. G. *Macromol. Symp.* **1995**, 92, 13. (b) Stutman, D. R.; Kleln, A.; El-Aasser, S. M.; Vanderhoff, J. W. *Ind. Eng. Chem. Prod. Res. Dev.* **1985**, 24, 404.

32. (a) Takaki, M.; Asami, R.; Ichikawa, M. *Macromolecules* **1977**, *10*, 850. (b) Takaki, M.; Asami, R.; Kuwata, Y. *Polym. J.* **1979**, *11*, 425.

33. (a) Kee, R. A.; Gauthier, M. *Macromolecules* **1999**, *32*, 6478. (b) Li, J.; Gauthier, M.; Teertstra, S. J.; Xu, H.; Sheiko, S. S. *Macromolecules* **2004**, *37*, 795.

34. Ferry, J. D. *Viscoelastic Properties of Polymers*, 3rd ed.; Wiley: New York, 1980; p 267.

35. Graessley W. W. *Adv*. *Polym*. *Sci*. **1982**, *47*, 67.

36. Bretas, R. E. S.; Powell, R. L. *Rheol*. *Acta* **1985**, *24*, 69.

37. Chiu, W.-Y.; Hsueh, T. C. *J*. *Appl*. *Polym*. *Sci*. **1986**, *32*, 4663.

38. Scherbakoff, N.; Ishida, H. *Polym*. *Mater*. *Sci*. *Eng*. **1991**, *65*, 337.

Chapter 7

Concluding Remarks and Suggestions for Future Work

7.0 Concluding Remarks

The research presented in this dissertation focused on the synthesis and the characterization of arborescent polymers and of closely related grafted latex particles, of interest either as model systems or for large-scale applications. Among branched macromolecules, star-branched[1] and arborescent polymers[2] are particularly significant because of their well-defined architectures enabling the establishment of structure-property relations. Both polymer families are synthesized predominantly by living anionic polymerization. The absence of termination and chain transfer in these reactions allows the preparation of macromolecules with predictable molecular weights and narrow molecular weight distributions, with a degree of control difficult to attain by other means.

A divergent synthetic scheme was developed for the synthesis of novel high branching functionality hybrid polymers from carbosilane dendrimer substrates and 1,4-polybutadiene side chains. Carbosilane dendrimers containing either 32, 64, or 128 peripheral Si-Cl functional groups were first coupled with 1,2-polybutadienyllithium chains with a number-average molecular weight $M_n \approx 1000$ and a narrow molecular weight distribution. The polybutadiene-grafted substrates were then hydrosilylated with dichloromethylsilane and reacted with high 1,4-microstructure content polybutadienyllithium chains to generate the high branching functionality arborescent-dendrimer hybrids. Three series of hybrid polymers were synthesized containing 1,4-polybutadiene side chains with $M_n \approx 1500$, 5000, or 30000. A narrow molecular weight distribution was maintained for all samples ($M_w/M_n \leq 1.16$), and the hybrid polymers had branching functionalities up to 10 times higher than for star-branched polybutadienes synthesized previously.[3]

A grafting procedure developed previously for the small-scale (10 – 15 g) synthesis of arborescent polystyrenes,[4] based on end-capping of polystyryllithium with 2-vinylpyridine units in the presence of LiCl, led to a low grafting yield (e.g. 75 % for a linear substrate) when scaled up to 100 g. The decreased yield was linked to side chain dimerization and deactivation of the macroanions. A modified 100-g scale procedure was developed, using end-capping of the polystyryllithium with 1,1-diphenylethylene in the presence of LiCl, followed by the addition as a dilute solution of 3 – 6 equivalents of 2-vinylpyridine per side chain. This approach eliminated side chain dimerization and led to grafting yields of up to 95 %. Successive acetylation and anionic grafting reaction cycles were used to synthesize arborescent polystyrenes of generations up to G2 with low polydispersity indices ($M_w/M_n \leq 1.04$), and molecular weights and branching functionalities increasing in an approximately geometric fashion for successive grafting cycles. These materials are useful as model weakly interacting branched polymers with a well-defined structure, but there is also considerable interest in producing arborescent copolymers such as polystyrene-*graft*-poly(2-vinlypyridine), potentially useful as branched polyelectrolytes and microencapsulation agents. To prepare large amounts of samples for physicochemical investigations, the 100-g synthesis of arborescent polystyrene-*graft*-poly(2-vinlypyridine) copolymers based on acetyl coupling sites was achieved by modification of a reported procedure. Two arborescent copolymer families with $M_n \approx 5000$ or 30000 P2VP side chains were thus synthesized, and a narrow molecular weight distribution (M_w/M_n = 1.08-1.10) was maintained for graft copolymers of successive generations.

The compact structure of the arborescent poly(2-vinylpyridine) copolymers led to interesting polyelectrolyte behavior upon protonation by a strong acid such as trifluoroacetic acid (TFA). A compact molecular structure could lead to enhanced expansion when compared with linear poly(2-vinylpyridine) samples, due to the close proximity of the ionic groups leading to stronger interactions. At the same time, branching also increases the structural rigidity of the molecules, potentially hindering conformation changes and opposing the electrostatic repulsion forces. The relative importance of these two contributions was explored by examining their solution properties as a function of structure, protonation level, solvent type, and the addition of salt. The reduced viscosity (η_{sp}/C) of arborescent polyelectrolyte solutions in polar solvents (methanol, DMF, H_2O) was investigated as a function of polyelectrolyte concentration (C) for the two families of P2VP copolymers synthesized. The viscosity of the copolymer solutions was also compared with that of linear P2VP samples under the same conditions.

Finally, the synthesis of model filler particles was achieved by grafting polyisoprene chains onto cross-linked polystyrene latex particles using the acetyl coupling site chemistry. These materials, which can be viewed as an extreme case of an arborescent copolymer structure, were then used to investigate the influence of filler-matrix polymer interactions on the rheological behavior of linear polyisoprene blends. The rheological behavior of the blends was examined by dynamic mechanical analysis in terms of frequency-dependent complex viscosity, storage modulus, and damping factor. All the blends exhibited enhanced complex viscosity and storage modulus, and lower damping factor values relatively to the matrix polymer. A decreased damping factor,

indicative of lower heat dissipation, is interesting for applications where the generation of heat is undesirable such as tires.

7.1 Suggestions for Future Work

The carbosilane dendrimer-arborescent polybutadiene hybrids synthesized should be excellent model branched polymer systems for further investigation of their elastomeric properties, due to the very low entanglement molecular weight of the polybutadiene chains. The zero-shear viscosity of polybutadiene star-branched polymers is known to increase exponentially once the number of entanglements per side chain (M_{arm}/M_e) exceeds a value of 3 – 5.[5] This is attributed to enhanced entanglement formation in the branched polymers relatively to the linear polymers, if the side chains are sufficiently long. The rheological behavior of polybutadienes with branching functionalities as high as the ones obtained in this work has never been investigated, so it would be interesting to compare them with the star-branched polymers. The dendrimer-arborescent polybutadiene hybrids synthesized in the present study indeed have side chain molecular weights reaching values up to 17 times larger than the entanglement molecular weight of 1,4-polybutadiene (M_e = 1800).[6]

The large scale (100-g) synthesis of arborescent polymers from styrene and 2-vinylpyridine using a *grafting onto* method based on acetyl coupling sites was achieved in up to 95 % grafting yield. This confirms the suitability of the acetyl coupling chemistry for large scale reactions and opens the door to further scaling up of the reaction, to 1000 g and above. Reactions yielding more than 100 g of material would be highly desirable for certain types of physical tests (e.g. tensile measurements) requiring large samples, in

particular when the reproducibility of the results and a range of different sample compositions must be examined. The large-scale synthesis of other copolymers (e.g. arborescent polystyrene-*graft*-polyisoprene, arborescent polystyrene-*graft*-polybutadiene) would also be of interest for applications as elastomers.

The polyelectrolyte behavior of arborescent poly(2-vinylpyridine) copolymers was barely explored in this thesis. The properties of these materials should be investigated under a much wider range of conditions, for example using different acids such as HCl and HBr, quaternization with alkyl halides such as methyl iodide, and medium- to low-polarity solvents including THF ($\varepsilon = 7$), to examine ionic aggregation phenomena and reversible gelation effects not considered in the present study.

The core-shell polymers synthesized by grafting polyisoprene chains onto cross-linked latex particles appear to be excellent model filler systems to study the reinforcement of elastomers, since their size and surface functionality can be controlled accurately. The scope of the investigation could be easily broadened by examining a range of cross-linked polystyrene particle sizes and controlling the thickness of the shell by varying the size of the grafted chains over a broad range.

7.2 References

1. (a) Rempp, P.; Franta, E.; Herz, J.-E. *Adv. Polym. Sci.* **1988**, *86*, 145. (b) Hsieh, H. L.; Quirk, R. P. *Anionic Polymerization*: *Principles and Practical Applications*; Dekker: New York, 1996; Chapter 13.
2. For a recent review on arborescent and other dendrigraft polymers see Teertstra, S. J.; Gauthier, M. *Prog. Polym. Sci.* **2004**, *29*, 277.

3. Roovers, J.; Toporowski, P.; Martin, J. *Macromolecules* **1989**, *22*, 1897.

4. Li, J.; Gauthier, M. *Macromolecules* **2001**, *34*, 8918.

5. Roovers, J. *J. Non-Cryst. Solids* **1991**, *131-133*, 793.

6. Fetters, L. J.; Lohse, D. J.; Richter, D.; Witten, T. A.; Zirkel, A. *Macromolecules* **1994**, *27*, 4639.